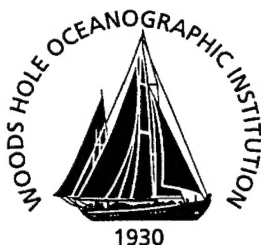


Woods Hole Oceanographic Institution



Instrumentation for Open Ocean Aquaculture Monitoring

by

James Irish, Megan Carroll, Robin Singer
Art Newhall, Walter Paul, Craig Johnson, Nick Witzell

Woods Hole Oceanographic Institution
Woods Hole, MA

and

Glen Rice
Dave Fredricksson

Ocean Engineering Program
University of New Hampshire

October 2001

Technical Report

20020328 033

Funding was provided by the National Oceanic and Atmospheric Administration for the Open Ocean Aquaculture Project under Contract No. NA86RG0016 to the University of New Hampshire and under Subcontracts 00-394 and 01-442 to the Woods Hole Oceanographic Institution.

Approved for public release; distribution unlimited.

WHOI-2001-15
UNH OOA

Instrumentation for Open Ocean Aquaculture Monitoring

by

James Irish, Megan Carroll, Robin Singer
Art Newhall, Walter Paul, Craig Johnson, Nick Witzell
Woods Hole Oceanographic Institution
Woods Hole, MA 02543

and

Glen Rice
Dave Fredricksson
Ocean Engineering Program
University of New Hampshire

October 2001


Technical Report

Funding was provided by National Oceanic and Atmospheric Administration for the Open Ocean Aquaculture Project under Contract No. NA86RG0016 to the University of New Hampshire and under Subcontracts 00-394 and 01-442 to the Woods Hole Oceanographic Institution.

Reproduction in whole or in part is permitted for any purpose of the United States Government. This report should be cited as Woods Hole Oceanog. Inst. Tech. Rept., WHOI-2001-15.

Approved for public release; distribution unlimited.

Approved for Distribution:


W. Rockwell Geyer, Chair

Department of Applied Ocean Physics and Engineering

1.0 Abstract

The University of New Hampshire (UNH) is working on an Open Ocean Aquaculture (OOA) demonstration program off Portsmouth, New Hampshire in the Gulf of Maine. This site has two fish cages moored with four anchor moorings each. To understand these systems and model their behavior, the forcing by currents and waves, and the response of the mooring (tensions) and the fish cage (motions) required measuring. UNH has an environmental mooring with an ADCP current profiler to obtain the current forcing. WHOI constructed a wave rider buoy, load cell and recorder systems and a fish cage motion package, and with UNH diver and ship support, deployed them at the OOA demonstration site.

To measure the tension in the critical mooring lines of the fish cage, load cells were constructed and deployed with the mooring when it was serviced during August 2000. To record the load cell measurements of tensions, low power recording systems were constructed, tested and deployed on the load cell mounting bars by divers. Single load cells were deployed in the four anchor lines at the top of the rope where it attached to the grid line rings. In the NE corner, load cells were also placed in the two grid lines and the riser line to the fish cage. Finally at the fish cage, two load cells were mounted on the cage rim and attached to the NE corner upper bridle line. A single data system recorded the tensions at the NE corner, and the two load cells on the fish cage were designed to be recorded with the fish cage motion package. The recorders were deployed in 22 October 2000 and recorded good data through January, when they were turned around and redeployed. The three single load cell recorders were left in place until July 2001 and recorded through 23 June when their data storage filled. The four load cell system was recovered in March after a large winter storm, and had failed due to short in a load cell or wiring in early March. A preliminary look at the data shows that the mooring was tensioned in the NW-SE direction. The nature of the signal changed significantly during storms and at other times related to fish cage servicing.

To measure the wave forcing of the fish cage and mooring, a wave rider buoy was constructed. The sensor is a 3-axis accelerometer that measures the motion of the buoy as it follows the waves. The acceleration is recorded and integrated twice to obtain vertical displacement characteristics (related to wave amplitudes) and spectra. The buoy is moored with a compliant elastic element to allow it to move freely in the waves, yet remain in its moored position to the east of the northern UNH-OOA fish cage. The wave rider buoy was deployed on 4 January 2001 and recovered on 17 March 2001 after a major Northeast storm. It recorded data throughout its deployment that was used to estimate wave forcing for the winter of 2001, and captured several severe storms.

To measure the motion of the moored fish cage, a 6-axis motion package was constructed and deployed. The system used a 6-axis Motion-Pak as the sensing element and a PC-104 based data system with A/D and hard disk data storage. The system was battery powered and mounted in a pressure case for surface or submerged deployment. The motion package was deployed on the Northern fish cage from Jan into March 2001 and recorded motions throughout without difficulty. It observed the major storm in early March where the counter weight was lost from the fish cage, and its increase in motion thereafter.

2.0 Table of Contents

1.0 Abstract	2
2.0 Table of Contents	3
2.1 List of Tables	4
2.2 List of Figures	4
3.0 Introduction, Need and Approach	6
4.0 Part 1: Mooring Line Tension Monitoring	7
4.1 Load cell system	7
4.1.1 Load cells	8
4.1.2 Load cell mounting	10
4.1.3 Electronics pressure case, strongback, and diver servicing	13
4.2 Recorder	16
4.2.1 Persistor controller/recorder	16
4.2.2 Sampling plan, software, and power	19
4.3 Northeast corner assembly	21
4.3.1 Load cell and mooring line assembly at grid corner	21
4.3.2 Northeast Corner Telemetry Link	22
4.3.2.1 Telemetry component in the load cell recorder	23
4.3.2.2 Electrical conductor on mooring rope	25
4.3.2.3 Telemetry component on fish cage	31
4.4 Deployment, field operation, servicing, and results	35
5.0 Part 2: Wave Forcing Monitoring	41
5.1 Accelerometer Options	41
5.2 Data System and Telemetry	43
5.2.1 Persistor controller, signal conditioning, recorder, sampling	43
5.2.2 Spread spectrum telemetry link	45
5.3 Telemetry Buoy and Compliant Elastic Mooring	47
5.3.1 WHOI telemetry buoy	47
5.3.2 Solar panels, batteries, and power system	51
5.3.3 Compliant elastic mooring	53
5.4 Deployment, operation, results	53
6.0 Part 3: Fish Cage Response Monitoring	60
6.1 Motion sensor and recording system	60
6.1.1 Systron Donner 6-axis motion sensor	60
6.1.2 Power requirements	61
6.1.3 PC-104 data system	61
6.1.4 Software and sampling program	65
6.1.5 Spread spectrum telemetry link	65
6.2 Mounting, battery and electronic pressure cases, antenna	66
6.2.1 Battery supply and life	66
6.2.2 Pressure cases	67
6.2.3 Mounting silos	67
6.2.4 Spar in-water mounting system	68
6.3 Environmental sensor package	69
6.3.1 Sensors (pressure, temperature, OBS and currents)	69
6.3.2 Mounting on fish cage	70
6.3.3 Environmental Sensor Data system	71

6.4 Deployment, operation and preliminary results	73
7.0 Acknowledgements	80
8.0 References	81
9.0 Appendices	83
9.1 Load Cell Electronics	
9.1.1 Power switch on load cell recorder	83
9.1.2 Telemetry link in recorder	84
9.1.3 Telemetry link on fish cage	85
9.2 Load Cell Mechanical	
9.2.1 Strongback for load cell only	86
9.2.2 Strongback for load cell and recorder only	87
9.2.3 Recorder pressure case	88
9.2.4 Fish cage telemetry package	89
9.3 Wave Rider Electronics	
9.3.1 Electronics dchematic	90
9.4 Wave Rider Buoy and mooring	
9.4.1 Buoy assembly drawing	91
9.4.2 Mooring component list	92
9.5 Motion Package	
9.5.1 Electronics and battery pressure case	93
9.5.2 Silo assembly on spar	94
9.5.3 Silo assembly with pressure cases	95

List of Tables

Table 4.1 Conductor Cable Wrap Details	28
Table 4.2 Instrument Start and End Times	35
Table 4.3 Load Cells, Recorders and Positions	35
Table 5.1 Accelerometer comparison	41
Table 5.2 High Acceleration Events	57
Table 6.1 Motion-Pak Specifications	61
Table 6.2 Motion-Pak Power Requirements	61
Table 6.3 Motion Package start and end times	73
Table 6.4 Statistics from 6 February Storm	75

List of Figures

Figure 3.1 UNH-OOA fish cage and mooring system	6
Figure 4.1 Northern Fish cage mooring with load cell locations	8
Figure 4.2 Load cell prototype open for inspection	9
Figure 4.3 Load cell with amplifier, case and wire	10
Figure 4.4 Load cell eye and wire guard	11
Figure 4.5 Load cell on wire guard showing operation	11
Figure 4.6 Load cell off strongback detail showing eye nut	12
Figure 4.7 Load cell on strongback	12
Figure 4.8. Load cell on strongback with cable guard and recorder pressure case	13
Figure 4.9 Schematic view of recorder ready to attach to strongback	14
Figure 4.10 Schematic view of recorder attached to strongback	15
Figure 4.11 Picture of pressure case on strongback	15
Figure 4.12 Persistor microcontroller with PicoDAC and compact flash card	16
Figure 4.13 Recorder attached to end cap of recorder	17
Figure 4.14 Battery in pressure case ready to attach recorder	19

Figure 4.15 Recorder attached, initialized and ready to closer	20
Figure 4.16 Drawing of NE corner and load cells	21
Figure 4.17 Picture of NE corner with 4 load cells in place	22
Figure 4.18 Schematic of motion of load cells in relationship to wiring	23
Figure 4.19 Telemetry electronics for bottom and top	24
Figure 4.20 Telemetry electronics with Persistor recorder on end cap	24
Figure 4.21 Walter Paul measuring riser line	26
Figure 4.22 Spiraled Element wrapped around Compliant Core	27
Figure 4.23 Stretch Natural Wrap Angle versus Conductor Rope Stretch	29
Figure 4.24 Electrical cable on riser line for telemetry link	30
Figure 4.25 Electronics on board with regulator and battery	31
Figure 4.26 Electronics with spread spectrum radio	32
Figure 4.27 Telemetry package ready to mount in silo	33
Figure 4.28 Silo systems for top of fish cage	34
Figure 4.29 Average tension of load cells in mooring	36
Figure 4.30 Standard deviation of tension of load cells in mooring	38
Figure 4.31 Average tensions of four load cells in Northeast corner	39
Figure 4.32 Corrosion on stainless tie rods of pressure case	40
Figure 5.1 Summit Instruments accelerometer	42
Figure 5.2 Wave rider electronics board	44
Figure 5.3 Spread spectrum radio modem and solar regulators	46
Figure 5.4 WHOI telemetry buoy	48
Figure 5.5 Walter Paul by UNH-OOA wave rider buoy under construction	49
Figure 5.6 UNH-OOA wave rider buoy deployed	50
Figure 5.7 System battery voltage time series	52
Figure 5.8 Wave rider mooring schematic	54
Figure 5.9 One burst record output	55
Figure 5.10 Summary data statistics - mean and variance	56
Figure 5.11 Acceleration and integrated displacement from 6 March storm	58
Figure 5.12 Spectra of sensor noise, signal during storm and displacement	59
Figure 6.1 Systron Donner Motion-Pak	60
Figure 6.2 Block Diagram of fish cage data system	62
Figure 6.3 Fish Cage Motion Package	63
Figure 6.4 Battery discharge	66
Figure 6.5 Silos and instrument cases for motion package installation	67
Figure 6.6 Schematic drawing of silos on the top of the fish cage	68
Figure 6.7 Mounting frame for motion package	69
Figure 6.8 Motion package in mounting frame	69
Figure 6.9 Environmental sensing pack in frame	71
Figure 6.10 Environmental sensor digitizing electronics	72
Figure 6.11 Time series plot from 6 Feb Storm	74
Figure 6.12 Spectra of accelerations	75
Figure 6.13 Spectra of rate sensors	76
Figure 6.14 Fish Cage Average Accelerations	77
Figure 6.15 Fish Cage Variance of Accelerations	78
Figure 6.16 Fish Cage Average Rate Sensors	79
Figure 6.17 Fish Cage Variance of Rate Sensors	80

3.0 Introduction, Need, Approach

There is an increasing need for open ocean aquaculture to fill the Nation's requirement for seafood that is continually increasing at a time when our natural fisheries are decreasing. Near-shore aquaculture and aquaculture in protected waters have proven successful with species such as salmon and catfish, but not with cold-water fish such as cod and haddock. The water conducive to these fish is found in open, unprotected waters and the technology to design and moor appropriate fish cage or pen systems in these locations has not been developed and tested. Also, as the population increases the availability of protected water sites for aquaculture is decreasing and open ocean sites must be considered, and the methodology to carry on open ocean aquaculture must be examined and developed.

The University of New Hampshire (UNH) has established an open ocean aquaculture (OOA) demonstration site just south of the Isle of Shoals off Portsmouth New Hampshire in the Gulf of Maine (Baldwin, et al., 2000). This demonstration project purchased two Ocean Spar fish cages and designed, constructed and deployed a mooring to hold the fish cages in position in 52 meters of water. Each fish cage had four anchors to hold it in position (Figure 3.1). The fish cage has two stable positions, one in the "up" position with the fish cage at the surface (shown in Figure 3.1), and the second in the "down" position, with the counter weight (the line from the cage down in Figure 3.1) on the bottom. The South cage was being used in the down position, and the North cage was serviced in the summer of 2000, instrumented and kept in the up position during the winter 2000-2001.

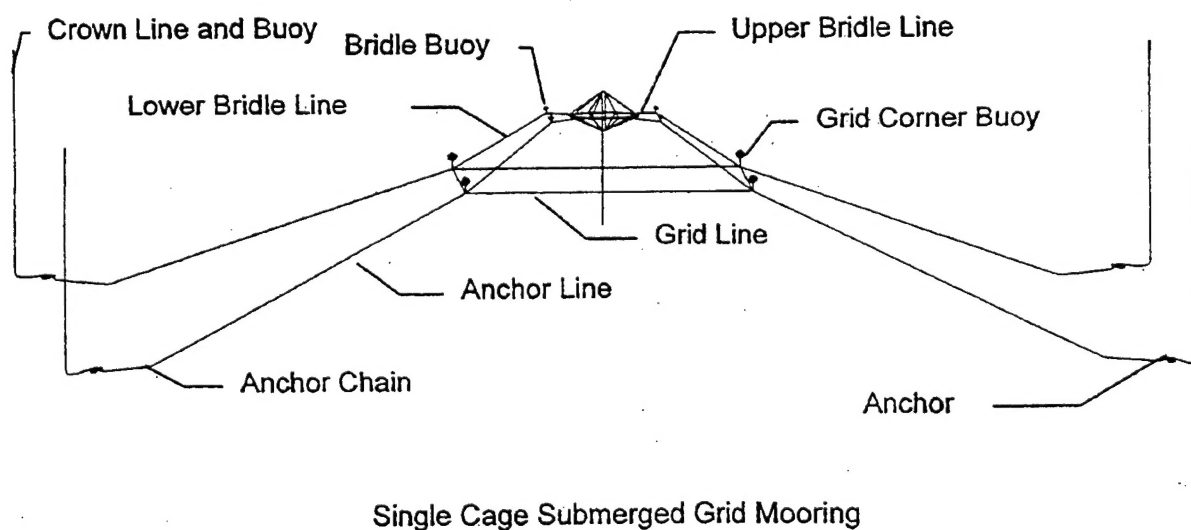


Figure 3.1. The UNH-OOA mooring schematic. Two such moorings (North and South) are deployed at the OOA site. (from UNH-OOA WEB site)

As part of the UNH-OOA project, physical scale model tests (Fredriksson, et al, 2000), finite element modeling (Tsukrov et al., 2000), and monitoring instrumentation of the full fish

cage and mooring system are being conducted. This effort is aimed at developing an understanding of mooring elements, materials and methodology to carry on open ocean aquaculture. This understanding is coming about through a three tiered approach of computer modeling the systems, scale physical model testing, and instrumentation of the full system as described in Fredriksson (2001). The Woods Hole Oceanographic Institution (WHOI) is working with UNH to instrument the mooring system, the fish cage, and to monitor the wave forcing. The water current forcing and environmental properties at the site are being measured by an Acoustic Doppler Current Profiler (ADCP) on an environmental mooring deployed by UNH (Bub and Brodeur, 2001).

Therefore, the current forcing, the wave forcing, the mooring line tensions and the fish cage response were measured with the fish cage at the surface. By comparing these observations with the scale physical and computer models, greater understanding of the processes involved in open ocean aquaculture is being achieved and incorporated in the computer models. These models can then be used by others to design viable open ocean aquaculture systems with the assurance that the models contain the relevant physics and have been validated at the UNH-OOA site.

This report covers the WHOI monitoring instrumentation development and deployment and is divided into three sections covering the load cells for mooring tension (Part 1), the wave rider buoy for wave forcing (Part 2), and the fish cage motion recorder (Part 3). Each section is divided into parts discussing the sensing elements, the recorder and telemetry, the mounting system and concluding with some preliminary data plots. An analysis of these data (including the ADCP currents) is written up in an additional report (Irish, et al., 2001b). A subset of the schematics and drawings are given in the appendices.

4.0 Part 1: Mooring Line Tension Monitoring

James Irish⁺, Megan Carroll⁺, Robin Singer⁺, Walter Paul⁺, Craig Johnson⁺,
Glen Rice^{*} and Dave Fredriksson^{*}

⁺Woods Hole Oceanographic Institution, ^{*}University of New Hampshire

4.1 Load cell system

An understanding of the fish cage mooring behavior and design criteria requires knowledge of the tensions in the mooring lines as a function of current, waves and biofouling of the fish cage (drag). To accomplish this, load cells and recorders were placed at several critical locations of the fish cage mooring to measure the tensions (Figure 4.1). Previous physical scale modeling and finite element computer models suggested that the tensions in the mooring lines would typically be 1,000 to 3,000 lbs, with peak tensions approaching 15,000 lbs. Therefore, it was decided that the load cells should be capable of measuring tensions to 20,000 lbs. and remain linear. To survive the catastrophic event (e.g. tangling with fishing activities), the load cells would have to be capable of withstanding 50,000 lb tensions to make them compatible with the strengths of the mooring lines and hardware.

The load cells were mounted on strong steel bars that allowed them to be shackled into the mooring, and also to hold the recorder and batteries. As the load cells were the critical element they will be discussed first, followed by the mounting, recorder and other details. A brief discussion of deployment and a brief data summary is given at the end of Part 1.

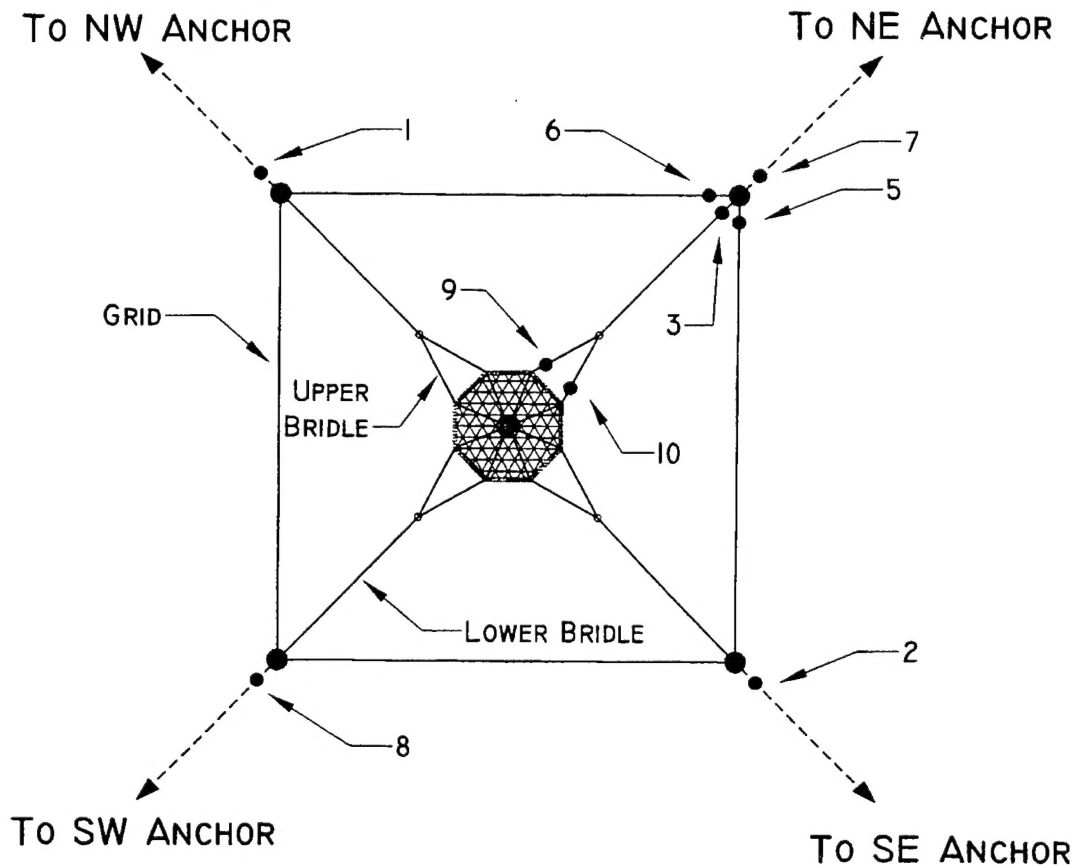


Figure 4.1. The Northern fish cage mooring as instrumented for the UNH-OOA program for the winter of 2000-2001. Load cells (serial number identified) positions are indicated. (Fredriksson, 2001).

4.1.1 Load cells

After a search of the various load cell manufactures, Sensing Systems Incorporated of New Bedford, MA was selected to make the load cell sensing elements. This company is small, located nearby WHOI so that we could visit and discuss program requirements with them, and they were willing to listen and design load cells that matched our application requirements. In addition to the specifications outlined above, the load cells had to be insensitive to torque in the mooring line. As most fiber lines are made of twisted fibers, as the tension in the line varies, the torque applied at the end will also change. Therefore, producing a design that was insensitive to torque was important. This was accomplished by constructing the load cells with the webs between the inner and outer rings wider in the angular direction rather than in thickness (see Figure 4.2). This simple design minimized the effects of torque. The strain gauges themselves were then placed on the thin part of the web near the inner and outer rings (Figure 4.2).

As the load cells were a part of the fish cage mooring, the recorders had to be constructed so divers could disconnect them (mechanically and electrically) from the load cells and bring them to the surface for servicing. An Impulse underwater matable connector was selected (IM-4-LP) that has proven successful in many applications. This plug could be mated and unmated

by divers at the expected 20-meter depths of the load cells and recorders. It was important to minimize the effects of contact resistance in the connector between the load cell and recorder. A preamplifier was mounted on each load cell so the largest signal (voltage) would be on the connector to prevent milliohm resistance changes in the contacts from having large effects on the results. This amplifier is relatively insensitive to battery input voltage changes and produces an output matched to the 2.5-volt range of the A/D converter in the Persistor data system (see below).

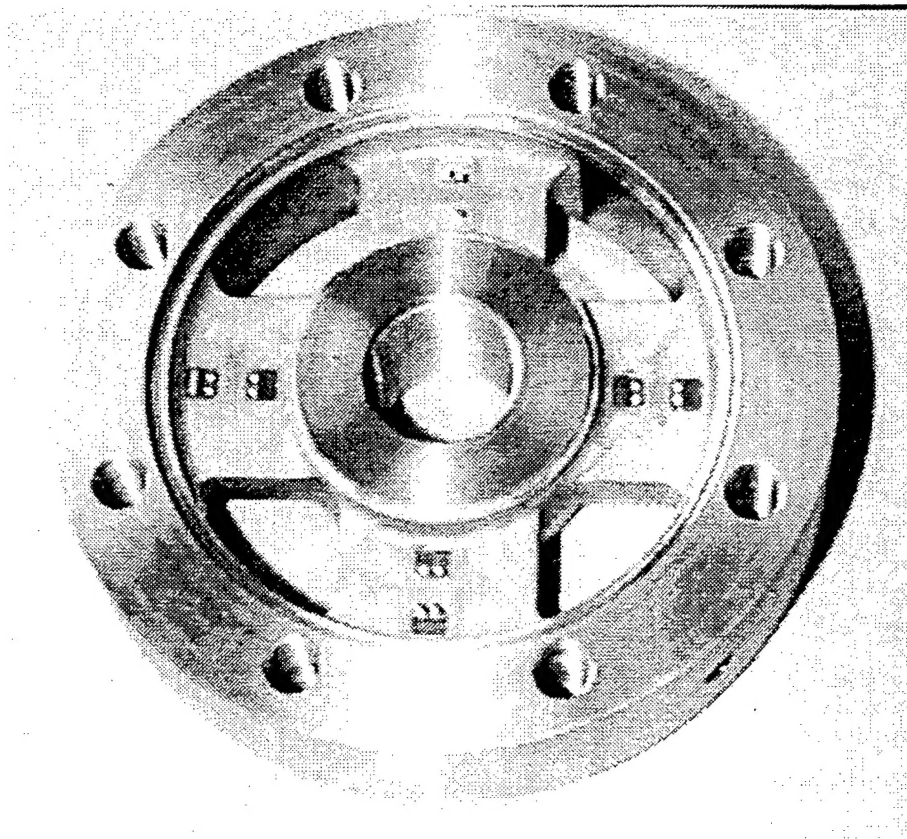


Figure 4.2. The prototype load cell after machining and testing. To complete it, covers would be welded in place between the inner and outer rings, and the electronics/connector case added. The strain gauges are seen on each web assembly (note top strain gauges are partially missing). The wide webs are to minimize the effects of rope torque on the load cell.

The amplifier was mounted in a metal box attached to the side of the load cell with the underwater connector on the end of a short length of wire (Figure 4.3). A problem with this wire was how to connect it with the electronics without having it being moved about with the currents and waves. A weak point in any connector is where the wire attaches to the sensor and the recorder. If the wire were to move about, then there is a stress concentration point where the wire joins the potting of the connector or bulkhead fitting, and the wire will break there after about a year of normal activity. To hold the wire firmly, a wire guard was cut from metal or plastic and attached to the load cell between the cell outer ring and mounting plate (Figures 4.4, 4.5, 4.7 and 4.8). This not only holds the wire in position, but also protects it when the load cells were being launched and when there were in the water. No simple banging against a firm object or rubbing by a line would damage the cable.

To minimize the corrosion effects in salt water and to provide a material that met the strength requirements, 17-4PH stainless steel was used. This is readily machined and welded as required, and the mild steel used in the mounting bar would act as an anode to protect the material. The interior of the load cell was filled with foam to further protect it from water penetration. The load cells were designed and tested to have linear output from 0 to 20,000 lbs tension, and to have no permanent deformation under these loads. They were also designed for a greater than 50,000 lbs failure, but were not tested to failure to assure that this was so. The load cell as delivered by Sensing Systems Inc, is shown in Figure 4.3.

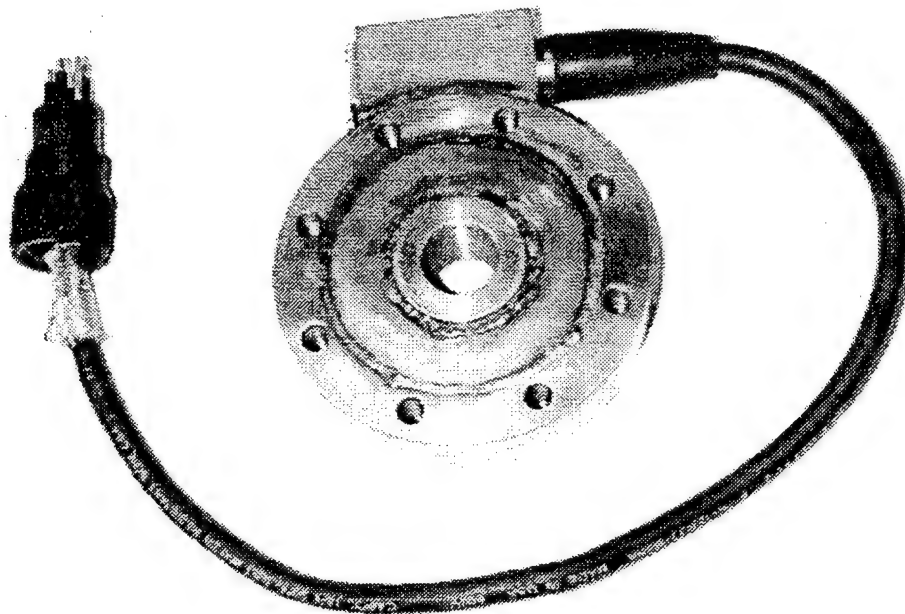


Figure 4.3. Load cell with amplifier in an attached pressure case (top box) and an Impulse 4 conductor underwater matable connector that runs to the load cell recorder. The load cell is mounted with an eye screwed into the center and a plate that is bolted to the outside ring.

4.1.2 Load cell mounting

To mount the load cell in the mooring, hardware needed construction with an eye on either end. This would allow the load cell to be shackled into the mooring line at the required position, only lengthening the line by the amount equal to its length (less than 1 m). Therefore an eye was required that screwed into the threaded hole in the center of the load cell (see Figure 4.4, 4.6, and 4.7). This eye was secured in place by a nut and cotter pin on the backside of the load cell. The load cell with eye and nut in place is shown in Figure 4.6. The other end of the load cell was more complicated. A plate that could be screwed into the bolt holes in the outer ring of the load cell was required, but it also had to be spaced away from the load cell to allow space for the nut and cotter pin on the back of the eye. This was accomplished by using the wire guard as a spacer (Figure 4.7). The plate was then welded to a bar with a hole for a shackle in the other end. Both the holes in the eye and the bar were protected by plastic insulators to

provide smooth wearing surfaces and to provide electrical insulation between the mild steel bar, the 316 stainless steel eye and the galvanized shackles [see Appendices 9.2.1 and 9.2.2].

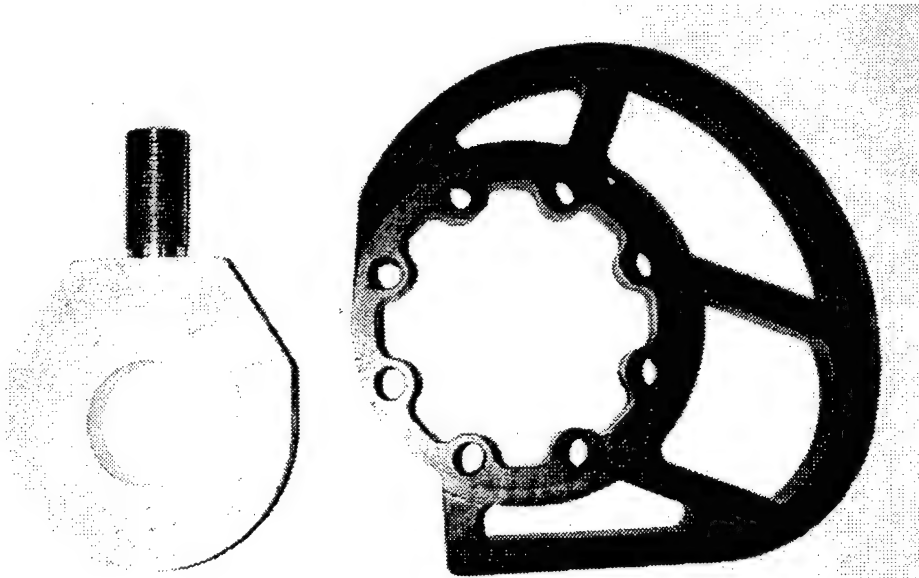


Figure 4.4. Eye for center of load cell (left), and wire guard to protect wire (right). The eye was made from 316 stainless, with a hole large enough for insulating washers and a standard 1 1/4" shackle. The wire guard at right is made of Delron, but others were made of stainless steel also. The holes for the bolts and the cable run are seen assembled in Figure 4.5 below. The guard in place with the wire and pressure case is shown in Figure 4.8.

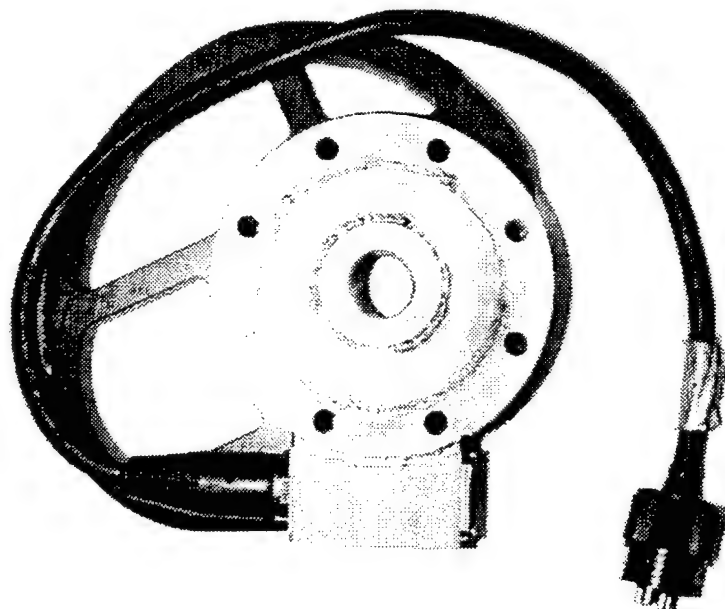


Figure 4.5. Load Cell sitting on wire guard to show how protects wire from damage and leads it to the recorder.

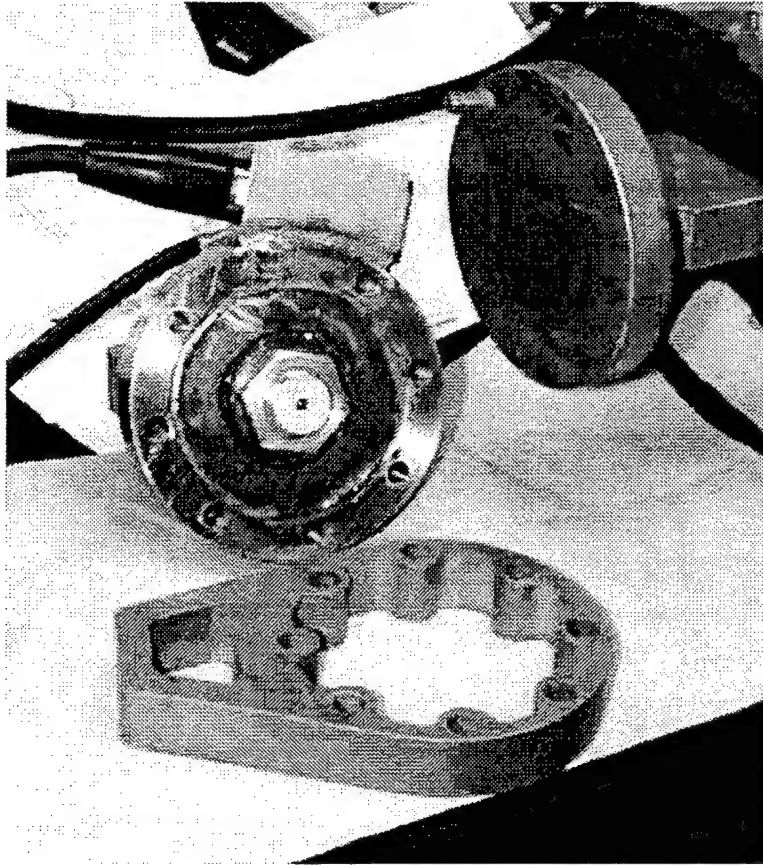


Figure 4.6. Detail of the safety nut on eye (no cotter pin in place yet) and the first design for the wire guard that was determined to be inadequate. The plate on the end of the steel mounting bar is seen at the right, with one bolt protruding.

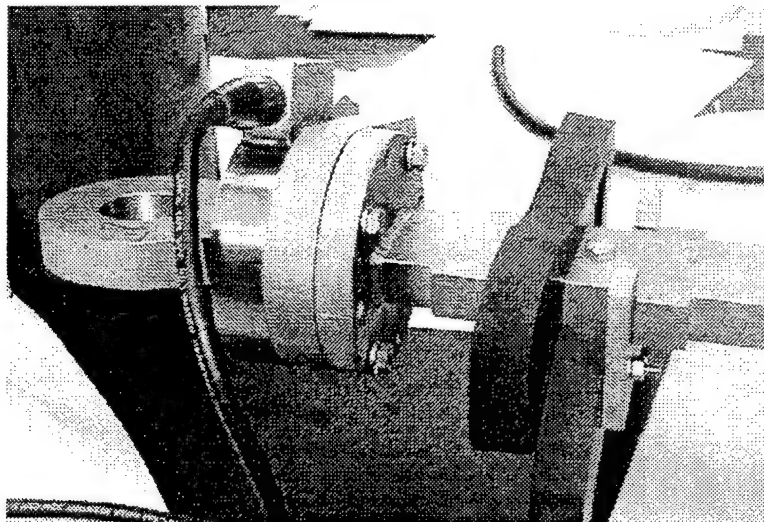


Figure 4.7. The eye in place and the load cell mounted to the steel bar with an early version of the wire guard. The rubber block (black block on the steel bar) helps hold the electronics pressure case to the steel bar. The titanium c-shaped piece that holds the pressure case is also shown.

The bar on the back of four of the load cells was lengthened beyond what was required for a shackle to allow for the attachment of the recorder and battery pressure case (Figures 4.9, 4.10 and 4.11) [see Appendices 9.2.1 and 9.2.2 for the two strongback configurations]. This allowed the system to move as one piece in the water column with the mooring, yet allow for servicing without removing the load cell from the mooring system.

4.1.3 Pressure Case, Strongback and Diver Servicing

The length of the bar or strongback on the back of the load cell to which the recorder's pressure case was attached was based on the length of the pressure case required to hold the batteries to power the system for 4 months between servicing. Once this was determined, then the rest of the system to be sized accordingly. A main design factor was to allow for removal of the pressure case and servicing by divers. This was accomplished by cutting the bar or strongback so that the recording package could be slipped onto the bar relatively easily by the diver and temporarily held by titanium c-shaped pieces that gripped the bar, then secured by pulling rubber locking pieces into place and by placing two screws through the bar into blocks on the pressure case (Figures 4.7, 4.8, 4.9, 4.10, and 4.11) [see Appendix 9.2.3].

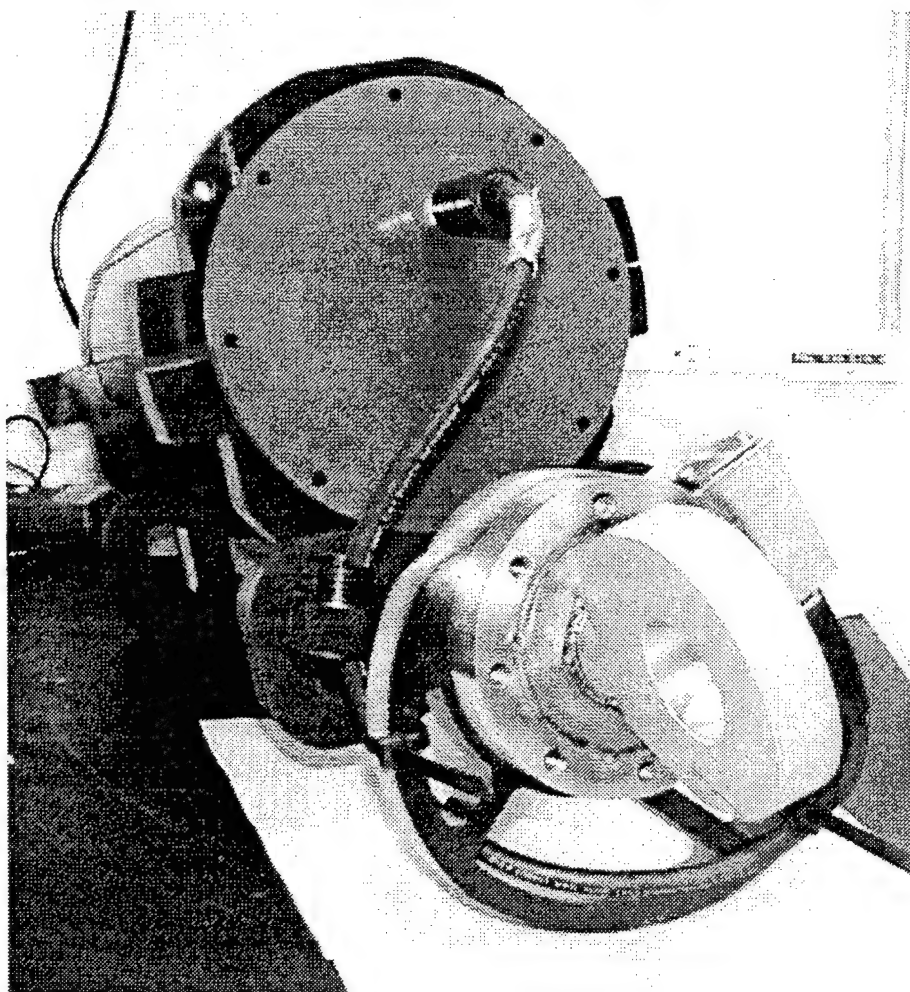


Figure 4.8. Eye in place load cell on the load cell, the load cell bolted to the strongback bar and proper wire guard in place. The pressure case is set in place with the wire running to it from the load cell. The slack allows for unplugging and replugging during servicing.

The diver would swim down with the load cell recorder, slip it onto the strongback and secure it with the rubber blocks and bolts. The pressure case with recorder and battery weighed about 7 lbs in water, and was buoyed with a small plastic net float for safety and ease in handling. The diver would then remove the dummy plugs from the connector on the load cell cable and on the pressure case, and plug the load cell into the recorder. The only requirement on timing of this activity was that it was not to take place when the recorders were powering the underwater connector, that is for 20 minutes every three hours. If the power were applied, the female connector on the recorder would be damaged, and data possibly missed (as well as requiring replacement of the connector). This method worked well, except that the dummy plugs were hard for the divers to handle without dropping, and should probably be attached with lanyards to the cables or some such safety feature in the future. Since leaving them at the site on lanyards would increase the movement and wear of any rubbing parts with the currents and waves, they were not attached, and the loss of several dummy plugs did occur during the several winter servicing cruises of the load cells and fish cage motion package.

The c-shaped hooks and how they hook over the load cell bars is shown in drawings in Figures 4.9 and 4.10. The c-shaped hooks are pushed over the bar, then slid away from the load cells to the left. Then they will stay there under the weight of gravity. The rubber pieces are the slipped down in to position to prevent the case from falling off (Figure 4.10 and 4.11). At this point, two bolts are screwed through holes in the steel bar, into the Delron pressure case mounting blocks to really secure the pressure case to the load cell strongback bar (Figure 11).

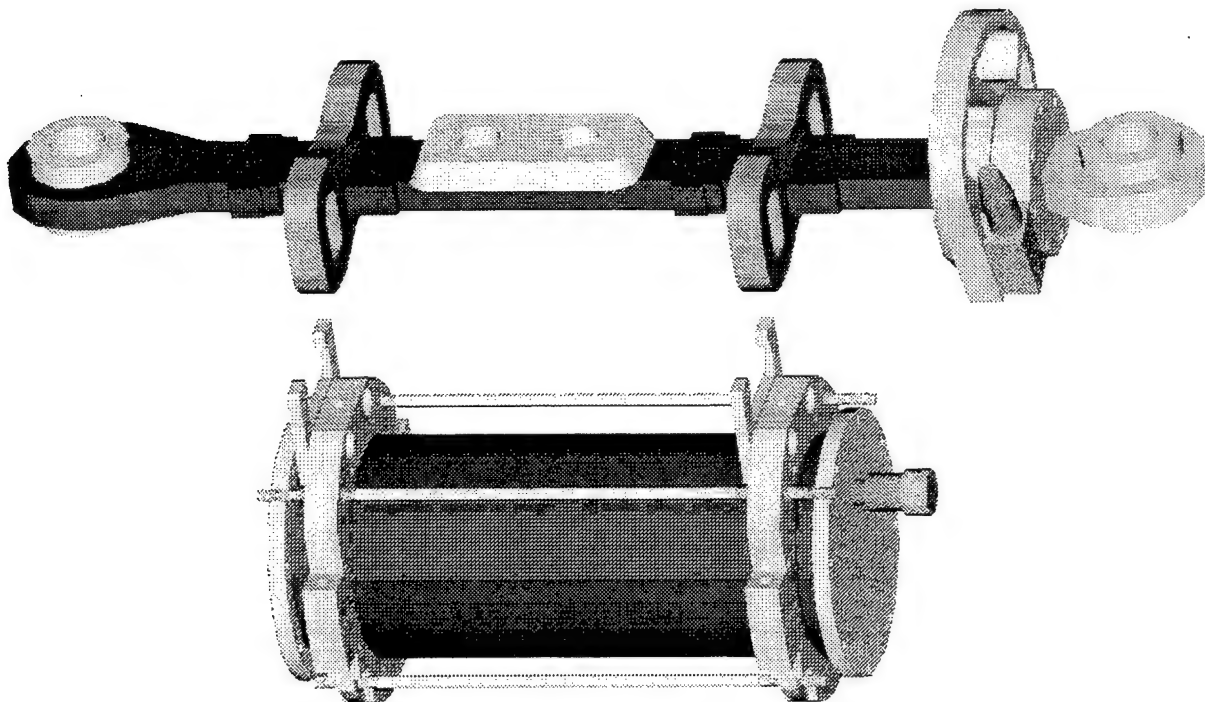


Figure 4.9. Schematic of the pressure case ready to mount on the load cell strongback. The two c-shaped hooks that slide over the bar can be seen. They are mounted on brackets that clamp around the PVC pressure case and held separated proper distance by stainless steel rods.

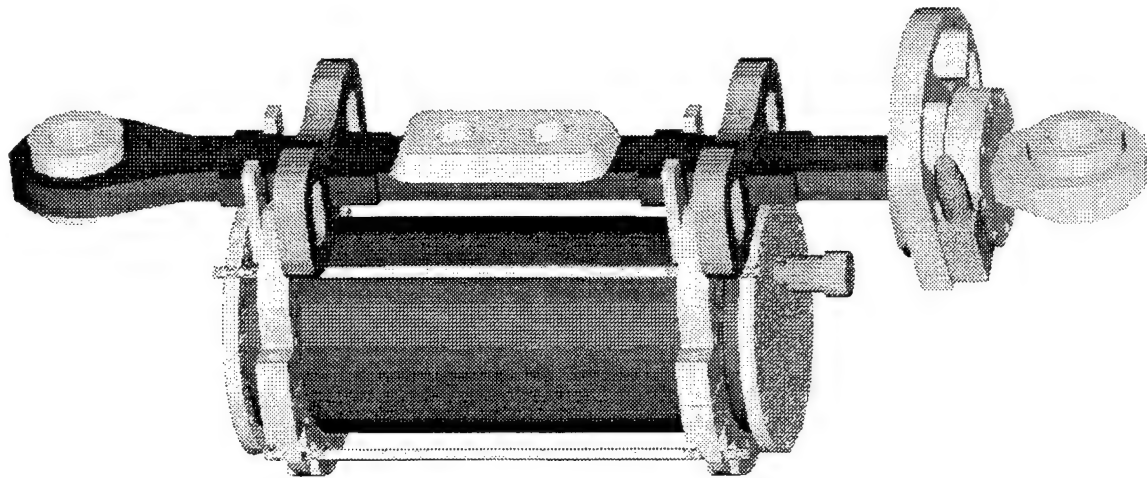


Figure 4.10. Schematic view of pressure case mounted in strongback. The c-shaped hooks have been slid into final position ready for the rubber blocks to be moved into place, and for the screws to be installed.

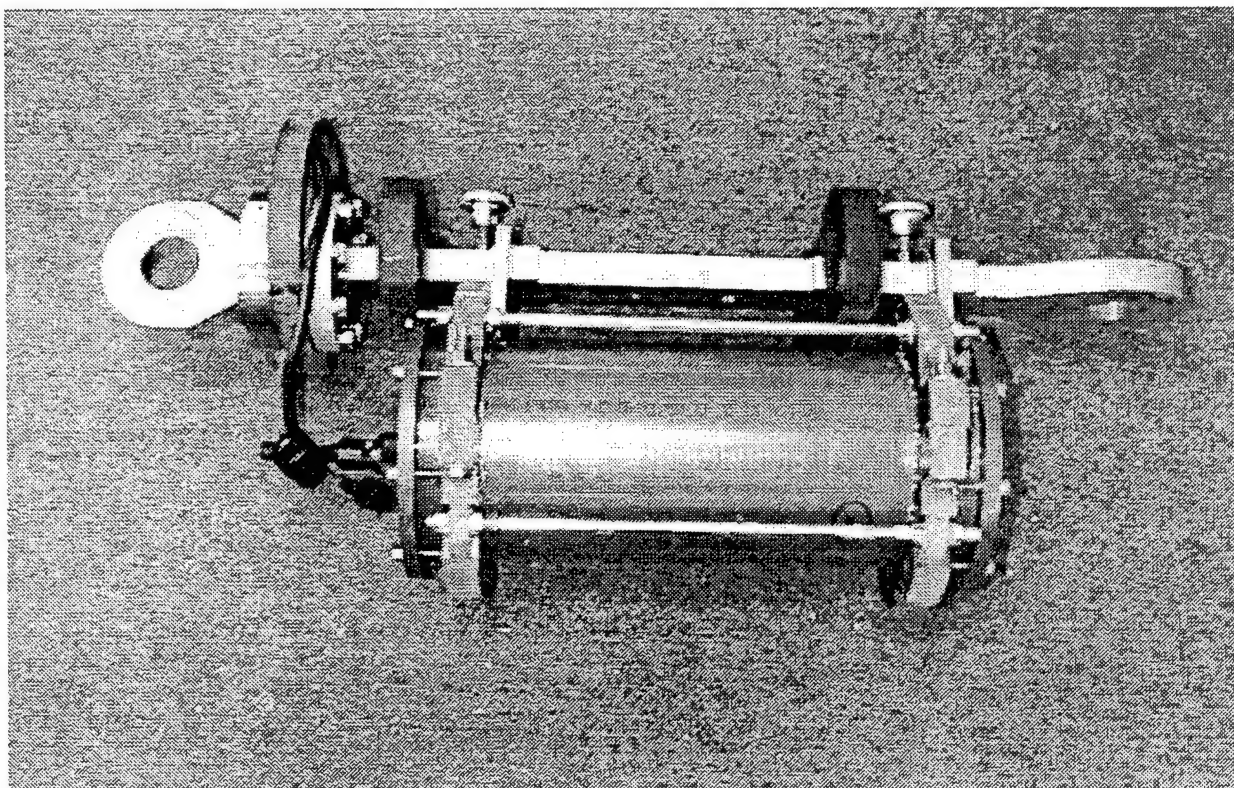


Figure 4.11. Photograph of the pressure case and load cell mounted on strongback with locking screws in place. The rubber holding blocks are not slipped into place in this picture. The load cell cable is run to the connector, but not plugged in nor properly attached to the strain relief and wire guard with tie wraps and tape. The hand screwed bolts are visible at the top.

4.2 Recorder

4.2.1 Persistor Controller/Recorder

The load cell recorder/controllers were constructed around a Persistor CF1, a Motorola 68CK338-based microcomputer, enhanced with an 8 channel 12 bit A/D, internal clock with backup power, low power circuitry, serial output and compact flash data storage media (Figure 4.12). A similar system was also used in a wave rider buoy and is described in Part 2. The CF1 system used compact flash cards of varying size for data storage, depending on the application. These cards are readily available at low cost due to their use in digital cameras. This program used cards between 48 and 128 MB to store the data for greater than 120 days between servicing. The single load cell recorders would last for about 5 months on a 48 MB card, and the four load cell recorder required 128 MB as it was recording 2.5 times the data. The four-month interval between servicing was specified by the UNH Ocean Engineers to match their fish cage maintenance and servicing plan.

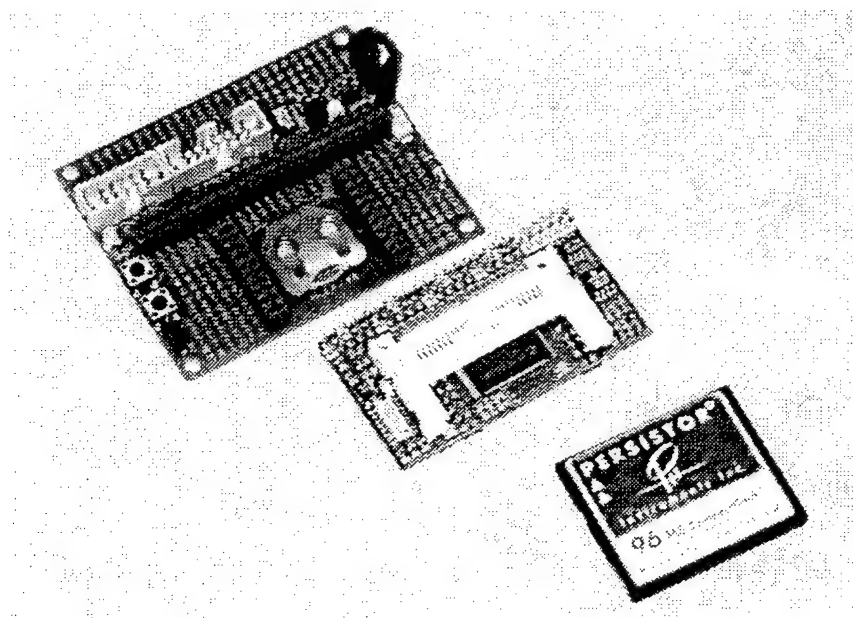


Figure 4.12. A Persistor microcontroller (center) with a 96 MB compact flash card (lower right) and a PicoDAQ A/D board with backup clock battery and connectors (upper left).

The Persistor CF1 systems run PicoDOS, which is a robust embedded version of DOS that provides many useful features and tools for the development of software. The Code Warrior C/C++ development system was used to write, compile, link and load the data collection and storage software. As CF1 systems were relatively new, some interaction with the manufacturer was necessary, and they responded quickly to assist in constructing the software sampling packages. The CF1 came with an extensive library of subroutines and examples, and with superb technical assistance by the Persistor staff to answer questions and get us going.

The basic controller board was supplemented by a PicoRecipe board (also from Persistor) that had power input filtering and protection, a serial port connector, the 8 channel 12 bit A/D chip and its input connector, a clock and RAM backup Lithium battery and spare space for some additional circuitry (Figure 4.12). This additional space was used for an FET switch to power

the load cells under software control. The PicoRecipe card also was a two-piece card with a second development board that could be broken off and used for additional user-developed circuitry to keep the footprint of the package small, or left as delivered for a larger, lower data system configuration. This additional card was populated with a diode protection circuit for the six parallel battery packs and the battery connector (see Figure 4.13) [see Appendix 9.1.1].

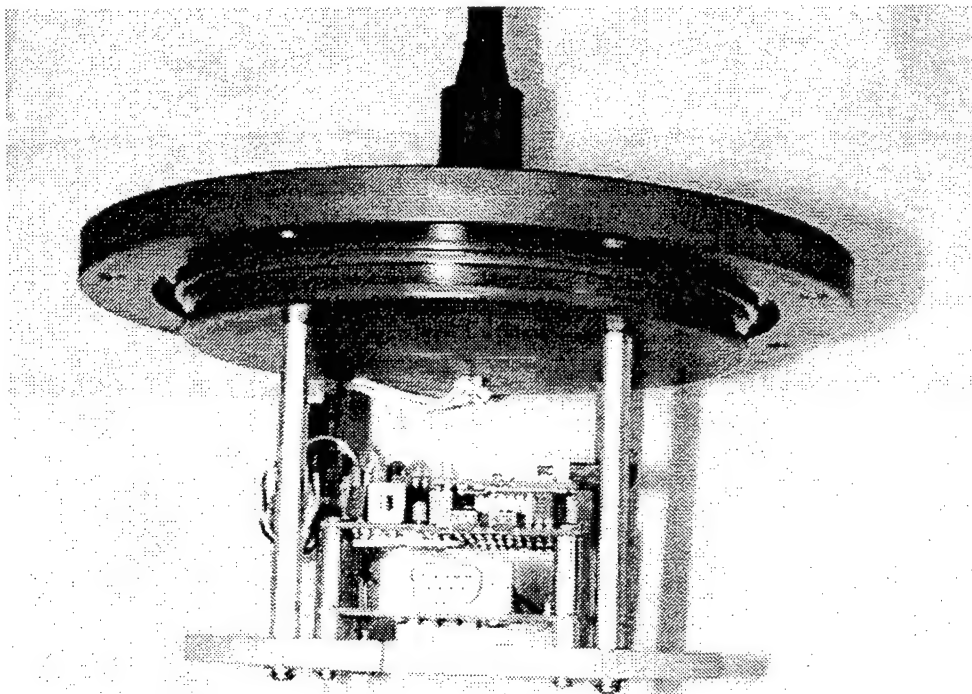


Figure 4.13. The load cell recording electronics mounted to the end cap of the recorder pressure case. The top board is the Persistor CF1 with compact flash card, the middle board has the PicoDAQ A/D with battery backup and an FET switch to control the battery power to the load cell, and the bottom board is a six-diode array and plug for battery power input.

The Persistor CF1 and PicoRecipe Card draw less than 20 ma of current when sampling, depending on the application, and have several low power modes to conserve overall energy. This low power drain coupled with the computational, I/O, interrupt and A/D capabilities, made the unit ideal for this application. The A/D operates over the Motorola QSPI interface and routines for its use were provided by Persistor. The low power wakeup was accomplished with the on-chip periodic timer interrupt (PIT), which is built into the 68338 chip. The CF1 has more than 20 pins that can be used for general purpose I/O if they are not used for other functions. There were often useful for power switching and debugging. One logic line was used to control the power switching FET to power up and down the load cell and amplifier under software control [see appendix 9.1.1].

We used one of the simplest low power modes, and brought the sleep mode current down to 1 ma. The only problem we have had with these systems is when a solder flake shorted a logic line to the 12-volt battery, and burned out some circuitry in the microcomputer, causing the

standby current drain to jump to 40 ma. The rest of the system continued to work, but the power consumption was up because the logic line was midway between Vcc and Vdd with both sides conducting current.

The flash card data storage has also proven to be very reliable. A SanDisk USB port flash card interface, and alternatively a flash-to-PCMCIA adaptor, were used to plug the flash card into a notebook computer that was then networked to another computer with CD-ROM writer to backup the data. The data was stored on both computers and CD-ROM before the data was erased from the flash card for the next deployment. We overcame the drawback that under PicoDOS the number of files that can be written to the flash card under the root directory is limited to 511, by making a subdirectory called L1 (for load cell recorder number 1), or L2, or L3, or L5 (for the 4 load cell recorder). The files could then be dynamically allocated, and any number could be used. In the second deployment in 2001, the three single load cell systems ran for 5 months and saved 1,233 files each on 48 MB flash cards. The systems did not have a catastrophic failure after the flash cards filled, but instead continued to operate despite not being able to write the data to files.

For identification of the files and the time of sampling, the file name was made up of the load cell recorder ID, the month, the day and hour. Thus, for recorder 3, on January 23 at 1800 UTC, the file name would be L3012318.dat. As the records started on the hour and lasted for 20 minutes, this was an unambiguous scheme that put a time stamp on each record. The file name was constructed by using the Persistor real-time clock to give day, month and hour. This approach, initially used in a scanning sonar system (Irish et al., 1999) and now in the Persisor CF1 based systems, has worked well, and is also being used in the motion package and the wave rider buoy (see Parts 2 and 3 below).

The real-time clock was also used to control the sampling program. The system was programmed to sleep for one minute, then wake up, check the time and look for the three-hour start time. If the time were not appropriate for the start of the sample, the system would then revert to low power mode for another minute. When the selected minute of the three-hour arrived, the system would start, power up the load cell, open the file with the proper name, and sample the data, writing it to the flash media. When the record was done, the system would go back into its low power mode. This system worked well, and allowed simple control of the sampling.

The recorders and batteries were placed in the pressure case and firm foam padding inserted to prevent battery movement. The Persistor based data system was mounted on a plate that was attached to the end cap (Figure 4.13), so that the electronics was separated from the battery by this plate. The plate had cutouts on four sides, so that the battery cable could be run past the plate to plug into the electronics diode board (Figure 4.14 and 4.15). Figure 4.14 shows the battery in the bottom of the pressure case, with foam packing in place to prevent movement. The recorder on the end cap is in position ready to plug in the power with the notches in the electronics plate clearly visible. Figure 4.15 shows the system with the power plugged in. The system could then be closed and deployed. In this case, a serial communications cable was plugged into the CF1, the time checked, the flash card checked (no files present, and the proper subdirectory name on the flash card), and the first few diagnostic printouts from the 1-minute wakeups were monitored to assure that the system was operating properly. Then the system was closed and readied for deployment.

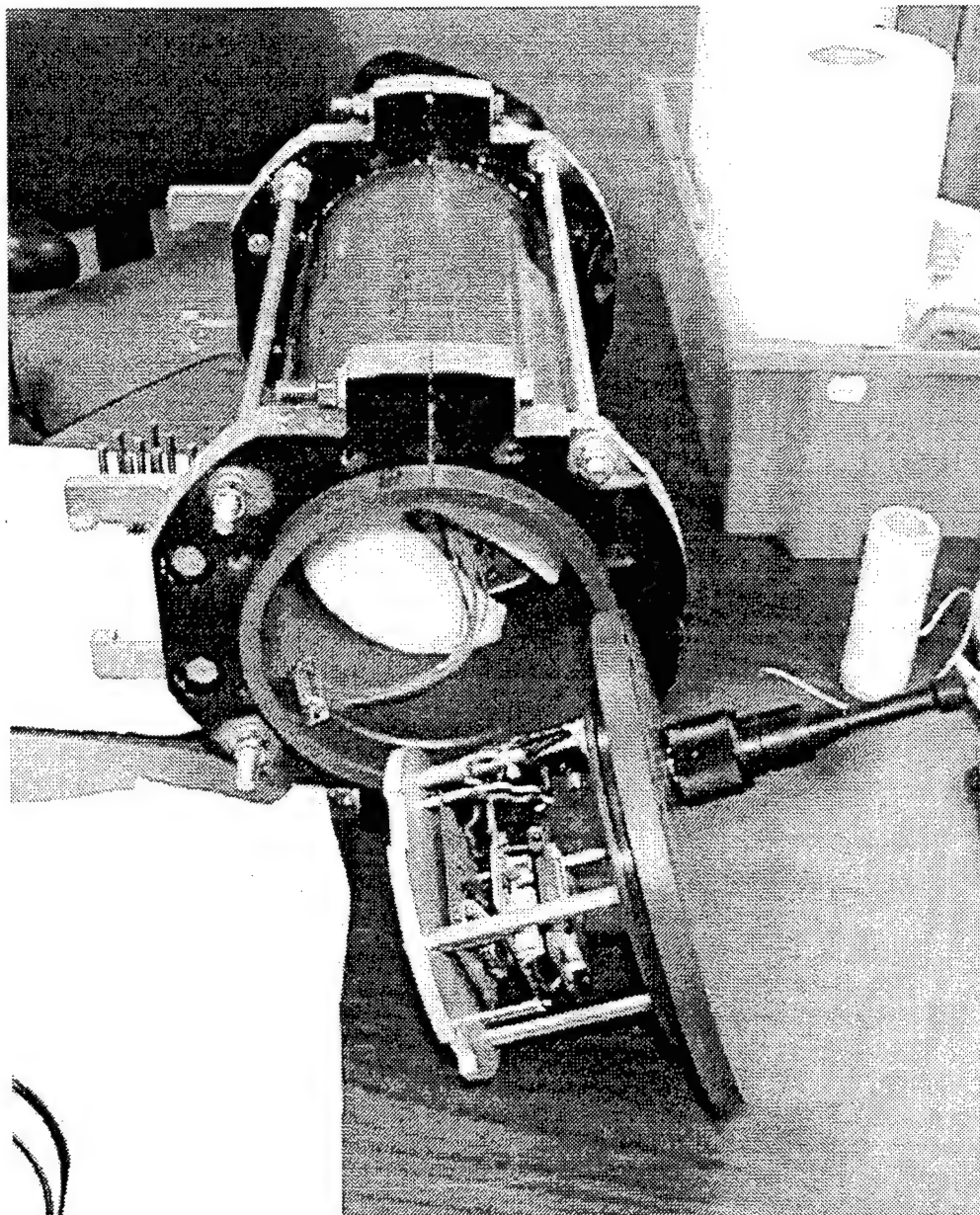


Figure 4.14. The battery pack in the pressure case, the foam spacer in place, ready to plug the battery into the electronics and start the system.

4.2.2 Sampling Plan, Software and Power

The sampling plan for the load cell recorders was coordinated with the motion package and wave rider buoy. The wave field changes statistics on about a 3-hour time scale, so that was selected for the burst interval for all instrumentation. To resolve the highest frequency waves without aliasing with the low-pass filter on the wave rider accelerometer and in the fish cage motion package, a 10 Hz sampling frequency was optimum. To obtain a record long enough to get good statistics of the wave field, a 20-minute burst was selected. However, for simplicity in the first sampling programs written for the three single load cell recorders, a smaller burst was required to fit in memory so the sampling rate was reduced to 8 Hz instead of 10. The four load cell recording system required software to record "on the fly" and a full 20 minute sample at 10

Hz was collected to be compatible with the wave rider and fish cage motion package (see below).

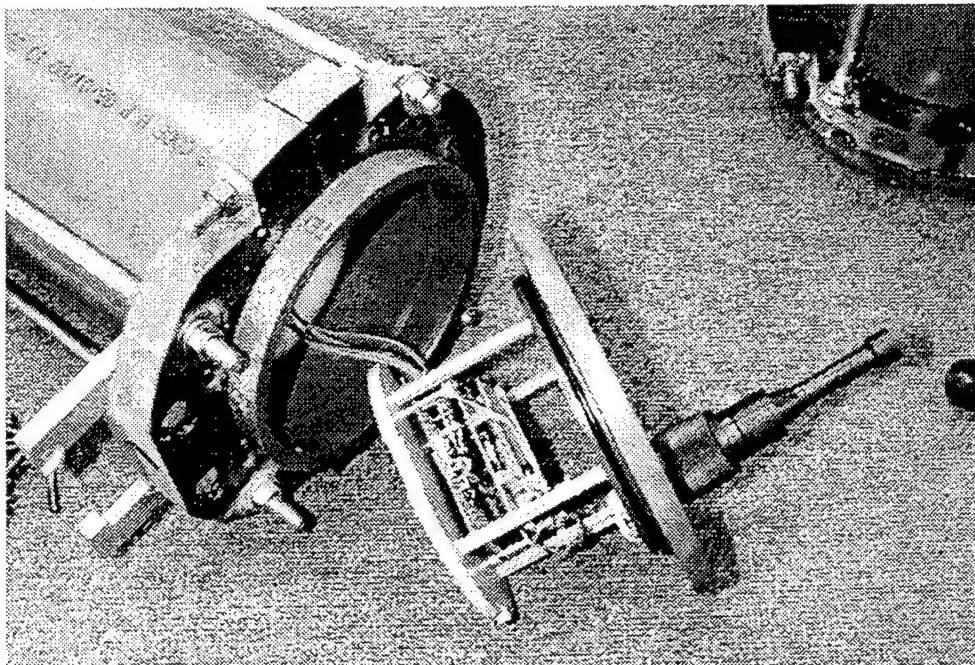


Figure 4.15. The electronics plugged into the battery pack in the pressure case ready to assemble. This configuration allows a computer to be plugged into the Persistor CF1 data system to check the system time and the flash card before the case is closed.

Due to time constraints to get the load cells into the water when the fish cage mooring was being serviced in the summer of 2000, the estimated power required for the system for a 4 month deployment was made before the data systems and load cells were delivered and so could be measured. The pressure cases had to be designed, material acquired and machined, the strongbacks and load cell mounting designed and constructed and the whole mechanical system made diver friendly for servicing. The power requirement estimates with a 50% safety factor suggested a battery pack of six parallel stacks of 8 alkaline "D" cells each would last over 4 months. However, after assembly and testing, it became apparent that we had significantly overestimated the amount of power required to write to the flash cards. During the single load cell deployments, the battery packs were down about 30% after a 10-months. This implies that the 48-cell battery pack could last for more than two years! However, the four-load cell system, since it powers four load cells and has to write more data to compact flash media, would not last a year, but would easily last for more than 4 months. This system also had a 128 MB flash card to store the additional data. Therefore, power was not a major problem, and the single load cell systems could be set to burst sample each hour, deployed for 5 months, fill the flash card memory and still have power remaining.

The firmware for the Persistor CF1 sampling program was loaded into RAM for testing and evaluation, during the development period. When the program was completed and tested, it was "burned" into on-board flash EEPROM memory for deployment. This allowed the systems to be set up, so that one could set the time, unplug the battery and wait for deployment. The on-board battery would keep the clock going, and when the main battery was plugged in, the system would wake and automatically go into its sampling program without any initialization being

required. This feature was not used in the first year at the OOA site, but would be an advantage when instrumentation was being delivered to others who would deploy it when they were able to obtain a weather window.

4.3 Northeast Corner Assembly

4.3.1 Load Cell and Mooring Line Assembly at Grid Corner

The Northeast corner of the mooring was of interest because that is the side that the severe Northeast storms would come from, and from which the largest waves should be seen (Panchang et al., 1990). Therefore, in addition to the load cell on the anchor line, additional load cells were placed on the two grid lines and the lower bridle line to the cage (Figure 4.1). Figure 4.16 shows the layout of these four load cells and how they were shackled onto the grid corner ring. The 37" flotation sphere that supported the anchor lines and grid ring was attached to the center of this ring by a section of 3/4" chain (Fredriksson et al., 2000). This assembly can be seen deployed in Figure 4.17 with the chain going up out of the picture to the float. A detailed discussion of the assembly and deployment of the mooring and the Northeast grid corner is given in Irish et al., 2001a.

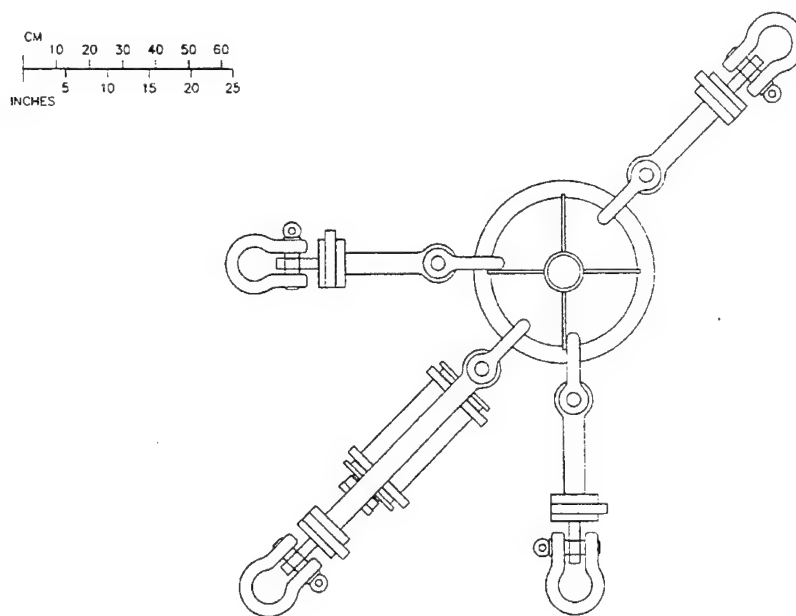


Figure 4.16. Top view sketch of the four load cells mounted on the Northeast corner ring. The top right load cell is attached to the anchorline, the bottom left to the fish cage mooring riser line and the other two to the grid lines. The recorder system is mounted on the load cell to the riser line with an electrical cable running to the fish cage.

It was found during the installation of the Northern net cage in August of 2000 that there was significant movement and some tangling of the ropes connecting the grid corner rings. The movement during the deployment operations was in response to current force, but later it also included movement due to wave forces. The modeling of the fish cage motion (Tsukrov et al.,

2000) indicated horizontal movement and tilt of the fish cage cause relative movement and even slack in some of the lines. Therefore, the four heavy load cell packages at the NE grid corner rings need to move on the grid ring in response to the movements of the mooring and fish cage. Insufficient electrical cable lengths between the four load cells and recorder at the NE mooring corner in response to this movement would pull or abrade the conductor cable (as may have occurred in March 2001, see below). Figure 4.16 shows the design position of the load cells around the Northeast grid corner, and Figure 4.18 shows some of the possible position variations of same load cells under slack conditions.



Figure 4.17. A picture of the Northeast corner with four load cells attached to the corner ring shown schematically in Figure 4.16. The bridle line to the fish cage is in the foreground, the two grid lines are on the right and left and the anchor line in the background by the diver. The grid corner float is above on the chain. The load cell wire guard can be seen at the bottom of the picture. (Picture by Glen Rice, UNH).

4.3.2 Northeast Corner Telemetry Link

The Northeast corner measurements were important to the program, so it was decided to telemeter the load cell data from the four load cell recorder to shore for analysis and input into the fish cage management program. This involved four components: (1) additional telemetry electronics in the load cell recorder as well as the additional software that was borrowed from the wave rider buoy (see Part 2 below), (2) a wire running up the lower and upper bridle lines from the recorder to the fish cage, (3) a spread spectrum radio on the fish cage (which was to be at the surface), and (4) mounting of the radio and antenna on the fish cage with solar powered battery and wave protection. Most of the work discussed was completed, but the full telemetry link was not implement because of several problems discussed below.

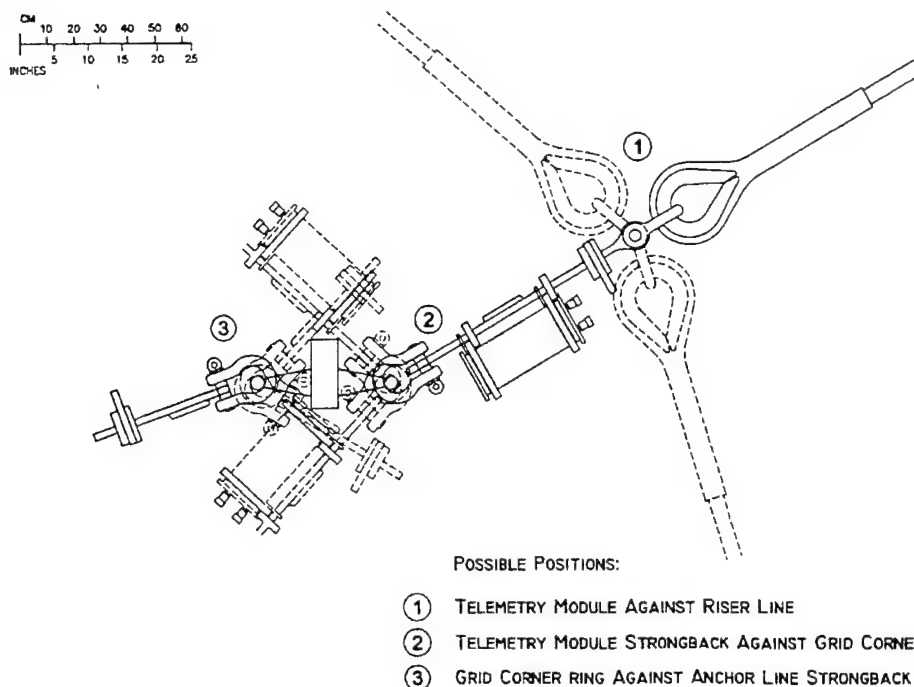


Figure 4.18. The electrical cables connecting the electronics to the load cells need enough slack and abrasion resistance to allow all possible movement of the load cells, anchor, grid, and lower bridle lines.

4.3.2.1 Telemetry Component in the Load Cell Recorder: The load cell recorder system was easily capable of waking up at a prescribed time and sending the data recorded in the last file out the serial port of the Persistor. This is the software component designed and tested for the wave rider buoy (see Part 2 below). This addition was easily implemented and then additional electronics was required for sending the data up the cable (see below) to the fish cage, connection and powering up the radio and telemetering the data to shore. Initial discussions were related to using another telemetry buoy similar to the wave rider for this purpose, and to recharge batteries in the recorder down the cable. However, after a study of the dynamics of the system and the scope of the buoy and relationship with the cage, this concept was abandoned, and the wire up the rope adopted. The telemetry buoy would have potentially tangled with the bridle line and flounder plate (see geometry of mooring in Irish, et al, 2001a).

In addition to sending the data up a wire, the trick is to do this in such a way as not to jeopardize the load cells or recorder if a problem were to occur in the telemetry link. A special circuit was built that electrically isolates the telemetry link from the rest of load cell recorder (Figure 4.19) [see Appendix 9.1.2 for schematic]. This circuitry also has drivers for the RS232 serial data lines. Normally this protocol would not be used over this distance, but the more robust RS422 or RS485 would be used. However, as WHOI has build drivers that are capable of transmitting RS232 over the couple hundred meters of cable used here, and the systems on each end of the wire were set up for RS232 (and not RS433 or RS485), it was decided to use this technology. Figure 4.19 shows the PC boards made for this application with the transmitting electronics in the board on the left what is in the physical format to go in the Persistor stack (Figure 4.20) [see appendix 9.1.2].

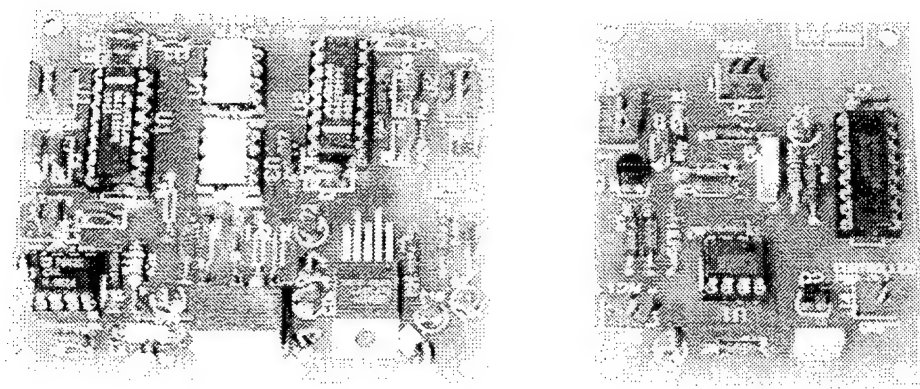


Figure 4.19. Telemetry electronics to send serial RS232 data up the cable from Persistor data system, isolating the telemetered signal from the data system and load cells. The electronics at the left goes in the four load cell recorder (Figure 4.20). The electronics at right receives the RS232 signal, turns on the spread spectrum radio (Figure 4.25) and passes the serial data to it for transmission to shore.

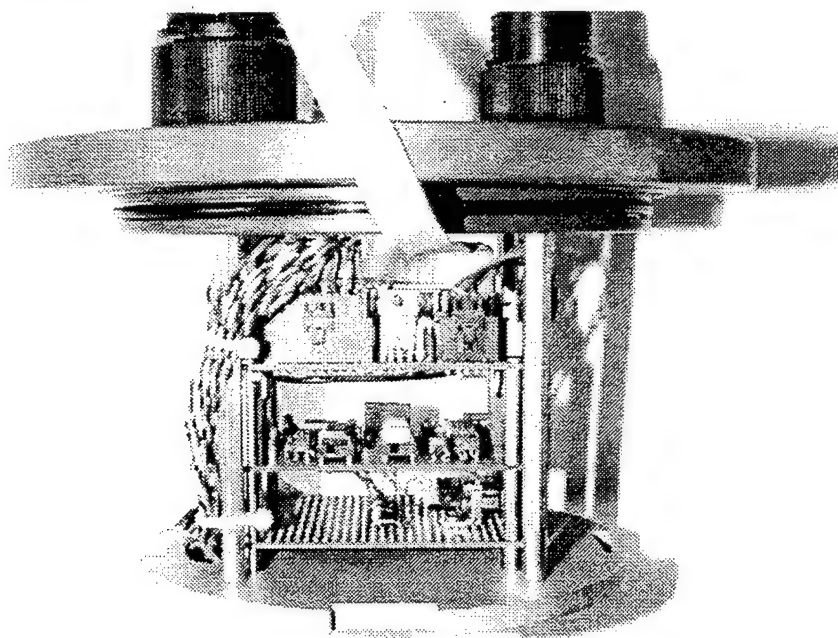


Figure 4.21. Four load cell recorder electronics. A 8 pin underwater connector (partially visible on the left top of end cap) connects with the load cells. The set of 5 twisted pair of wires seen at the left of the package connects the load cells with the A/D connector on the data system. The ribbon connector going out the top is the standard RS232 serial data port to a computer for system initialization (removed for deployment). The power switch in the middle of the top board controls power to the load cells. The connector at the top right provides power and signals to the telemetry board (Figure 4.19 left) in the middle of the stack. The diodes and connector to the battery pack can be seen on the bottom board. The connector on the right top, is the telemetry cable to the surface up the bridle lines.

4.3.2.2Electrical Conductor on Mooring Rope: An electrical connection was required between the load cell recorder located at the Northeast grid corner ring, and the spread spectrum telemetry module mounted on the fish cage central spar. The conductors were attached to two ropes in the mooring. An underwater matable connector allowed the two ropes to be deployed separately. The electrical cable runs along the 103-foot *lower bridle line* to the flounder plate, and then one 36-foot long leg of the *bridle line* to the fish cage (for mooring configuration see Figure 3.1, Fredriksson et al, 2000 and Irish et al., 2001a). The attachment of the conductor to the mooring rope was done at WHOI after antifouling material had been applied. The lower bridle line measured 2¼ inch in diameter, and was of eight-strand plaited construction. The rope was manufactured from a copolymer polyolefin fiber material by The American Group, and is sold under the trade name "Blue Steel." Puget Sound Rope manufactured the upper bridle line, a twelve-strand braid allegedly from polyester fibers, measuring about 1.22 inch in diameter. The nominal diameters of these two ropes were 48 mm (1-7/8 inch) and 24 mm (~1.0 inch) respectively (Muller, 1999).

A problem with attaching electrical cables to ropes which have a greater stretch capability, is how to stretch the rope and the cable without fatiguing the copper wire to the breaking point. Copper has only 0.5 percent or less of elastic elongation. Since all fiber ropes stretch considerably more under working loads, special configurations of conductors and rope have to be made in order to not overstretch, yield and thereby quickly destroy the electrical conductors. Spiraling the conductor cable around the rope solves this problem, but the correct wrap angle range for the conductors is critical. A helical configuration can extend its length by reducing its wrap diameter and thereby increasing its pitch length without stretching the length of conductor cable axis itself. This technique is used in the design of telephone hand set coil cords.

The larger the wrap angle, measured between conductor cable and rope axis, the easier the coiled conductor cable can be stretched. The smaller the conductor cable, compared to the rope diameter around which it is wrapped, the easier can it be stretched. Finally, the more the center rope contracts when elongated under tension, the easier it is for the spiraled conductor to extend. In order to establish the appropriate *zero stretch wrap angle*, the contraction of the bridle ropes' diameters at known stretch levels had to be found.

As a first step in determining the stress-strain relationship of the fish cage mooring lines, the amount of diameter contraction of the ropes at different load and stretch levels had to be measured. Each rope length was tensioned, using a forklift at one end and a bollard on the WHOI dock on the other. A load cell measured the amount of applied tension (the forklift could pull up to a maximum of 5000 lb.). At each tension level, the length of a marked distance along the rope axis was recorded, and the rope circumference at two distinct locations was measured (Figure 4.21). The Poisson Ratio, μ , is the ratio of the rope's circumference contraction to its axial strain (or rope contraction/rope stretch)¹.

¹ The rope contraction at a given load level is the reduction in rope circumference divided by the circumference measured under a small nominal pretension. The rope strain is the length increase of a marked rope section divided by the marked length at the nominal pretension. In some cases the *inverse* of the Poisson Ratio μ is used. It is called the Poisson Number n or v (= axial strain / lateral contraction). This can be confusing when comparing data.

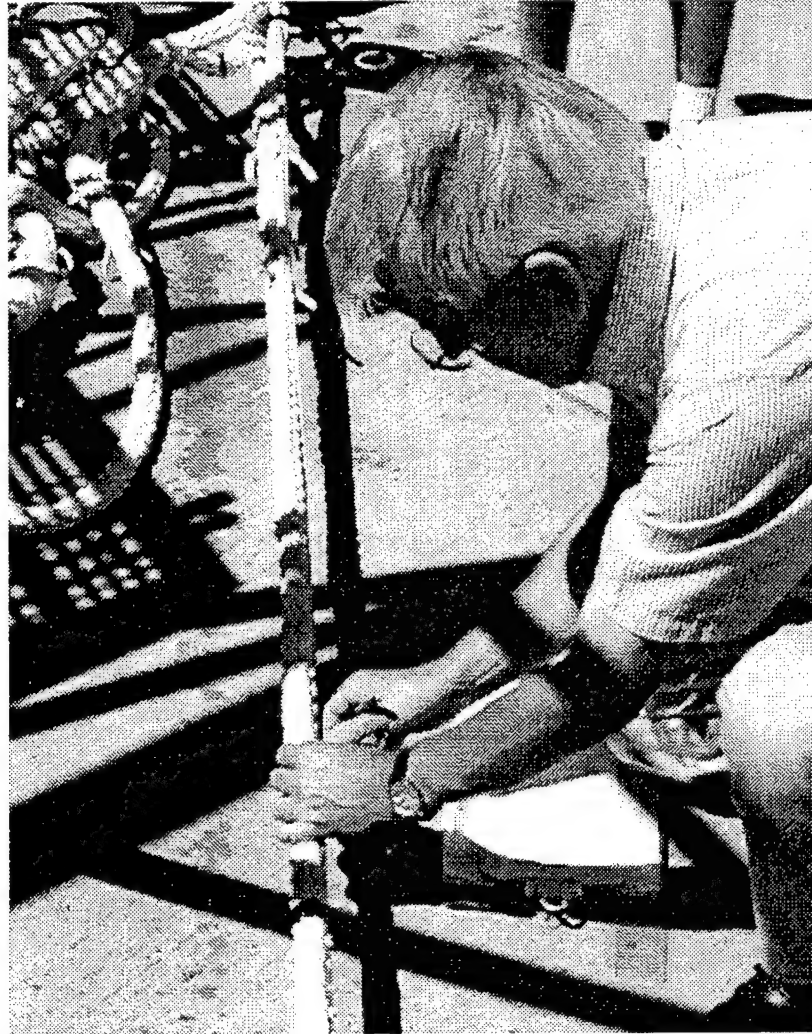


Figure 4.21. Walter Paul measures the circumference and stretch of the upper bridle rope to determine its Poisson's ratio. The black tape in front of his hand is one point for measuring the amount of elongation with tension.

Fiber ropes contract considerably more when stretched than metals due to their construction with a large number of soft textile fibers with significant amounts of air voids in the rope cross section. Poisson Ratios of metals are typically in a range of 0.23 to 0.33 (steel). Poisson Ratios for fiber ropes are between 0.5 and 2.5; or fiber ropes under tension and axial stretch contract laterally 1.5 to almost 11 times more than a piece of metal. The larger the numerical value of the rope's Poisson Ratio, the softer and more compressible is the rope under tension². The softer the rope structure, the easier it is for the spiraled conductor cable's wrap diameter to contract and thereby to increase its pitch length without stretching the copper conductors³.

² New, not yet tensioned ropes have larger Poisson Ratios than used ropes. In used ropes the fibers, yarns, and strands in the rope structure have contracted and compacted due to the applied tensions.

³ Used ropes have a more compact cross section and less elastic stretch, since initial tensioning has set and compressed the fiber assemblies. Used ropes are also longer due to the compacting process under load. The determination of the correct conductor wrap angle has to put these effects into consideration.

The average Poisson Ratio ranges for the *lower bridle line* was determined to be 1.296 (with a range of 0.785 to 1.427). A Poisson Ratio between 1.39 and 2.26 was measured in tests of the *upper bridle line*; its average value was 1.825. With known Poisson Ratios the stretch neutral wrap angle can be determined for each rope. The basic geometry of a conductor cable spiraled around a rope core is shown in Figure 4.22 and is used to create equations to determine the stretch neutral wrap angle (Paul, 2001).

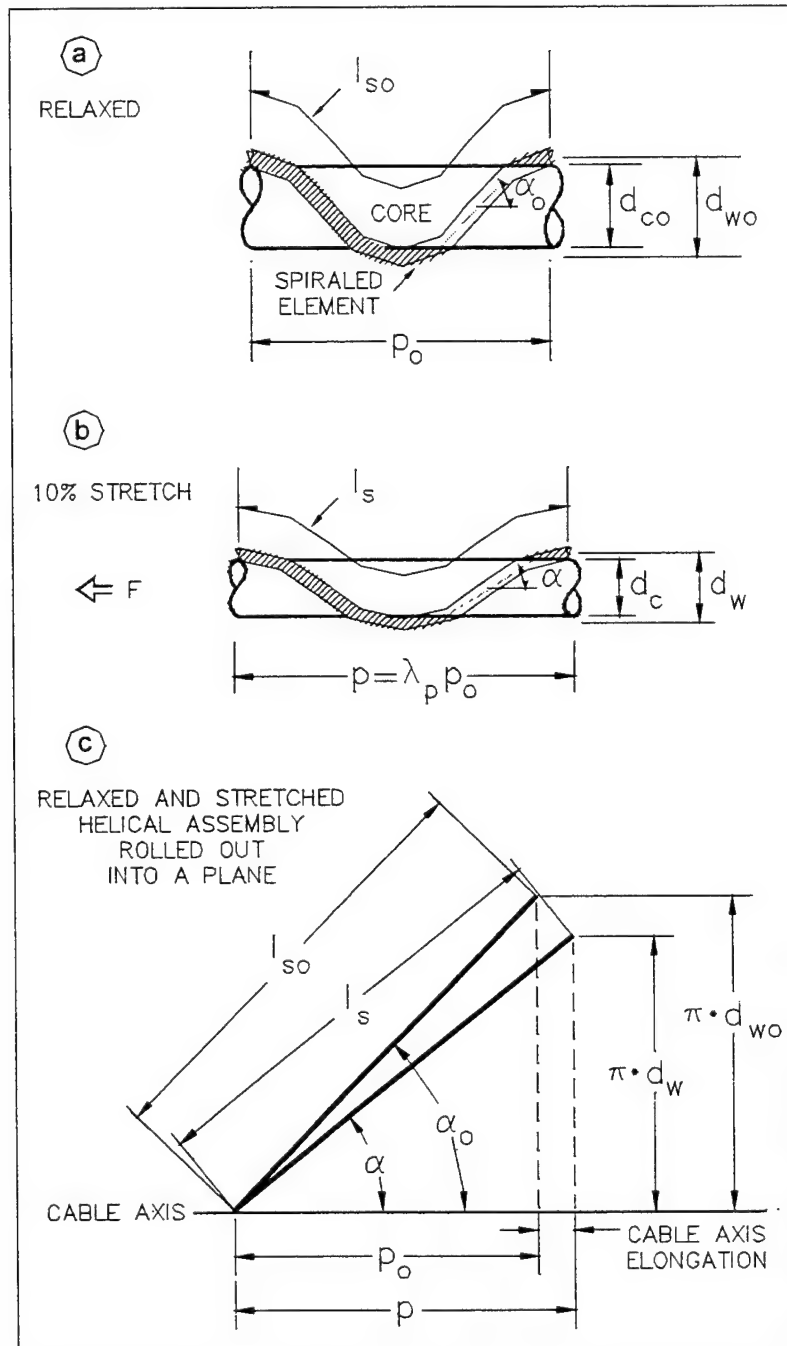


Figure 4.22. Spiraled Element wrapped around Compliant Core

The calculations simplify through the introduction of a stretch ratio $\lambda_p = p/p_0$ for the rope axis lengths; a stretch ratio for the conductor lengths $\lambda_s = l_s/l_{s0}$ ⁴; comparing the stretched and unstretched rope and conductor lengths⁵ (Figure 4.22). It is also helpful to use a ratio $k =$ conductor cable diameter divided by the unstretched rope core diameter [$k = d_e / d_{co}$], defining the basic geometric setup of the conductor rope.

The stretch neutral wrap angle α_0 can be calculated as (Paul, 1995):

$$\cos^2 \alpha_0 = (B^2 - A^2) / (\lambda_p^2 \times B^2 - A^2),$$

where: $B = (1 + k)$, $A = [1 + k - (\lambda_p - 1) \times \mu]$, and:

$(\lambda_p - 1)$ the conductor rope's axial strain [$= (p - p_0) / p_0$ in Figure 4.22 (C)].

Figure 4.23 shows examples or calculated stretch neutral wrap angle α_0 results for k values between 0.1 and 1.0, and values of 0.3 to 1.0 for the Poisson Ratio μ . While large wrap angles are required for steel ($\mu = 0.3$), the wrap angles for more compressible fiber ropes near the bottom of Figure 4.23 become more manageable. Small conductors relative to the rope core size (small k values) help to reduce the wrap angle as well. It is seen that even for high conductor rope stretches a suitable stretch neutral wrap angle for the conductor can be found. The conductor wrap angles α_0 and wrapping details were determined for the lower bridle rope and for the upper bridle line with the above equation and are listed in Table 4.1.

Table 4.1. Conductor Cable Wrap Details for Lower and Upper Bridle Lines

(1) Cage Mooring Rope	(2) Poisson Ratio Measured	(3) Conductor Dia. Rope Core Dia. = k	(4) Cable Wrap Diameter [inch]	(5) Calculated Wrap Angle ϕ_0 [degrees]	(6) Pitch Length of Cable Spiral $P_0 = \pi \times (4) / \tan (5)$ [inch]	(7) Conductor Length l_s per Pitch Length $l_{s0} = \pi \times (4) / \sin (5)$ [inch]	(8) Total Conductor Length = Rope Length $\times (7)/(6)$ [ft] **)
Lower Bridle Line 103 ft long	Min. 0.785*)	0.22	2.75	Max.: 51.7*)	Min.: 6.83*)	Min.: 11.0 *)	166*)
	Max. 1.427			Min.: 44.2	Max.: 8.88	Max.: 12.4	143
	Avg. 1.296			Avg. 46.2	Avg. 8.28	Avg. 12.0	149
Upper Bridle Line, 34.5 ft long	Min. 1.39	0.5	1.5	Max.: 46.3	Min.: 4.50	Min.: 6.52	50
	Max. 2.26			Min.: 39.7	Max.: 5.68	Max.: 7.38	45
	Avg. 1.83			Avg. 42.5	Avg.: 5.14	Avg.: 6.98	47

Notes: *) Measurement compromised due to previous tensioning
 **) Long "Pigtails" were added at each end to provide sufficient cable lengths at each termination during deployment, retrieval, and slack conditions in service, including lengths to bridge space taken up by load cell assemblies

⁴ The calculations are performed here assuming zero axial stretch of the conductor length, or $\lambda_s = 1.0$ since $l_s = l_{s0}$.

⁵ The subscript ₀ identifies the unstretched length dimension (or a not contracted diameter or wrap angle), in the stretched or contracted condition the subscript is omitted.

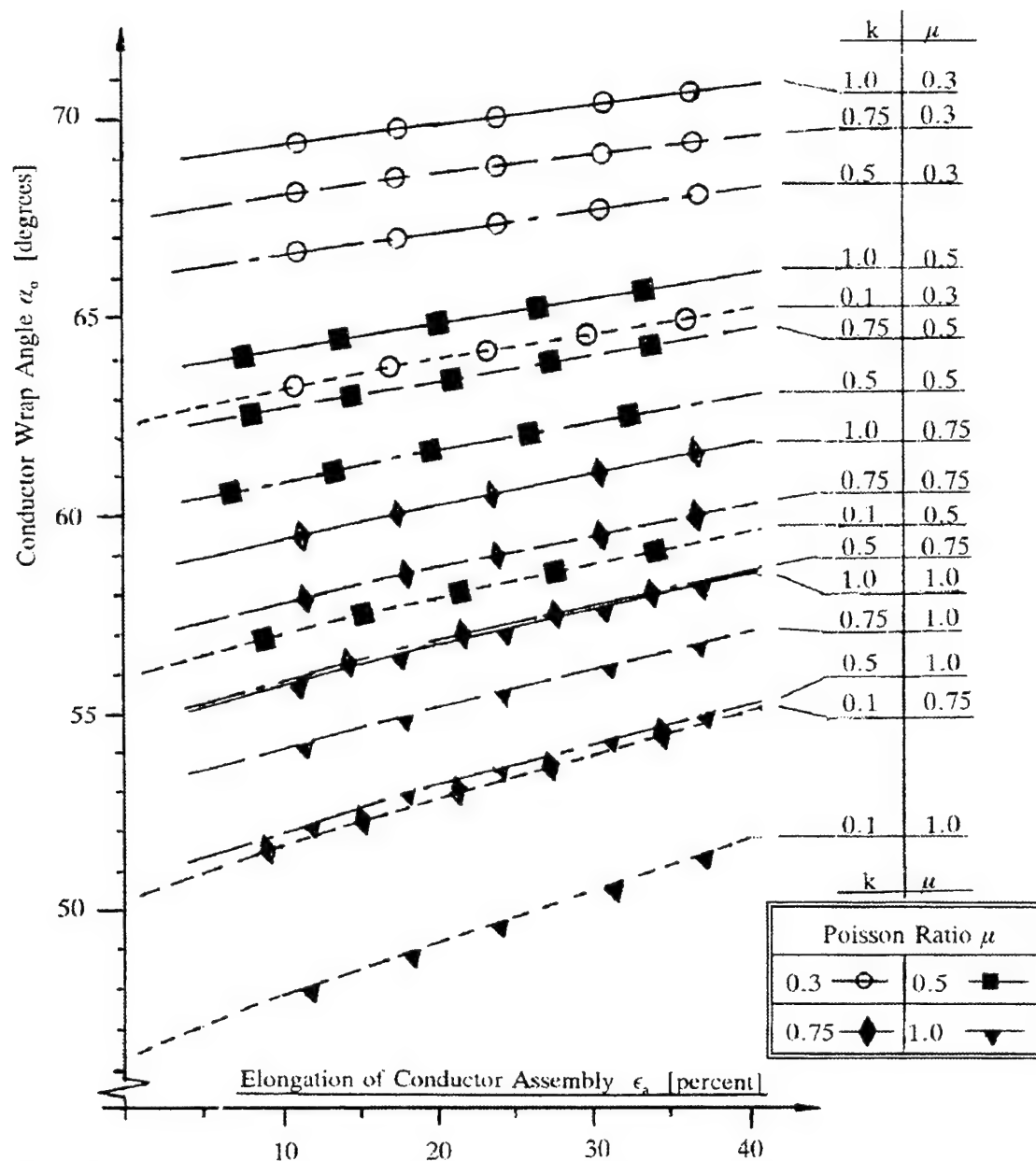


Figure 4.24. Stretch Neutral Wrap Angle Versus Conductor Rope Stretch

A sufficient length of conductor cable for the two bridle lines each rope was prepared following the data of column (8) in Table 4.1. The conductor cable has to be spiraled within fairly close limits of pitch length and wrap angle, in order to provide a near stretch neutral conductor path along the rope axis. A simple measuring template was made from cardboard for each rope. The gauge is long enough to span 4 to 5 wraps with cutouts positioned the required pitch length apart in order to assure that each wrap of the spiraled conductor cable is located within the required pitch length tolerance and stretch neutral wrap angle ϕ_0 along the rope axis.

Crewmembers of the F/V *Nobska* applied and secured the electrical cable along the bridle line ropes. The center of the conductor cable was positioned at the center of the stretched out and tensioned bridle rope and secured with suitable braided tying twine. The tying twine is made

from untreated “virgin” Nylon.⁶ The cable spiraling started from there towards each rope end by hand⁷, and at each full wrap the cable was secured to the center rope with the twine. It is easy to apply the cable with a slight slack during spiraling, which will help to assure that the copper conductors will not be overstretched. Sufficient cable at each rope end was left to allow pigtails needed to allow for the free movement of the load cell packages near the NE grid corner and the potential positions if the cage mooring experiences local slack and snap conditions due to sea state and current effects. The lower bridle rope with the spiraled and hitched conductor cable is shown in Figure 4.24.

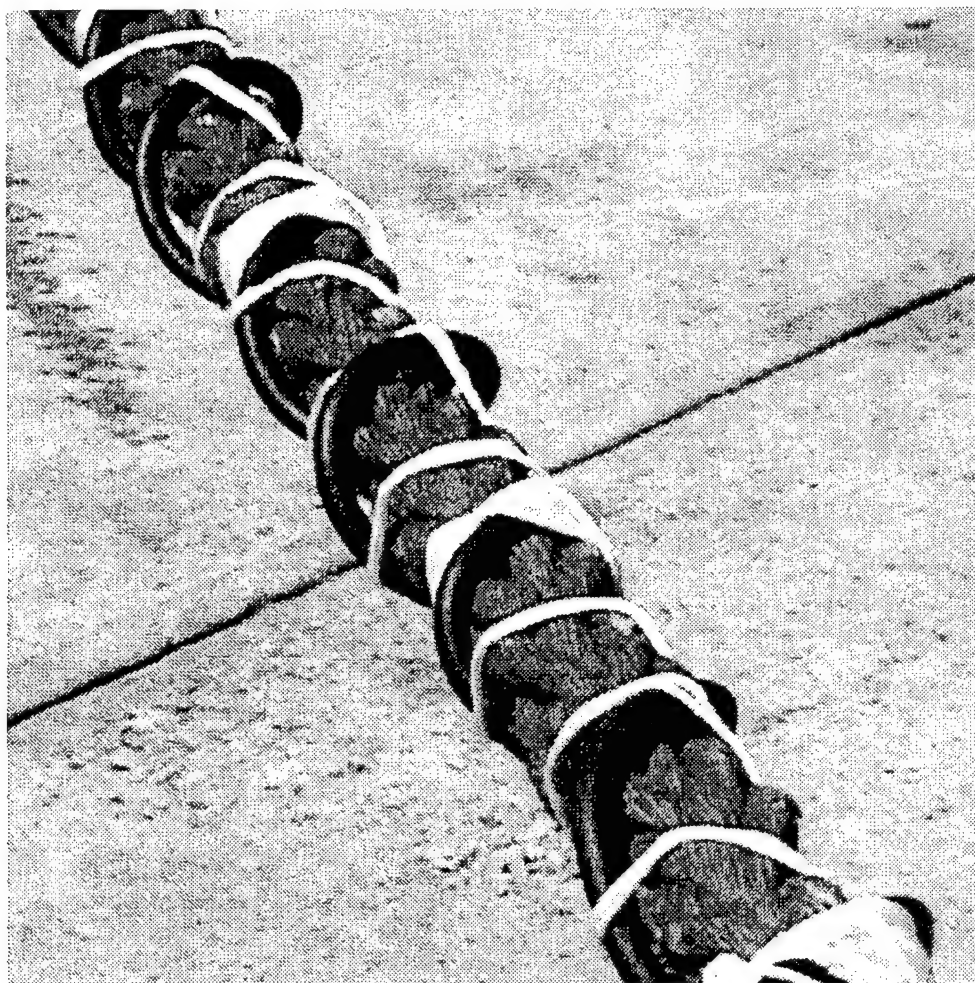


Figure 4.24. The photo shows the dark electrical cable helixed around the Lower Bridle rope. The position of the wrapped conductor cable was secured with “virgin” Nylon fish twine by crewmembers of the FV Nobska. An outer layer of polypropylene rope was hitched around the assembly for abrasion protection after this picture was taken.

⁶ Twines from virgin (untreated) nylon material will shrink and swell permanently once exposed to wet conditions, and thereby tighten and maintain the conductors in their position on the rope. The twines have enough retraction that they will maintain a tight grip of the conductors on the rope, when the rope stretches and contracts under applied tension.

⁷ Each half of the conductor cable length was spiraled on a wooden spool and the spool was rotated by hand

4.3.2.3 Telemetry Component on the Fish Cage

The RS232 signal coming up the wire arrives at the electronics mounted on the fish cage (Figure 4.25) (see Appendix 9.1.3 for schematic). This package contains the receiving electronics (Figure 4.19 and 4.25), a solar regulator to charge the battery (Figure 4.25) and a spread spectrum radio modem (Figure 4.26). The electronics are set up so that it normally is in a quiescent mode, drawing little power. When it senses signals on the RS232 line from the load cell recorder, it powers up the spread spectrum radio from the battery in the same pressure case (Figure 4.26) [see Appendix 9.1.3]. The system then relays all data output by the load cell to the spread spectrum radio. The link is two way, but in this application it was decided to try only the one way at first, as the software for interactive control of the load cell recorder was much more difficult to write and changing the software in-situ was risky and not within the resources of the UNH-OOA project.

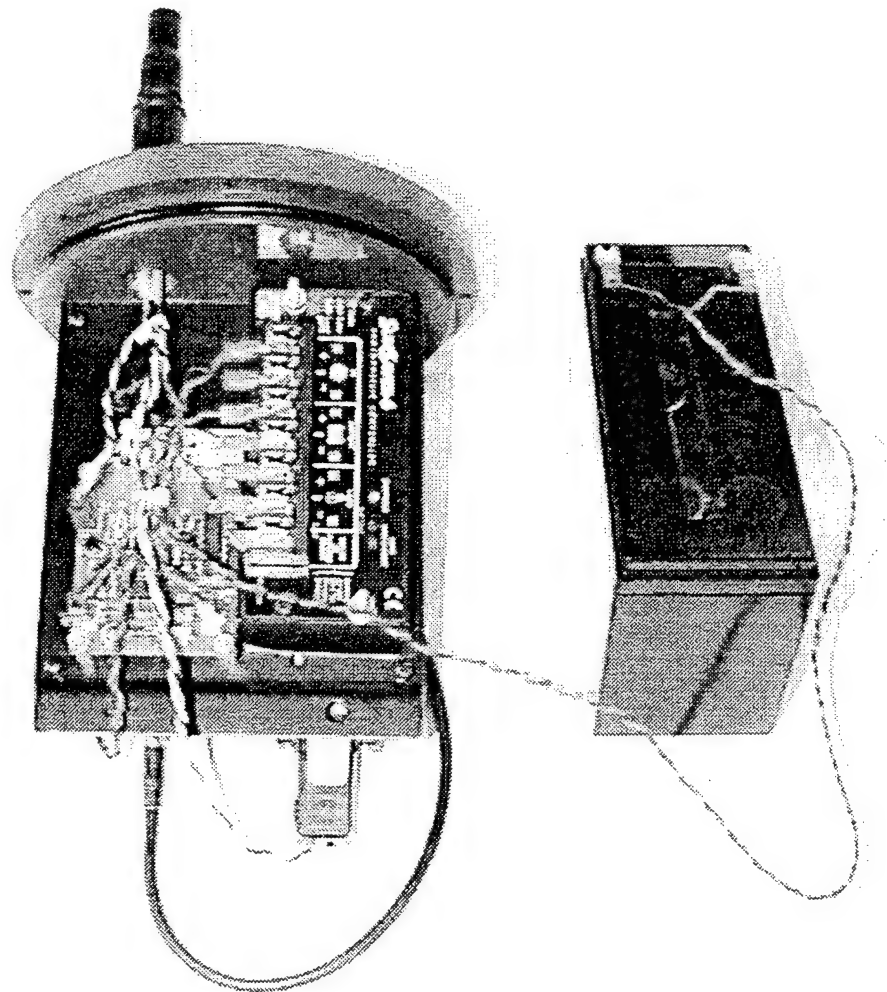


Figure 4.26. The electronics in the silo on top of the fish cage. The SunSaver-6 electronics is the shunt regulator for the 20-watt Solarex solar panel that charges the 7.5 ah sealed gel cell battery (right). The electronics board from Figure 4.19 is on the lower left, and the radio mounted below.

The telemetry package was initially planned to be mounted on top of the fish cage (Figure 4.28 and 6.5) in silos constructed to mount and allow servicing of the motion package. These silos also were to mount a 20-watt Solarex solar panel to charge a Panasonic 12 v 7.2 Ah battery through a Morningstar Corp., SunSaver-6 shunt regulator in the pressure case (Figure 4.25) [see Appendices 9.5.2 and 9.5.3].

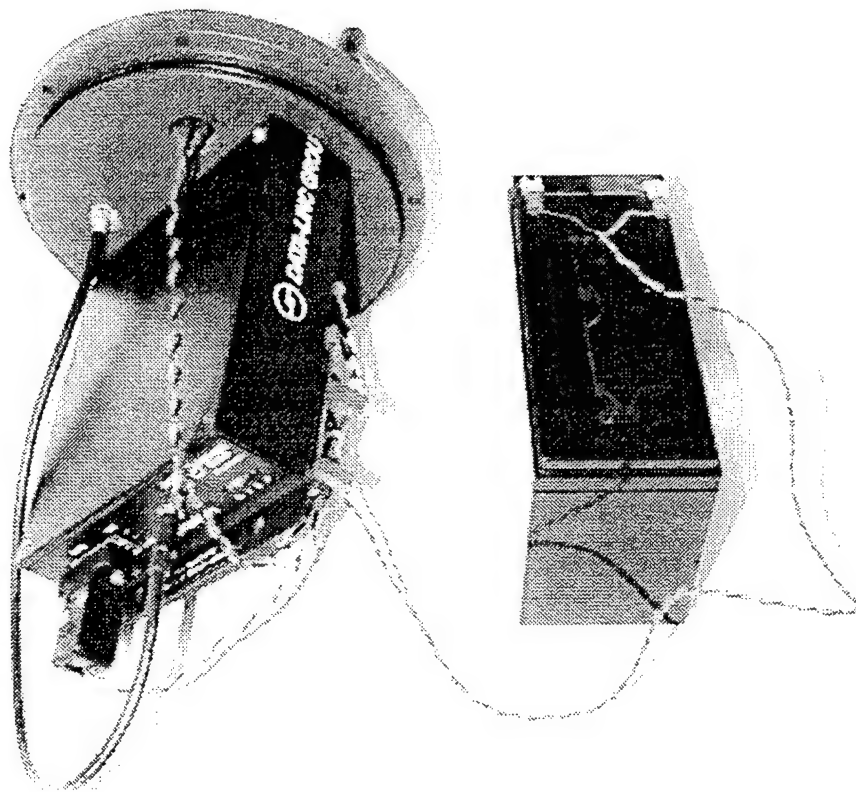


Figure 4.27. The Data-Linc spread spectrum radio modem is mounted on the back of the electronics-regulator board, and its coaxial connector runs out through a coaxial bulkhead connector through the wire seen. The RS232 data line runs to the telemetry electronics board shown in Figure 4.19 right and Figure 4.25.

The radio modem is the same used in the wave rider buoy, the motion package and the UNH environmental mooring. It is a Data-Linc Group SRM600 frequency hopping, spread spectrum radio modem (Figure 4.26). These radios communicate up to 20 miles in direct line-of-site applications so would reach the 8 nautical mile range from the fish cage to the UNH Seacoast Science center base. The Data-Link system can support up to 15 units talking to one another within range of each other, so would not be overloaded with the addition of this transmitter. Ken Morey and Karen Garrison (Ocean Process Analysis Laboratory at UNH) maintain the receiving station at the UNH Seacoast Science Center with computer and Internet connection to UNH to allow the relay of data to a workstation at UNH where it is available for subsequent analysis.

The DataLinc spread spectrum radio modem selected operates in the 902-928 MHz frequency band with packet data transmission. The system provides error free data with 32-bit CRC error detection, packet retransmission and acknowledgement for error free data. The radio data transmission rate is 144 KPBS and the limiting factor in the telemetry of data. Each unit is programmable to be a slave or master station, or a multiple slave to master as used in the UNH-OOA program. The radio's serial port could be programmed to any standard baud rate and configuration. When the radios first arrived, they were inserted between a computer and remote instrument, and preceded to work as reliably as if the instruments were connected with a hard wire.

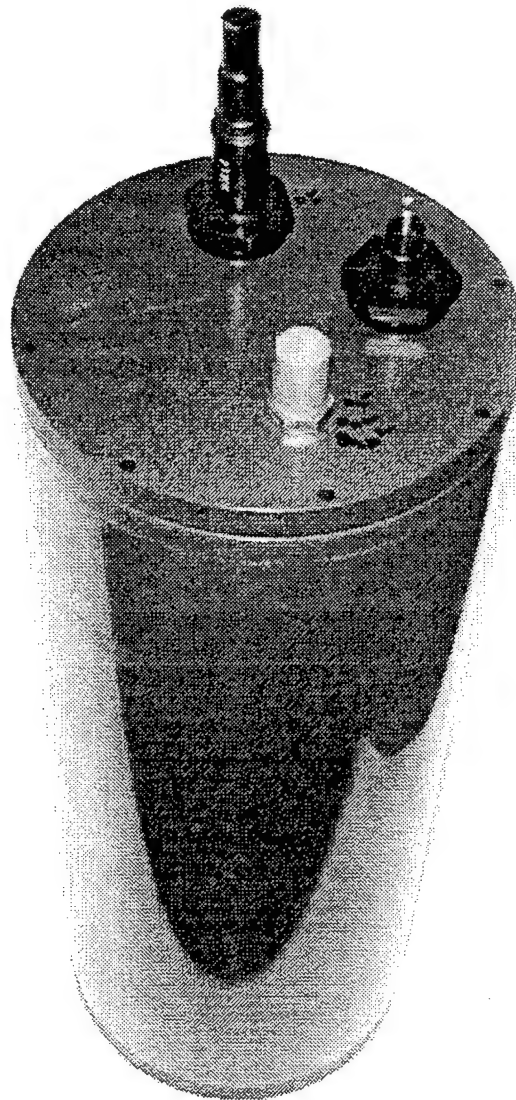


Figure 4.27. The telemetry package with electronics, radio and battery in a PVC watertight pressure case that was to be mounted in the silo on the fish cage. The system is capable of being submerged to the full extent of water depth at the site. The connector on the back of the top connects the load cell recorder in the water with the telemetry package through the wire running up the bridle cables. The connector on the right is for the solar panel, and the connector on the bottom is a coax to the antenna.

To coordinate the telemetry schemes, it was decided that each instrument would have its own time slot for telemetry. Thus, the four load cell system was assigned 38 minutes after the hour, the motion package 18 minutes after the hour, and the wave rider 48 minutes after the hour. This was comfortably after the UNH systems had transmitted and before they were scheduled to transmit again (UNH systems were on a 10 minute reporting schedule). The time slot allocation would mean that there were no collisions of messages, and we didn't have to have a two-way link with all the handshaking to assure that the system was able to complete its message without interference. During tests at WHOI we were did not see a message that was transmitted with errors, so the systems have proven reliable links.



Figure 4.28. Four silos built for the top of the fish cage to holds two battery pressure cases (one show front left) and motion package electronics pressure case (front right). The silos were to be bolted to the top of the UNH-OOA fish cage in holes drilled during survicing in summer 2000. They are connected at the top with square metal tubes to allow cables to be run freely between the electronics and antennas, and down to sensors mounted on the fish cage. The second silo from the left contains the mounting hardware for the telemetry module (Figure 4.27) and the cables from the fish cage to the motion package. The antenna bolts to the two tabs on the silo on the right, and a solar panel mounts on standoffs seen on the top of the right two silos. The solar panel provides power to the battery used by the load cell telemetry package to relay data from the four load cell recorder on the Northeast mooring leg to shore [see Appendices 9.2.4, 9.5.1, 9.5.2 and 9.5.3].

4.4 Deployment, Field Operation, Servicing and Results

The load cell system was deployed in two stages. The load cells and their strongbacks were deployed with the fish cage mooring during the week of 21 to 25 August 2000 (Irish, et al, 2001a). This was necessary as it would be difficult to insert the load cells into the mooring lines when they were under several thousand pounds tension in a safe manner by divers. Therefore, the systems were constructed and deployed with little testing and checks. A critical point was the four load cells on the Northeast corner ring (Figures 4.16 and 4.17) where electrical cables had to be run from the four load cells to the recorder in a manner that would allow movement of the system without wearing or damaging the cables. From the load cell records shown below it is obvious that this did not occur properly, either in the design or implementation.

The four recorder packages were deployed as soon as they were completed, calibrated and tested (see Table 4.2). They were stowed on 23 October 2000, transported to UNH and deployed from the R/V Gulf Challenger on 24 October 2000. As planned, divers deployed the load cell data recorders at a depth of seventy to eighty feet. All four recorders had to be carried by the divers to each grid corner, attached to the strong back, and then the load cell plugged in. Attachment required that the recorder be placed onto the strong back, and then slid so that two c-shaped brackets lined up and could be clamped on (see Figures 4.9, 4.10 and 4.11). Lining up these two brackets, while sliding, proved to be the most difficult part of load cell servicing. Two rubber locks were slid up the strong back, to hold the load cell in place, and then two bolts with graspable heads were inserted through the load cell recorder brackets into the strong back. The serial number of the load cells, recorders and their deployed location is listed in Table 4.3.

Table 4.2: Instrument start and end times

Recorder	Deployment	First Sample	First "On Bottom"	Last "On Bottom"	Last Sample
LC1	1	0000, 23 Oct 2000	1500, 24 Oct 2000	1200, 19 Jan 2001	0900, 21 Jan 2001
	2	2100, 22 Jan 2001	1800, 24 Jan 2001	1800, 25 Jun 2001	1800, 25 Jun 2001
LC2	1	0000, 23 Oct 2000	1500, 24 Oct 2000	1200, 19 Jan 2001	1500, 22 Jan 2001
	2	0000, 23 Jan 2001	1800, 24 Jan 2001	1800, 25 Jun 2001	1800, 25 Jun 2001
LC3	1	0000, 23 Oct 2000	1500, 24 Oct 2000	1200, 19 Jan 2001	1500, 22 Jan 2001
	2	0000, 23 Jan 2001	1800, 24 Jan 2001	1800, 25 Jun 2001	1800, 25 Jun 2001
LC5	1	0000, 23 Oct 2000	1500, 24 Oct 2000	1500, 18 Jan 2001	1800, 19 Jan 2001
	2	1800, 20 Jan 2001	1800, 24 Jan 2001	0300, 5 Mar 2001	0300, 5 Mar 2001

All times are in Coordinated Universal Time (UTC)

Table 4.3: Load Cell and Recorder Position

Load Cell Number	Location	Line Measured	Recorder
001	Northwest Corner	Anchor Line	L1
002	Southeast Corner	Anchor Line	L2
003	Northeast Corner	Lower Bridle Line	L5
004	Laboratory/Spare		
005	Northeast Corner	West Grid Line	L5
006	Northeast Corner	South Grid Line	L5
007	Northeast Corner	Anchor Line	L5
008	Southwest Corner	Anchor Line	L3
009	Fish Cage	Upper Bridle Line	Motion Package
010	Fish Cage	Upper Bridle Line	Motion Package

The North East corner load-cell-to-recorder connection required an extra cable upon initial deployment to connect the four load cells from the grid lines and anchor line to the recorder and load cell on the lower bridle line. Marking each cable before hand made this connection simple. A restriction on the servicing was that any electrical connections could not be made while the load cells recorders were recording. Then battery voltage would be present on the connector when exposed to salt water, and the contacts would be damaged. Recording occurred for twenty minutes after the hour every three hours during a multiple of three hours on GMT time, so careful watch on the time was required during diving operations.

After a 3-month period, all load cell recorders were recovered, serviced and redeployed. The recovery of the load cell recorders, done on 18 and 19 January of 2001, was a simple operation with the exception of the bolts that held the recorders in place. One of the two bolts on each recorder had lost its graspable head, requiring a wrench. This problem was easily corrected by welding the head to the bolts with 316 stainless rods for future deployments. The load cell recorders were redeployed on 24 January 2001, and the 3 single load cell recorders were left in place until 9 July 2001. They continued to record until 25 June, when the data storage was filled. The four load cell recorder was recovered on 27 March 2001, but had failed on 5 March 2001 as the major Northeaster storm of the season was starting. The symptom was indicative of a short in the underwater cable to the load cells, or in a load cell. We could not determine which without recovery of the cable (planned) and check of the load cells (visual check planned). The start, deployed, recovery and end times of the records obtained are listed in Table 4.2.

A diver serviceable, split-key type of shackle connecting one of the upper Northeast bridle lines to the net cage (Figure 4.1) failed during the winter, thereby breaking the electrical cable between the load cell record and the telemetry module on the fish cage. This also broke the cable running from the two load cells on the fish cage (Figure 4.1), so that the fish cage load cells and the telemetry option for the Northeast corner load cells could not be utilized.

Future deployments will use a lanyard to attach recorder dummy plugs to the recorders and load cell dummy plugs to the strong backs. This will simplify the diver recovery and deployment, and eliminate the loss of dummy plugs by dropping. The dummy plugs will be mated together while the load cells are attached to the recorders to avoid fouling of the plug-able surfaces. They will have to be secured to the system to prevent wear by moving about with the waves and currents.

For a quick look at a subset of the data, the four anchor line tensions (recorded in load cell output of volts), were converted to pounds tension using the nominal sensitivity of 8,000 lbs. per volt, and offset of 0.15 volt. (The actual sensitivity was adjusted to 8,000 lbs. per volt and calibrated by the manufacturer. The zero tensions offset numbers for each load cell were measured before deployment, and were close to these numbers.) The sensitivity of each load cell was a little different, but the means could change in tensions by as much as 500 lbs. depending on the temperature, excitation voltage and mechanical banging, so the absolute values will have to be adjusted later. The largest calibrated effect causing the mean tension offset to change with is the variations in supply voltage and temperature. We know the supply voltage from the record, and the temperature from the environmental mooring. Any change in sensitivity would show up in changes in peak size in the standard deviation records in Figure 4.30, but not affect the existence of a peak.

Figure 4.29 shows the averaged tension in each 20 minute burst sample from the four load cells in the anchor lines. The tensions were calculated (no editing for outlying bad points in a burst), and the mean calculated for each 20 minute burst. This is plotted as a time series versus year day in 2001, with the time as the start of the burst. (Note the year day is 1.5 for noon on 1 January). The high values before recorder deployment and after recorder recovery were removed (as they are noise since the recorder was not plugged into anything) to allow best viewing of the *in-situ* results. The scales on the plots were set to the same values, so that comparisons could be easily made of the signals. The most obvious feature is the strong visual coherence between the upper two plots and their difference from the lower two plots. Since the measurements were made by four different load cells and four different recorders, the observed differences are real. This implies that the main tension in the mooring holding the fish cage in position is in the Northwest to Southeast direction. This is the main orientation of the semidiurnal tidal ellipse, with about 1.5 times the amplitude in the NW-SE direction (top two panels) as in the SW-NE direction (the bottom two panels). The high frequency signals seen in the plot is semidiurnal tidal variations. It is interesting that this strong tidal signal is not seen in the lower two plots, even though the tidal currents in this direction are 2/3 those in the NW-SE direction.

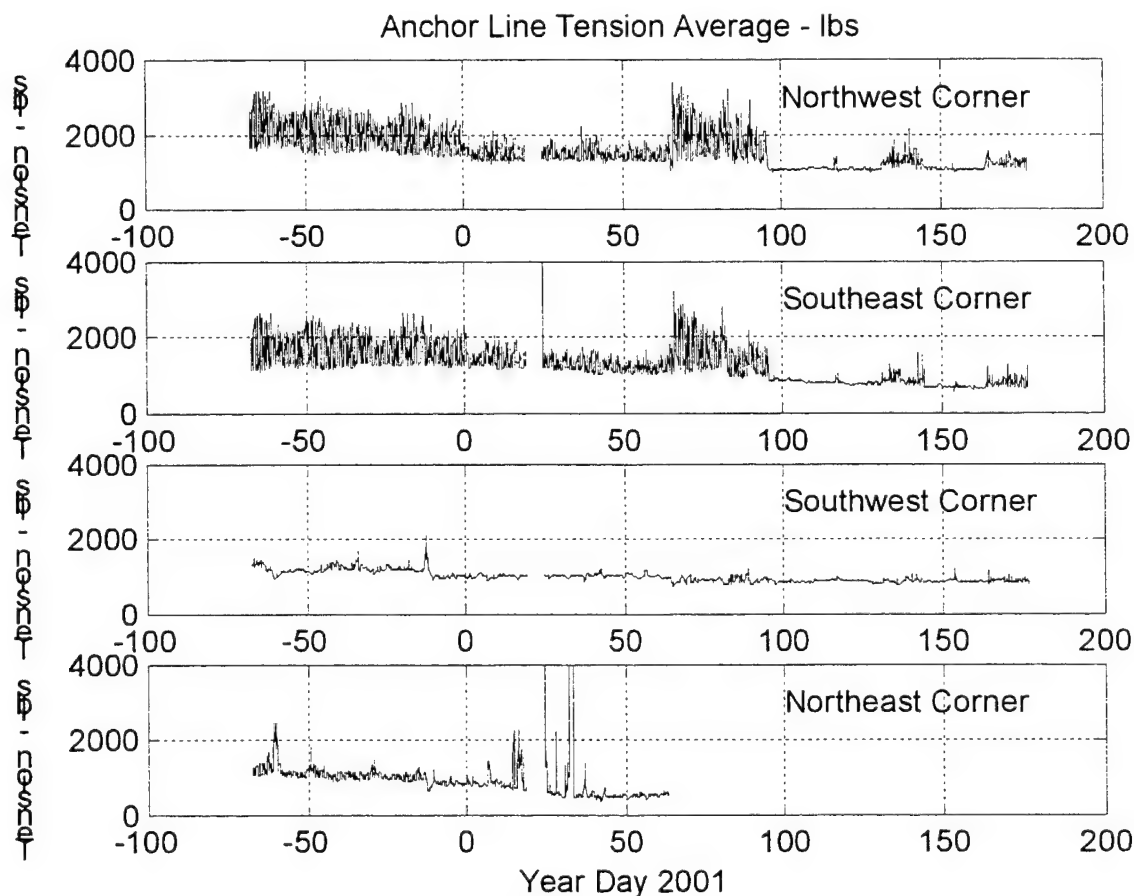


Figure 4.29. Plots of the average tension in the specified mooring anchor lines in pounds. The tensions were sampled at 8 or 10 Hz in 20-minute bursts every three hours. The average, without editing or removing bad points, was taken and plotted versus the start time of the burst in year day relative to 1 Jan 2001.

Also, there is the same low frequency trend toward lower tensions in all records. This is probably due to the lines elongating slightly with time as the fibers compress under wave and tidal current loading cycling. The reduction in tension could also be caused by the creep of the anchor in the bottom with tidal and wave loading, but is less likely if the anchor is properly embedded. The anchor would only move a few inches to more fully embed the fluke in the bottom.

There are coherent, abrupt changes in the mean tension record that are somewhat correlated with the storms, indicated by the peaks in the standard deviation records (Figure 4.30). The abrupt change in record about year day 65 is due to the counter weight becoming detached from the fish cage during a severe Northeaster. The higher tensions after that are due to fish cage motion at the surface. These abruptly end around year day 90 when a new counter weight was put on the fish cage, and it was moved to "down" or submerged position.

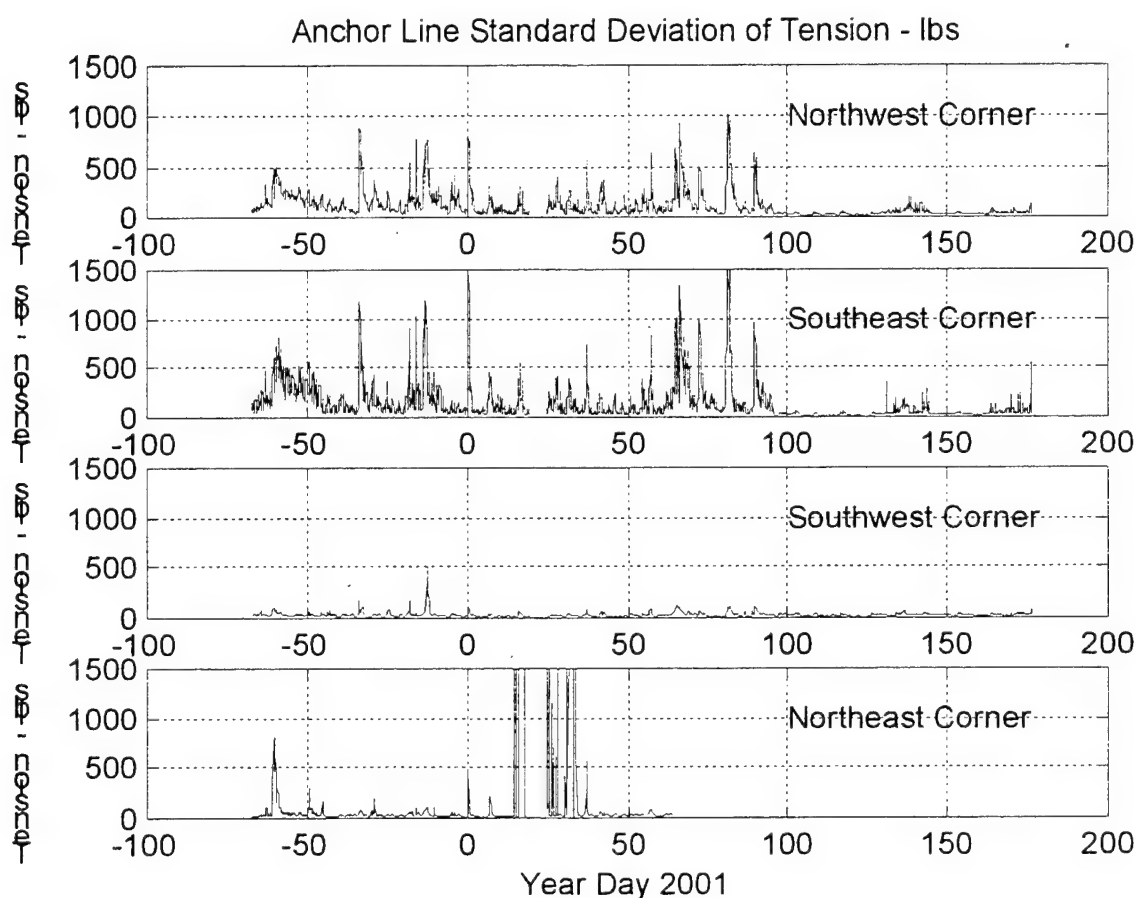


Figure 4.30. Plots of the standard deviation of the tension in the specified mooring lines in pounds. The tensions were sampled in bursts every three hours for 20 minutes at 10 Hz. The standard deviation, without editing or removing bad points, was taken and plotted versus the start time of the burst in year day relative to 1 Jan 2001 (although the plots say 2000).

The standard deviation records (Figure 4.30) show the individual storm peaks, particularly in the upper two panels. It is interesting that they do not show up in the lower two, which did not show the tidal fluctuations also. This further indicated that the major work of holding the mooring in position is by the Northwest and Southeast anchors. The sudden change

to lower standard deviation after year day 90 is due the addition of the new counter weight and the fish cage being submerged (see also Figure 4.29).

There are large spikes in the Northeast corner anchor line signal, and a shorter record, which are most likely due to electrical short in the wiring harness connecting the recorder to the four load cells. We should be able to replace this for the winter 2001-2002 season observations. The data should be usable for longer sections than shown by hand editing. There are significant questions than can be addressed by this data, and hopefully more will be answered than raised.

The Northeast corner recorder also had records from the other 3 load cells (Figure 4.31). Load Cell # 1 (top panel) is the anchor line shown in Figure 30. Load cells # 3 and 4 are the grid lines. Load cell #3 is noise (bad load cell or wire). Load cell #4 or its cable shorted about year day 14, causing the premature end of the record. The bridler line load cell # 2 was negative most of the time. This may have been caused by a mechanical shock to the load cell during deployment that changed the zero reading. The mean values are not good, and the load cell sensitivity may also have been affected. The riser line appears to be slack, or have little tension, in it much of the time. This result was also confirmed by diver observations that the bridler lines were often slack. This is another indication that the planned tensioning of the fish cage mooring lines above the grid lines was not realized.

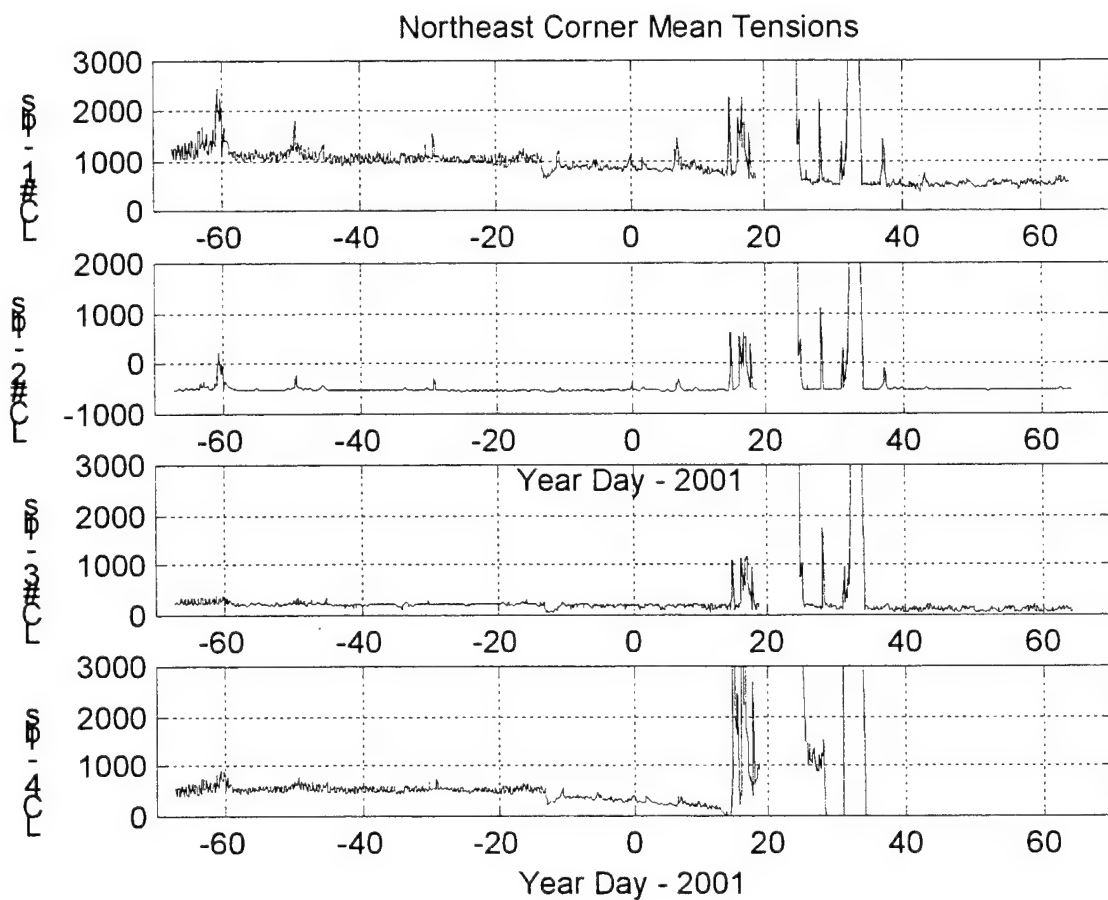


Figure 4.31. The means of each burst from the four load cells on the Northeast corner. The top panel is the anchor line tension, next the riser line, then the two grid lines (with first being bad).

The load cell recorder pressure cases were mildly fouled with growth after 9 months, but otherwise in good shape. As mentioned above the batteries were not exhausted, and the recorders and flash card data systems were working and behaved well after the flash cards were filled. The only mechanical problem observed was with the stainless tie rods on one of the pressure cases (Figure 4.32). These tie rods were used hold the two clamp blocks tight against grooves in the pressure case, to space the c-shaped hooks so they mated properly with the in-line load cell strongbacks (see Figures 4.9 and 4.10). Also, the end caps were bolted to these blocks to keep the case tightly closed and seat the O-rings against sea water intrusion. When recovered in July (after 9 months in the water), one rod broke off the recorder in the diver's hand, and could have lead to loss of the recorder and data. Upon close examination of all 16 tie rods from the four pressure cases, some small areas of typical looking anoxic crevice corrosion were observed under the bolts in the thread area. Also, some of the washers showed brown corrosion product and pits typical of crevice corrosion that is seen with prolonged exposure of 316 stainless steel to salt water in an anoxic environment. This corrosion is minimized if the tie rods are electropolished and passivated to remove surface contamination that will act as cells to start crevice corrosion. In the future, this problem can easily be avoided by using titanium hardware (as were the bolts holding on the end caps, and the c-shaped hooks, but at a higher materials cost.

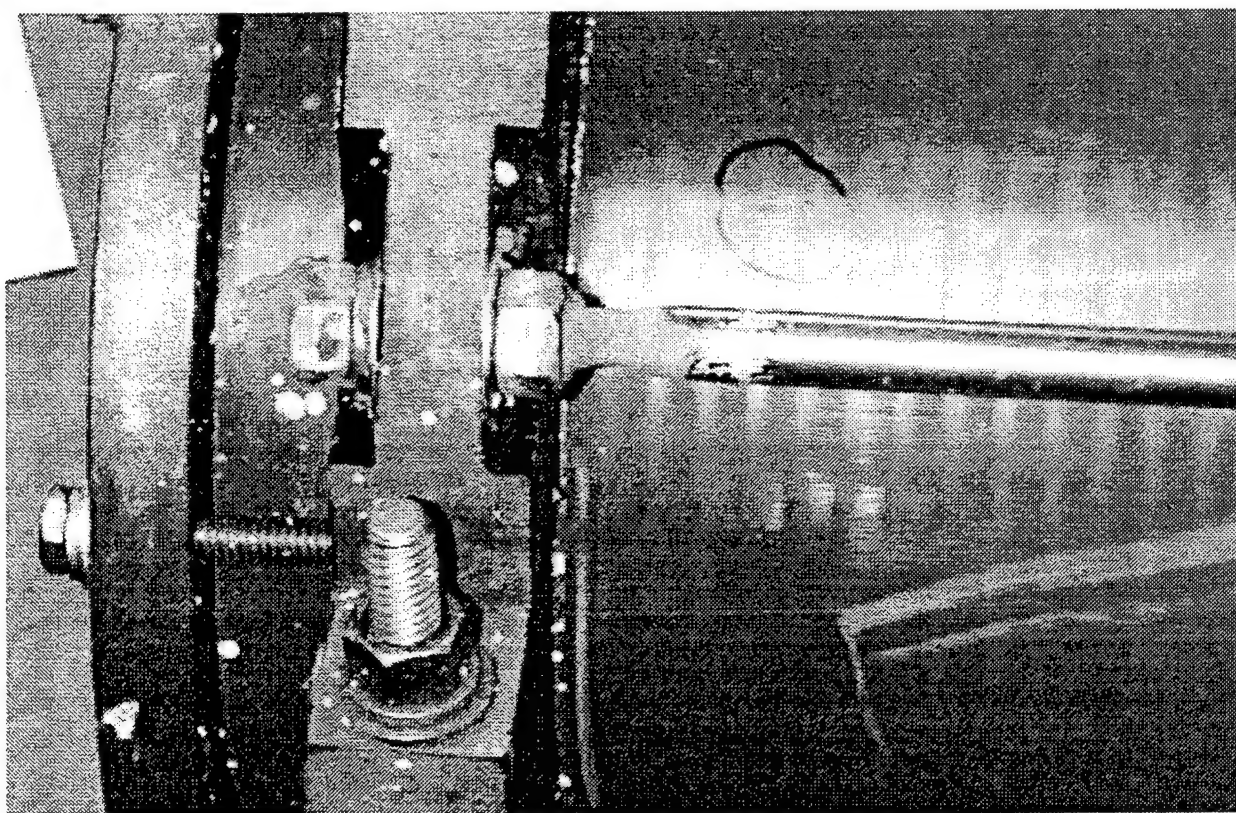


Figure 4.32. The corrosion on one of the stainless tie rods on a load cell recorder pressure case. Only one of the 16 rods used showed this corrosion. This photo was taken after three months exposure. After 9 months, the rod was so corroded so that it easily broke off.

5.0 Part 2: Wave Forcing Monitoring

James Irish⁺, Robin Singer⁺, Nick Witzell⁺, and Dave Fredriksson^{*}

⁺Woods Hole Oceanographic Institution, ^{*}University of New Hampshire

5.1 Accelerometer Options

To measure the non-directional wind wave spectra at the UNH-OOA site, WHOI constructed and deployed a wave rider buoy. The motion sensor in the wave rider buoy is a three-axis accelerometer that is digitized and integrated twice to obtain vertical displacements in post processing. This accelerometer is the low cost alternative to standard motion packages that are too expensive and power hungry for most remote applications. Jason Gobat and Mark Grosenbauch of WHOI (personal communication) have successfully used the Summit Instruments, Inc. accelerometer in engineering studies of oceanographic moorings, and suggested this might be a good solution for the UNH-OOA application. The Summit Instruments model 34103A accelerometers come with a user specified low-pass filter in each axis to reduce high frequency aliasing, so that no additional filtering needs to be build into the processing electronics. Crossbow also makes lower cost accelerometers that might be appropriate. Comparative specifications for the two accelerometers are given in Table 5.1.

Table 5.1. Comparison of Accelerometers

Manufacturer	Summit Instruments	CrossBow
Model	34103A	CXL02LF3
Range	±1.5 g on each axis	±2.0 g each axis
Sensitivity	1.30v/g on 3 axes	1.02 v/g on 3 axes
Cross Channel Coupling	< 0.25%	±3% FS
Linearity	0.2% FSR linear fit	±2% FS
Zero Drift	0.5% -40 to 85°C	30mg (0 to 70°C)
Power Requirement	5 v @ 25 ma	5 v @ 12 ma
Noise (DC to kHz)	5 mg rms to 100 Hz	1.5 mg rms
High Frequency Cutoff	4.5 Hz	125 Hz
Temperature sensitivity	<0.2 g (-40 to 85°C)	5 mg (-40 to 85°C)

Numbers from manufacturers published specifications

After studying the two systems, it was decided to use the Summit Instruments 34103A accelerometer (Figure 5.1) because WHOI has had success utilizing it. A Crossbow accelerometer was also purchased, and is being tested in another experiment to compare the results of the two instruments in open ocean applications. Early tests of the two indicated that the Crossbow had higher noise at low frequencies, which would adversely affect the integration from acceleration to displacement. (See discussion of results and spectra at the end of this report).

As the observations from the various instruments on the fish cage and mooring system would not be compared in real time, but statistically over the common sample interval (20 minutes every three hours), the accelerations could be integrated in either time space or in frequency space. Also, if the wave field were considered in equilibrium with the winds

(measured by a CMAN station at White Island on the nearly Isle of Shoals), a standard equilibrium wave spectral shape could be fit to the resulting spectra (see Fredriksson, 2001). Then, these results could be used to drive the wave tank for physical model tests, or the finite element computer models to predict the tensions and fish cage motion to compare with the observations.

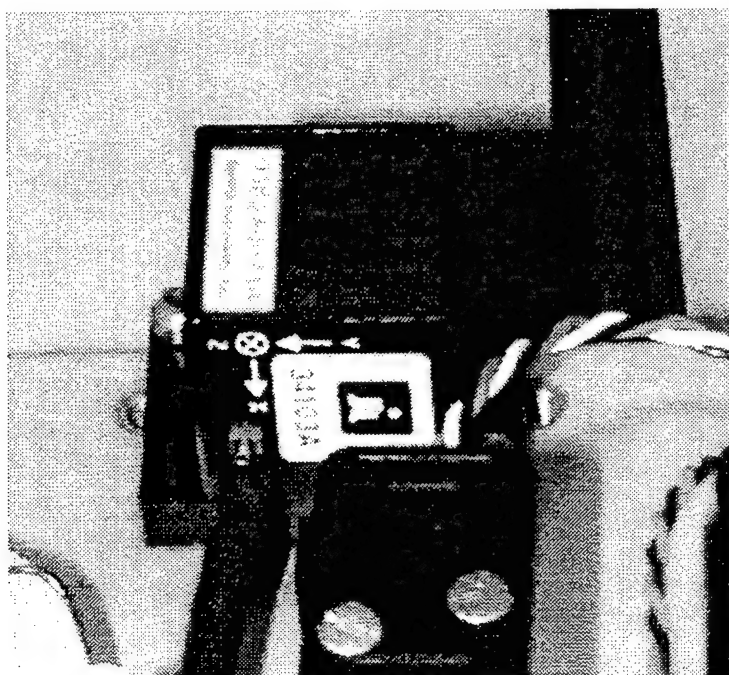


Figure 5.1. Summit Instrument 3-axis accelerometer installed on the electronics/signal conditioning board of the WHOI wave rider buoy. For the deployments, the y-axis was oriented down with the x and z axes in the horizontal plane. No buoy orientation measurements were made to enable some wave directional estimates to be made.

The Summit instruments accelerometer was selected largely because it had a built in low-pass filter compatible with a 10 Hz sample rate, so that we would not have to build electronic filters to prevent aliasing. Circuits were then built to reduce the output of the sensors from standard 0 to 5 volts output for -1.5 to +1.5 g acceleration to match the 0 to 2.5 volt range of the A/D converter in the data system. The operational amplifier network used could have easily filtered the data at the same time [see Appendix 9.3.1 for schematic]. The Summit specifications in Table 5.1 also indicated that it had lower drift and temperature sensitivity, which would affect the low frequency sensor noise level and reduce signal to noise and provide better data.

One factor critical in the operation of these sensors that affects the low frequency noise is the supply voltage. It must be accurately regulated or would show up as a low frequency drift in the record. Keeping this effect low is critical to the observations. Integrating the accelerations to displacements is the same as dividing the spectra by the radian frequency to the fourth power. As the noise of the accelerometer is essentially white (equal energy at all frequencies), the integration boosts the low frequency spectral levels of this noise, and is the signal against which we much measure the waves. The low frequency signal tends to high amplitudes at low frequency that dominate the record and must be dealt with in processing (see results section

below, and Irish et al., 2001b). The better the sensor, the less problems encountered with processing. However, the cost and requirements increase as one moves toward better sensors.

The main calibration of the system was the factory supplied calibration certificate. This was checked on a linear motion table at WHOI, and the results agreed with the factory calibration to within the accuracy of the table. Also, the system was tested with six different orientations to gravity force and the results tabulated. Again agreement was within measurement uncertainty, and we were comfortable with the results.

To obtain a system noise spectrum as a minimum level for the wave observations, a number of records were made with the system sitting upright in the laboratory, and on its side in the laboratory both before and after the deployment. These results are discussed in more detail in the Analysis report (Irish et al., 2001b). A typical noise signal spectrum is shown in Figure 5.15 along with the spectra from a significant storm. The signal to noise ratio is adequate, but not what might be expected in a motion package costing 15 to 20 times as much.

5.2 Data System and Telemetry

5.2.1 Persistor Controller, Signal Conditioning, Recorder Sampling

The wave rider data system was constructed around a Persistor CF1, a Motorola 68CK338-based microcomputer, enhanced with an 8 channel 12 bit A/D, internal clock with backup power, low-power circuitry, serial output and compact flash data storage media (similar to that used in the load cell recorders, see Part 1 above). The wave rider buoy used a 96 MB flash card to enable it to store data for more than 120 days between servicing. This four-month interval was specified by the UNH Ocean Engineers to match their fish cage maintenance and servicing plan.

The CF1 logic output lines were used to control external power to (1) the accelerometer, (2) a GPS receiver for time and position, and (3) a Data-Linc spread spectrum radio modem for data telemetry. This circuitry was placed on a separate circuit board on which the Persistor CF1 was mounted (Figure 5. 2) [see Appendix 9.3.1 for schematic]. An RS232 switch was also added to control the data output to the radio and input from the GPS receiver from the single serial port on the Persistor CF1. We used one of the simplest low-power modes, and brought the sleep mode current down to 1 ma.

The data is stored on flash media in a subdirectory called WR (for the wave rider buoy). For identification of the files and the time of sampling, the file name was made up of "WR" (for the wave rider), the month, the day and hour. Thus, for on 23 January 2001 at 1800 UTC, the file name would be WR012318.dat. As the records started on the hour and lasted for 20 minutes, this was an unambiguous scheme that put a time stamp on each record. The file name was constructed by using the Persistor's real-time clock to give the day, month and hour of the record (e.g. burst) start time.

The real-time clock was also used to control the sampling program. The system was programmed to sleep for one minute, then wake up, check the time and look for the three-hour start time. If the time were not appropriate for the start of the sample, the system would then revert to low-power mode for another minute. When the selected minute of the three-hour arrived, the system would start, power up the accelerometer and GPS receiver, open the file with the proper name, sample the 3 axes of the accelerometer and battery voltage, and write data to the compact flash media. When the record was done, the system would go back into its low-

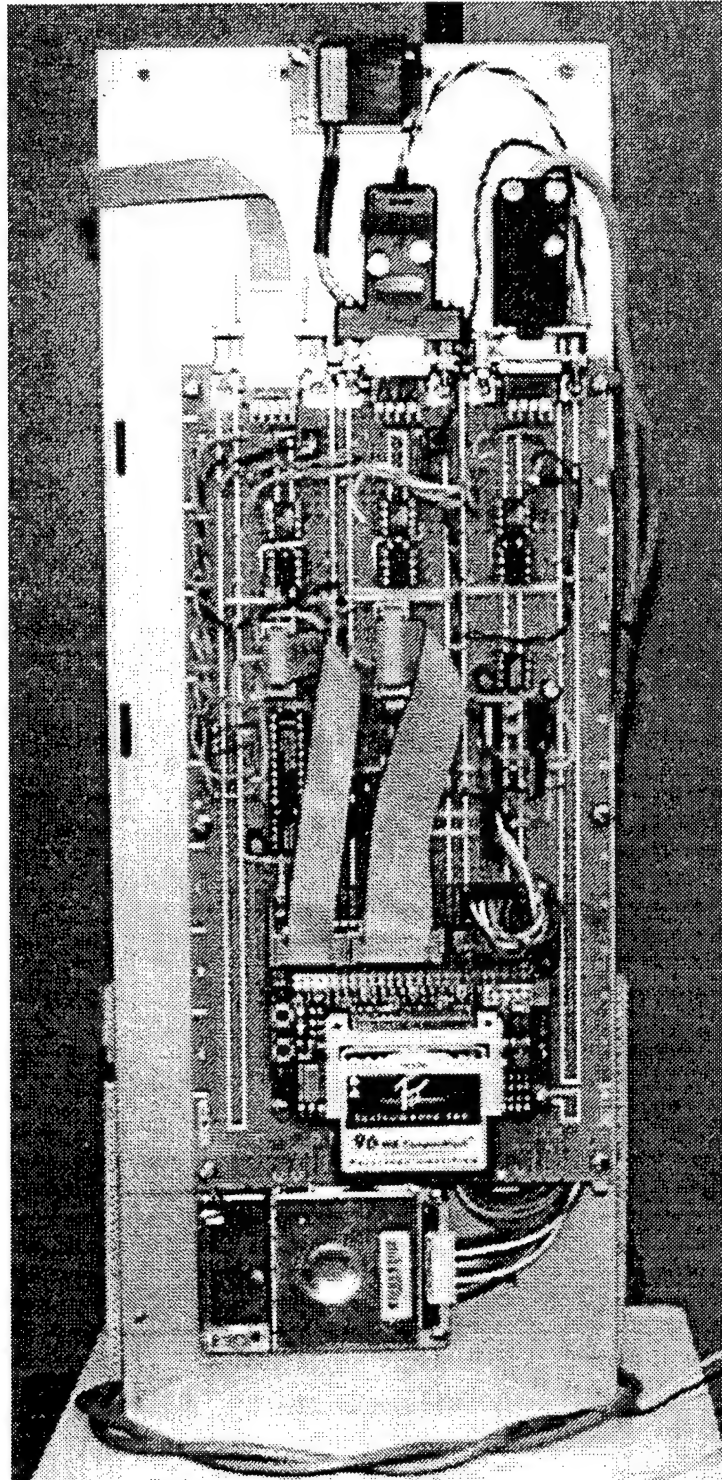


Figure 5.2. Wave rider buoy electronics showing the Persistor recorder with its 96 MB flash card, interface electronics, accelerometer at the top, and just below three DB9 connectors to the spread spectrum radio (left and Figure 5.3), accelerometer (right), and GPS (center connector). The Garmin GPS receiver is shown at the bottom of the board, but was later moved to the antenna mast with its antenna, so that a second coax connector wasn't required on the pressure case end cap.

power mode to wait the time for the radio transmission. At that time, the system would wake up, power up the radio and send the last file from the compact flash card over the radio link. When the transmission was complete, the system would then return to its low-power mode for the duration of the three-hour interval. This system worked well, and allowed straightforward control of the sampling.

To check the record times, a Garmin 25LP Series GPS receiver was built into the system. The GPS was turned on with the accelerometer, and thus had 20 minutes to lock on to the satellites, download the latest ephemeris information and obtain a good fix and time. As noted above, the GPS time and position were temporarily recorded on flash card storage and read and telemetered with the accelerometer data via spread spectrum radio modem to shore. This gave a time fix at the end of the burst from a separate clock as well as provided position information as a check that the wave rider buoy was still in position and had not moved.

Conditioning circuitry was built to adapt the 0 to 5v signals of the accelerometer to the 0 to 2.5 volt range of the A/D in the recorder (Figure 5.2) [see Appendix 9.3.1 for schematic]. The accelerometer was purchased with 4.6 Hz low-pass filters on each axis, to prevent aliasing, when sampling at 10 Hz bursts for 20 minutes (the same sampling program as the load cells and the motion package). The 20-minute burst was initially selected to obtain the full wave spectra with beating of all components, and the 10 Hz was selected to be well above any significant wave energy (and any system resonance) to capture all wave forcing and system response and be compatible with the 4.6 H cutoff (the lowest available) of the accelerometer. The three-hour interval between bursts was selected to allow the wave field to become somewhat decorrelated between bursts to optimize the use of the available data storage.

5.2.2 Spread Spectrum Telemetry Link

It was desirable to telemeter the wave spectra to shore for analysis and input into the fish cage management program. To accomplish this a Data-Linc Group SRM600 frequency hopping, spread spectrum radio modem was used (Figure 5.3). This is the same unit as discussed in the load cell telemetry section (see Part 1 above). These radios can communicate up to 20 miles in direct line-of-site applications so would do well in the 8 nautical mile range from the wave rider buoy to the UNH Seacoast Science center base, and was compatible with the UNH environmental mooring and base station. This allowed the relay the data to a workstation at UNH daily where it was available for subsequent analysis. To coordinate the various telemetry units, it was decided that each instrument would have its own time slot. Thus, the wave rider was assigned 48 minutes after the hour.

Some problems were encountered when three radios (the UNH environmental buoy, UNH tide gauge, and the WHOI wave rider) were transmitting (each in their own, non-overlapping time slot) to one base station. This will have to be resolved in the future for multi-point telemetry at the UNH-OOA site.

The wave rider records were often short, starting into the record and cutting off the end. This was weather dependent, the poorer transmissions occurring during bad weather. It was decided that the systems had not been programmed to work properly. When the radio was turned on, it knew the address of the base station and tried to connect. If the waves were high or the buoy were tilted over, it would be impossible to connect quickly as the waves would "eclipse" the line-of-sight path, blocking it momentarily. Also, Ken Morey reported that he had trouble

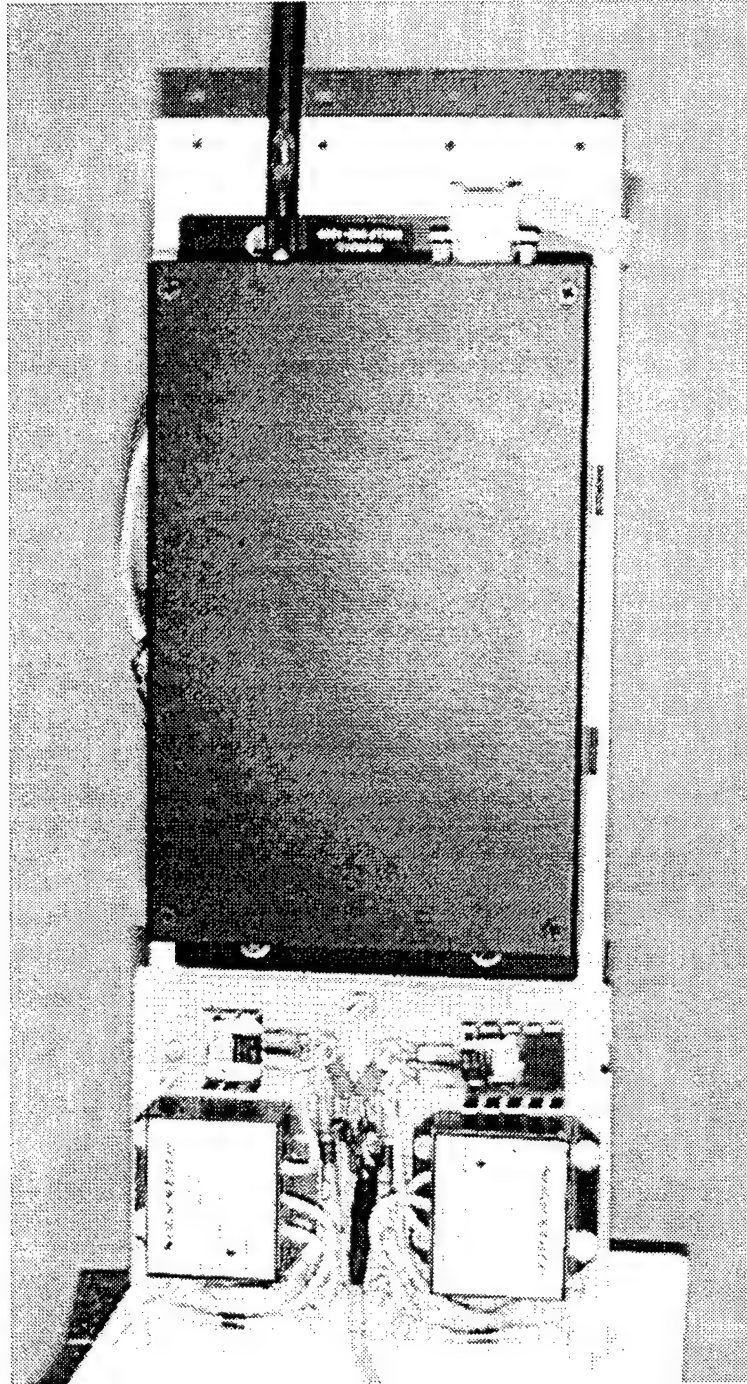


Figure 5.3. Spread spectrum radio (top large black box) and solar panel battery charger/regulator assembly (bottom) on the back of the electronics board, Figure 5.2. The antenna cable is the black wire going out the top of the picture that goes through the end cap in a D.G. O'Brien coaxial underwater connector. The DB9 RS232 connector is seen at the top right with its ribbon cable going around to the serial port on the electronics conditioning board (Figure 5.2). Power to the radio is also switched on this board. The solar regulators are the two boxes at the bottom connected to the solar panels by the four diodes mounted below them. The two diodes above them in the heat sinks connect the two batteries to the system power bus.

connecting to his environmental buoy located near the wave rider during very foggy conditions. Therefore, time should be allocated to wait to allow the system to connect before data is sent. During laboratory tests we did not see this problem, and therefore allocated about 10 seconds to connect (normal laboratory tests took two or three seconds). Then the data system started sending data. If the system was not connected and too much data were loaded into the buffer, then some would be lost as observed.

An additional problem appeared to be some interference with the nearby environmental mooring. About the time that the wave rider started transmitting, the environmental mooring appeared to change its time, and then was not telemetering its data at the right time, and there were some collisions of transmissions that loaded data. This should not have happened as we had allocated times so as not to overlap, to prevent having to program the base and remote stations for special handshaking protocol.

Finally, the records were cut off at the end when we powered down the radio after about 10 seconds after we had completed sending the data from flash card out the serial port to the radio. The radio has a large data buffer, and as it may take some time to establish the link, and more time to retransmit packets to get the complete message through, the power-up time could be exceeded and the radio shut off before the message was completely sent. This was again because of our lack of experience with the systems in the field, and can easily be corrected by allowing more time with the radio on, and shutting it off when the end of our time slot is reached. If the radio is done transmitting, it will go into its receive mode at much lower power. As power is not a problem, this shouldn't significantly change the power budget and should improve the telemetry. New software has been written to address this problem by allowing more time for the transmission, but not going to the extent of building in handshaking software with the base station, as it was not our computer or data retrieval software.

If the system is to become part of a two-way communications link for the offshore aquaculture demonstration project to the feed buoy and monitoring systems, some of these reliability issues will need to be addressed. Perhaps a relay station from White Island would improve the reliability of the transmission, as it could be high on the Island to get a good view of shore and the offshore instrumentation with minimal wave interference. The link from island to shore would be better as directional antennas could be used to improve signal to noise.

5.3 Telemetry Buoy and Compliant Elastic Mooring

5.3.1 WHOI telemetry buoy

The wave rider buoy was constructed utilizing a WHOI NOPP telemetry buoy designed and extensively used by WHOI in a variety of small buoy applications (McDonald and Peters, 2000) [see Appendix 9.4.1]. This buoy utilizes a Surlyn flotation collar from Gilman Corp as the principle flotation with a 6" diameter pressure case running through the foam as the electronics/battery well (Figures 5.4, 5.5 and 5.6). The bottom of the pressure case has been fitted with underwater bulkhead connectors to bring signals up the mooring cable and into the buoy for processing and telemetry (not used in this application). The top end cap does have penetrations (including coaxial connectors) to carry power and signals in and out of the pressure case. The foam flotation collar and pressure case provide about 500 lbs. of positive buoyancy which is adequate for use in coastal waters with a standard wire mooring configuration. WHOI has also used larger foam blocks providing over 1200 lbs. of positive buoyancy.

Above the flotation collar, a tower extends upward holding the solar panels (new for this application), the flashing guard light, a radar reflector and the antenna mast (Figures 5.4 and 5.6). The top end cap of the pressure case with connectors can just be seen below the solar panels in Figure 5.6. The guard light is a 600 Series from Carmanah Technologies that is self-contained with its own solar panel and battery. A photocell switch shuts the light off during the daylight hours to save power, but turns it on when the light level falls. As a self-contained unit, these have worked very well in the small buoy application, but are limited power output (effective intensity 7 cd), with a range of 2 miles. The radar reflector is a Firdell Blipper made for pleasure boats, and is highly reflective to standard shipboard radar. It is mounted as high as reasonable on the buoy to provide signal over the longest range and not provide too much wind drag.

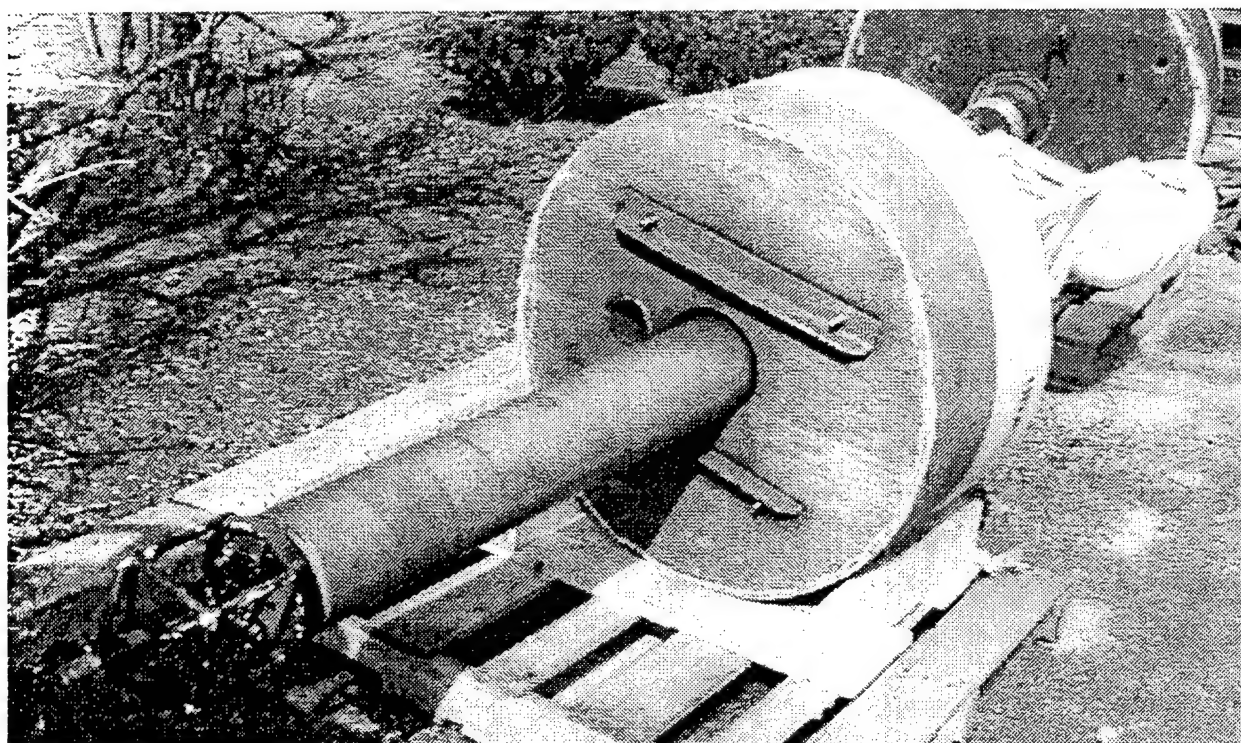


Figure 5.4. The bottom of a WHOI NOPP telemetry buoy showing the 6" pressure case going through the foam flotation collar with mooring attachment at the bottom (far left). The pressure case houses the batteries and electronics. The tower and radar reflector are just seen at the far right above the foam collar.

The antenna mast is made from a 2-meter long, 1.5" diameter fiberglass pole, and is mounted in the center of the buoy for symmetry. On top of the mast is the spread spectrum radio whip antenna. The GPS antenna is mounted just below the top of the mast (see Figure 5.6). The GPS antenna and electronics are packaged together and mounted on the mast just below the spread spectrum radio antenna, and the RS232 signals and power are run on cables inside the mast along with the coax cable to the antenna and through the pressure case end cap. The power to the GPS is controlled by the data system, and the data collected on the RS232 port. For assembly drawing of the standard WHOI telemetry buoy, see Appendix 9.4.1.

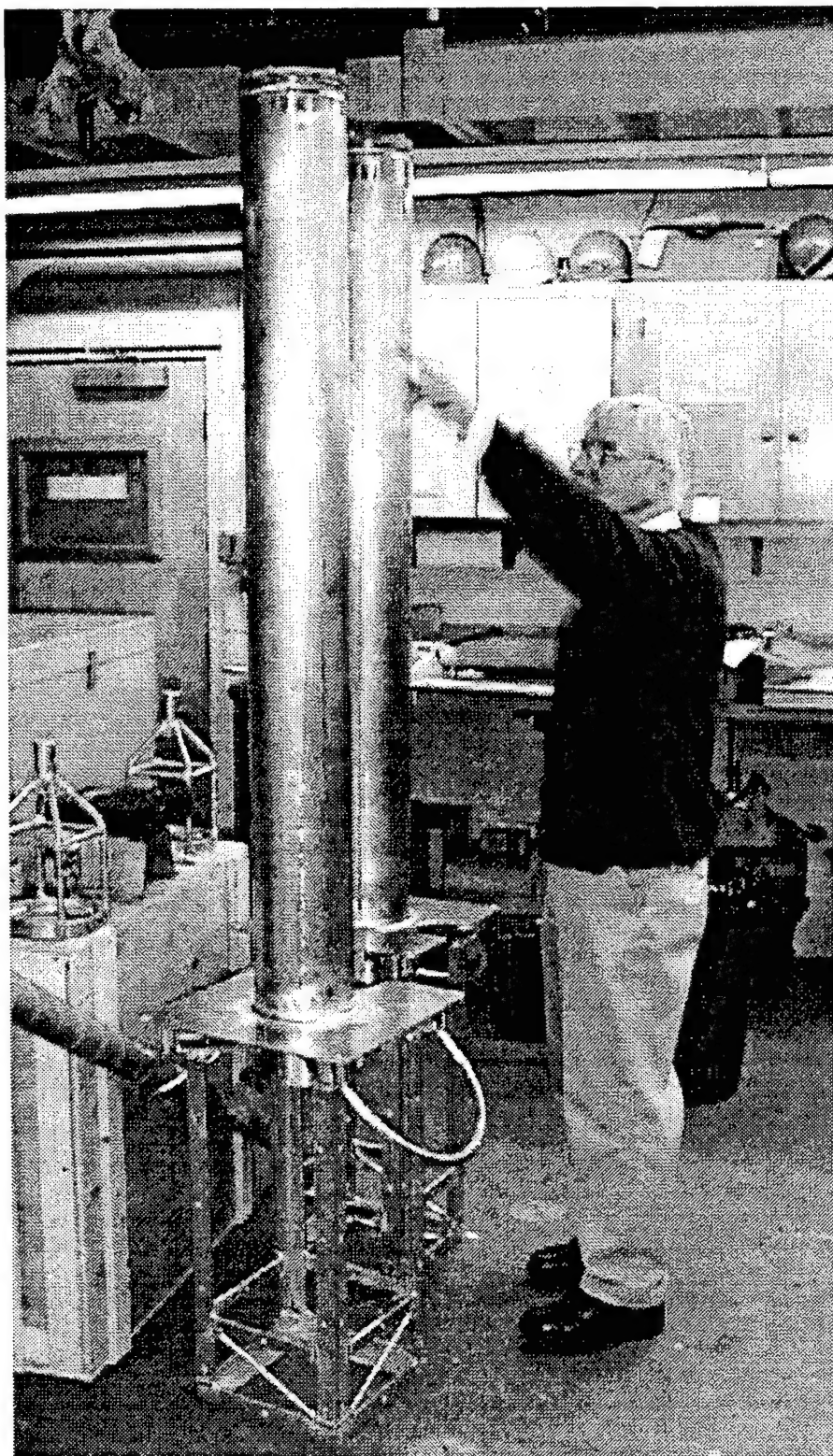


Figure 5.5. Walter Paul standing by two NOPP telemetry buoy pressure housings with towers (upside down) to give scale. The housings are fully machined/welded and ready for painting and assembly. The mooring brackets that attach to the bottom of the buoy and hold the end cap in place are seen on the box on the far left.

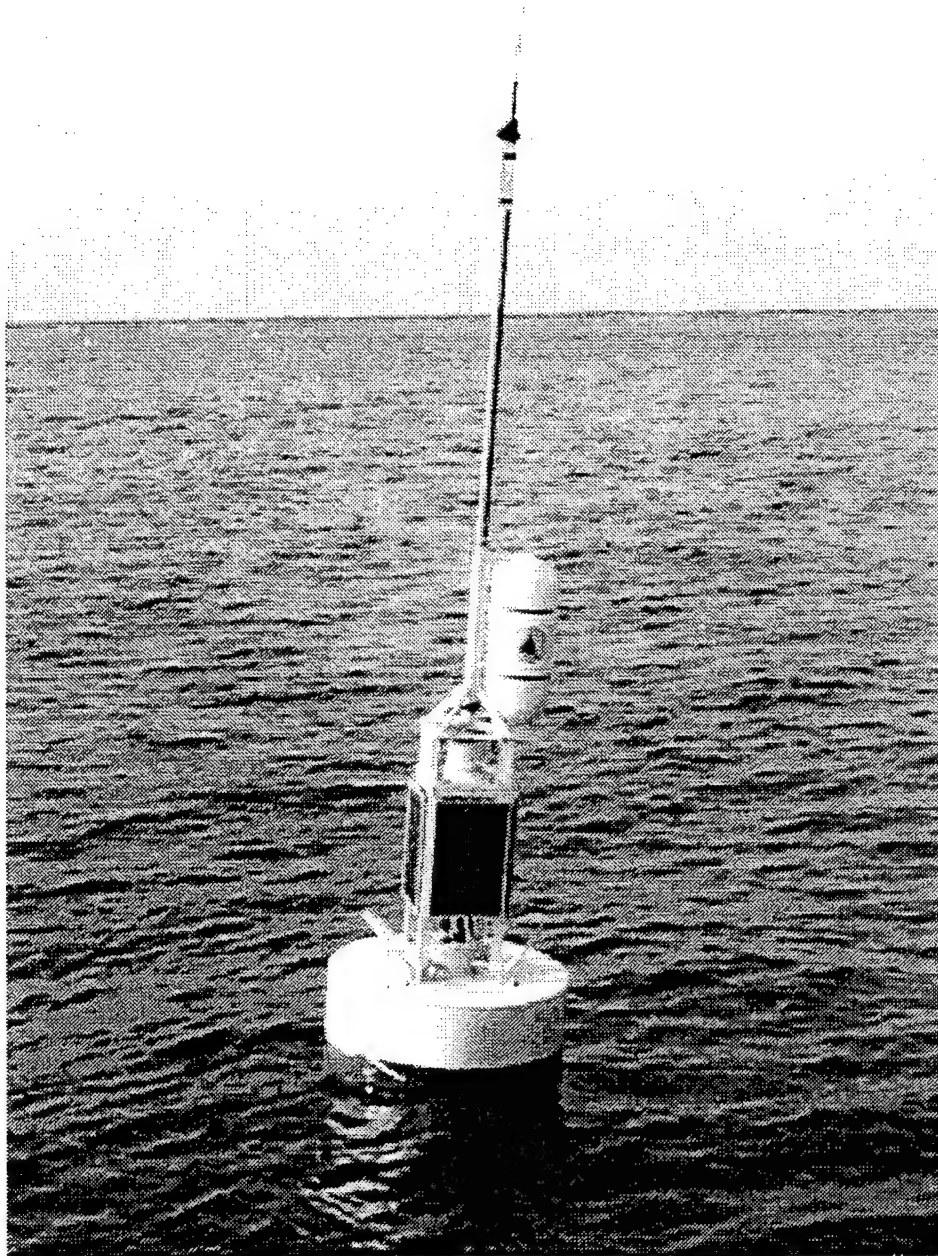


Figure 5.6. The WHOI wave rider buoy shown deployed east of the UNH northern fish cage at $42^{\circ} 56.733' N \times 70^{\circ} 37.679' W$ in 52 meters of water. The radio antenna is seen at the top of the mast, with the GPS unit (the black blob) mounted just below. The white radar reflector is visible at the top of the buoy tower that holds the solar powered Coast Guard navigation light. Four 10-watt Solarex solar panels power the system indefinitely. Flotation is supplied by a Gilman Surlyn foam flotation collar. An aluminum pressure case in the center holds two gel cell batteries (in the bottom for stability) and the electronics with accelerometer (attached to the top end cap).

The concept behind the wave rider buoy is that it follows the surface; so measuring the motion of the buoy is the same as measuring movement of the sea surface. In order for the buoy to follow the surface, the mooring must have the necessary compliance to allow the buoy the freedom to move up and down with the waves. For the UNH-OOA application it was decided that a rubber compliant elastic element would be best. UNH and WHOI have experience in using these in more substantial moorings (Wood and Irish, 1987, Irish, 1996, Irish and Kery, 1997, Paul et al., 1999). To function properly the response to wave forcing must be near 1 for the primary wave frequencies. Therefore, any buoy-mooring-mooring resonance would be disastrous if they were in the wave spectrum. Quick calculations showed that the resonance was around 1 second, and so not critically affecting the wave measurements.

5.3.2 Solar panels, batteries, and power system

The large advantage of a solar powered buoy with telemetry, is that its deployment is not limited by either power or data storage, and the deployment can continue until the mechanical hardware is worn or some failure in the sensing system is observed. To power the wave rider buoy, four Solarex MSX-10 solar panels were used. Each panel output is 10 watts under ideal conditions with peak currents of 0.58 amperes. It was initially planned to have two buoys, each with two 10-watt panels. However, programmatic changes eliminated the second buoy, so all four panels were placed on one buoy (see Figure 5.6). The 10-watt panels fit on the telemetry buoy's tower as if it were designed for them with minor modification to drill new mounting holes. This supplied more than enough power and the batteries never really were heavily drawn down. The battery voltage was recorded as along with the accelerometers, and a plot of the average voltage during the 20-minute burst sample every three hours is plotted in Figure 5.7.

The solar power was stored in two Panasonic LC-R127R2P 12 volt, 7.2 ampere hour sealed gel cell batteries. Two Solarex SSH1/12/3A/0 shunt regulators regulated the solar panel charging of the batteries. These regulators measured the battery voltage, and when it exceeded 14.5 v, shorted out the solar panels. The solar panels still produced a current flow, but now at millivolts, so the power dissipated in the regulator was milliwatts. When the voltage dropped below 14.5, the regulator turned on again allowing the battery to be charged.

Two solar panels were tied to one regulator through 1N5821 Schottky 3 amp blocking diodes to prevent the solar cell from discharging the battery at night. The two regulators were used to charge the two batteries, so there were two parallel power systems. This provided a 100% redundancy if there was a failure in one, and even if three solar panels were damaged, the system would continue to work. The two power systems were then tied to the system power through two more Schottky MBR1545 15 amp diodes to prevent a problem with one power system from drawing down the other, yet deliver any required power to the data and telemetry system (Figures 5.2 and 5.3). The power/charging control circuits were located on the bottom of the main conditioning electronics board by the spread spectrum radio (Figure 5.3). This design has worked well in solar power buoys UNH and WHOI have been using since 1985.

To monitor the battery voltage (Figure 5.7), the voltage was divided down by a factor of 6 from 15 to 2.5 volts to be compatible with the Persistor A/D. Precision 1k and 5k ohm resistors were used, and the resulting measurements, with a factor of 6 scaling were a few percent above the measured battery voltage, and adequate for system battery voltage status checks.

The system power requirements are minimal. The data system draws 7 or 8 ma when operating, the accelerometer about 25 ma more when on and the GPS about 75 ma. The largest power drain is the spread spectrum radio that requires 70 ma in standby mode while listening, and up to 650 ma when transmitting. The maximum current drain is less than 1 amp and well within the power system capability. The data system and accelerometer only draw their current during the 20 minute sampling interval every three hours, and the radio is only on for about 3 minutes every three hours. When the system is in low-power mode, the current drain is about 2.5 ma, much of that taken by the battery sensing resistors which were supposed to be 10 times the value used. Therefore, the total daily power requirement was about 1.5 ah per day. The two batteries could then power the system for about 2 weeks without recharging. One solar panel need only receive about 3 hours of optimum sunlight per day to replace the power used during one day. The arrangement of four solar panels always provided a panel toward the sun for optimum charging. The pair of solar panels on each power subsystem was mounted on opposite sides of the tower for optimum sharing of power and charging between systems. The system voltage plot (Figure 5.7) shows that the solar system kept the batteries topped up, and they never were really in danger of being discharged to the point that they became damaged and couldn't be recharged.

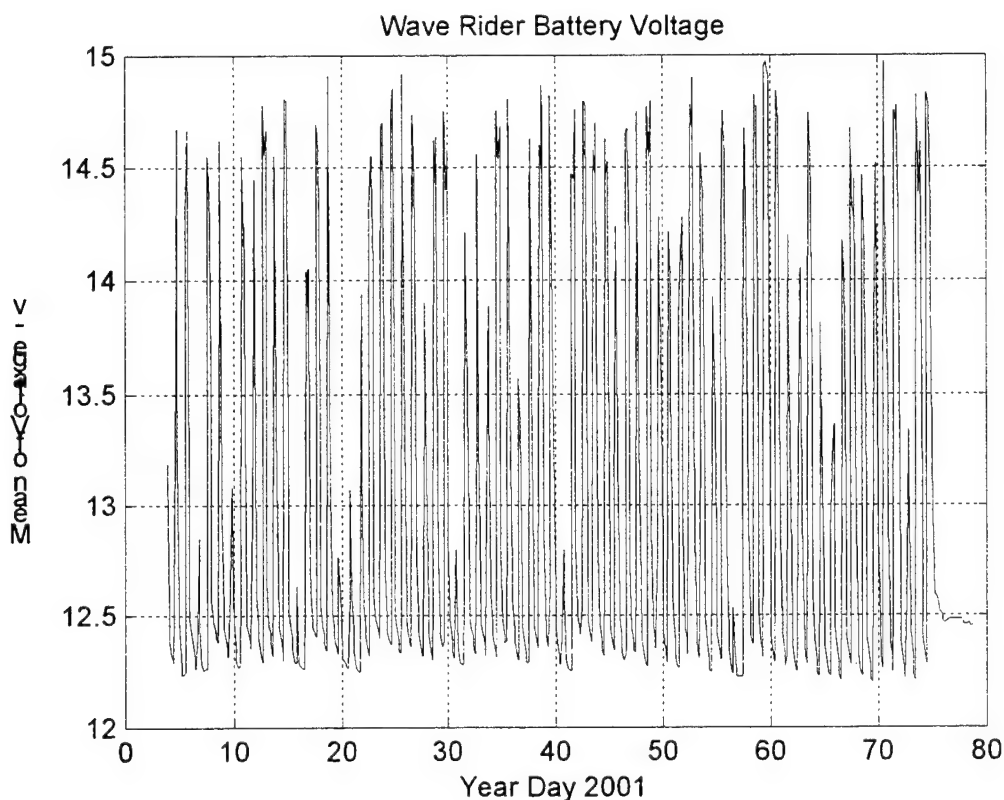


Figure 5.7. The time series of averaged system voltage during each 20 minute burst for the full deployment. The high voltage peaks are due to the solar panel changing the battery and the minimum voltages are obtained during the night when the system draws on the battery. The short section of nearly constant voltage at the end of the record was with the system running in the laboratory for a few days with no direct solar exposure, so were not charging.

5.3.3 Compliant elastic mooring

The compliant elastic element was made up of a single 1" diameter rubber band that is specially terminated to reduce stress concentration at the splice (Wyman, 1982). The mooring design (Figure 5.8) has the compliant elastic in the upper part of the water column and a 5/16" wire rope to the anchor. Because of the project policy to recover the entire system when possible, leaving no anchors or gear on the bottom, the design provided for recovery by divers. Because the elastic elements are not strong enough to recover the anchor safely, a diver has to swim down the elastic elements with a recovery line, and attach it to a pear link in the mooring between the elastic and wire rope. Then the mooring could be recovered without stressing the elastics and not leaving any pieces on the bottom. As the maximum UNH diver depth was 100 feet, then the wire rope was cut so that the ring at the bottom of the elastics would be at 100 feet. In fact the wave rider was deployed 10 feet deeper than planned because of an error in the depth sounder/positioning and caused a little concern for diver safety.

The elastic element used is fairly compliant, with a 90 lb tension for a stretch of 100%. (Paul et al., 1999). For this deployment two 10-meter long sections of elastic were used, so that with shackles, chain, swivels, etc. the elastics were stretched only about 70%, providing slightly more than 55 lbs tension at slack water. This nearly constant tension provided a righting moment to the buoy to keep the antenna up for telemetry, and to keep the buoy more or less on station (Irish and Kery, 1996 and Irish, 1997). Modeling of the mooring with WHOI Cable (Gobat et al., 1997) showed that in strong currents (1.5 kts or 0.75 m/s which is greater than the maximum current seen at the environmental mooring), the wave rider buoy would move about 27 meters horizontal, or about half the water depth. The tension in the mooring would increase from about 75 lbs. to about 125 lbs., well within the working range of the elastic elements. The buoy is still relatively free to move with the waves, and a 5 meter 10 second wave produces additional tension fluctuations about the 125-lb. mean of ± 25 lbs. Again, well within the working range of the elastic element. As a design criterion, a stretch of 5 times the original length at a tension of 600 lbs. is considered the maximum load before breakage. Therefore, the mooring is working in a good part of the stress-strain curve for the elastics and should have no problem surviving. It did survive from early January through the March storm with an estimated 13-meter wave. The buoy was then successfully recovered to retrieve the full data set for analysis, not because of mooring or equipment problems. The hardware was not worn and will be used again on the next deployment [see hardware list in Appendix 9.4.2].

5.4 Deployment, Operation and results

The buoy, electronics and mooring system were brought to UNH at Christmas time and the operation of the system reviewed with Dave Fredriksson and Glen Rice so that they could start the wave rider and deploy it without WHOI personnel being present if a weather window should open. The system was finally deployed from the R/V Gulf Challenger on 04 Jan 2001, and produced the first good record at 1500 UTC. The system was recovered after the 06 March 2001 storm to retrieve the data for analysis. It wrote its last record on 15 March 2001 at 1500 UTC, was recovered and carried to the UNH Ocean Engineering building. On 19 March, the system was shut down, the data system removed and the data dumped to computers and a CD-ROM burned. 561 good records were collected with the wave rider in place, or 1,683 hours (70 days) of wave information. It appeared that the system worked well for the 2½ months it was deployed, and recorded good records of acceleration.

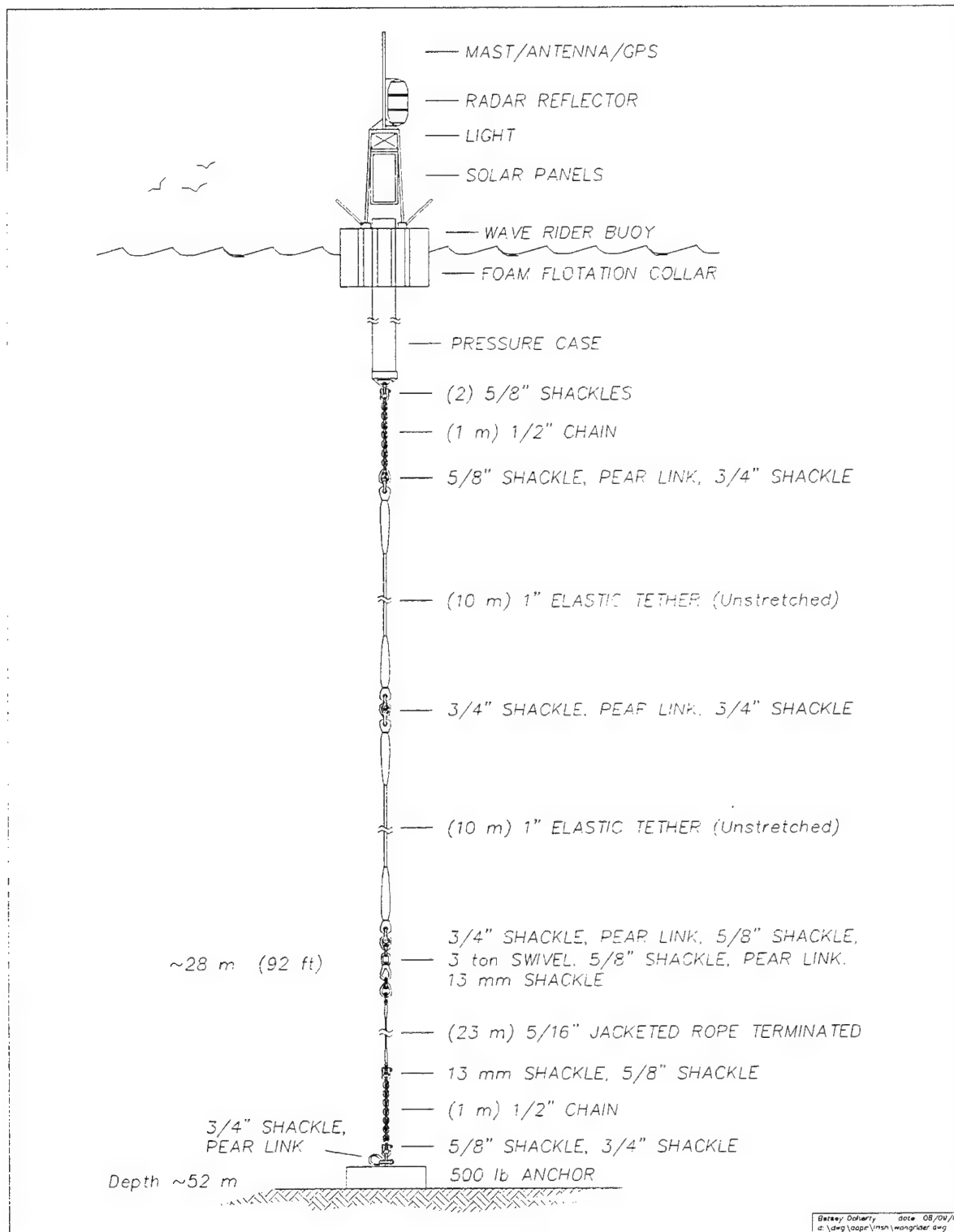


Figure 5.8. Schematic of the wave rider buoy mooring, with the compliant elastic tether in the top 100 feet of the water column, and 5/16" jacketed wire rope to the bottom. A swivel was located at the top of the wire rope between the wire rope and compliant elastic tether.

Figure 5.9 shows a normalized record (volts to g's acceleration) of the three axes and the system voltage for the March 6 storm. We were relying on the spread spectrum radio link to be the primary source of data (with the internal recorder as a backup) to shore, which would allow real-time analysis of the wave activity at the site. The record shown in Figure 5.9 is what would be obtained every three hours. However, there were several problems involved. The receiving station was located in the Seacoast Science Center some distance from UNH, and a good communications line had to be installed at this site. Ken Morey and Karen Garrison of the Ocean Process Analysis Laboratory at UNH set this system up, coordinated with the phone people, and established an ftp site at UNH where everyone could access the telemetered data that was collected daily from the Seacoast Science Center. When this was up and running, it became apparent that there were other telemetry problems as discussed above.

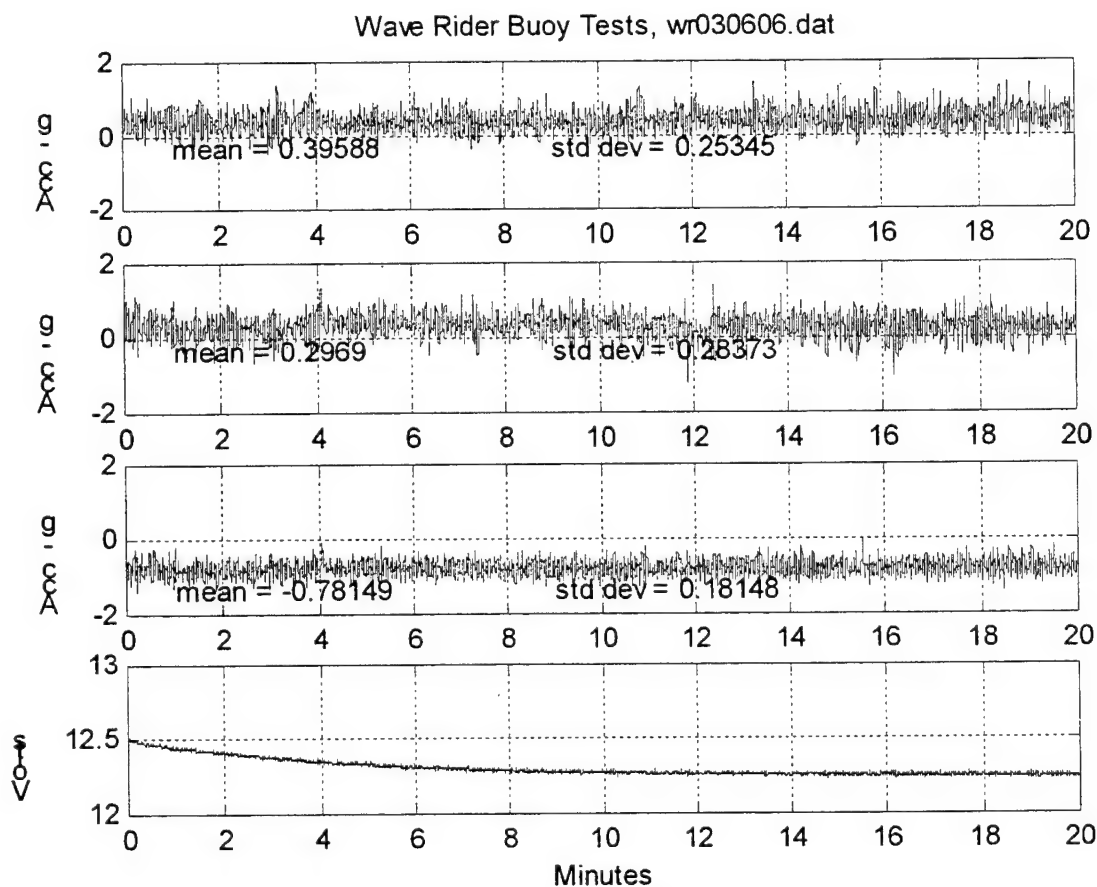


Figure 5.9. Signals recorded by the wave rider buoy during the 6 March 2001 storm. One 20-minute burst starting at 0600 UTC is shown sampled at 10 Hz. The two horizontal axes are at the top and the vertical acceleration is the third plot down. The system battery voltage is shown at the bottom.

A summary of the statistics (the mean and variance of the 1200 samples) in the 20 minute burst samples (e.g. the statistics from Figure 5.9 is one point in time) is given in Figure 5.10. The change in mean values (shown in the top panel of Figure 5.10) can indicate a tilt of the buoy,

as is clearly seen around year day 43. The storms are indicated by the increase in variance of the acceleration as seen in the bottom panel of Figure 5.10.

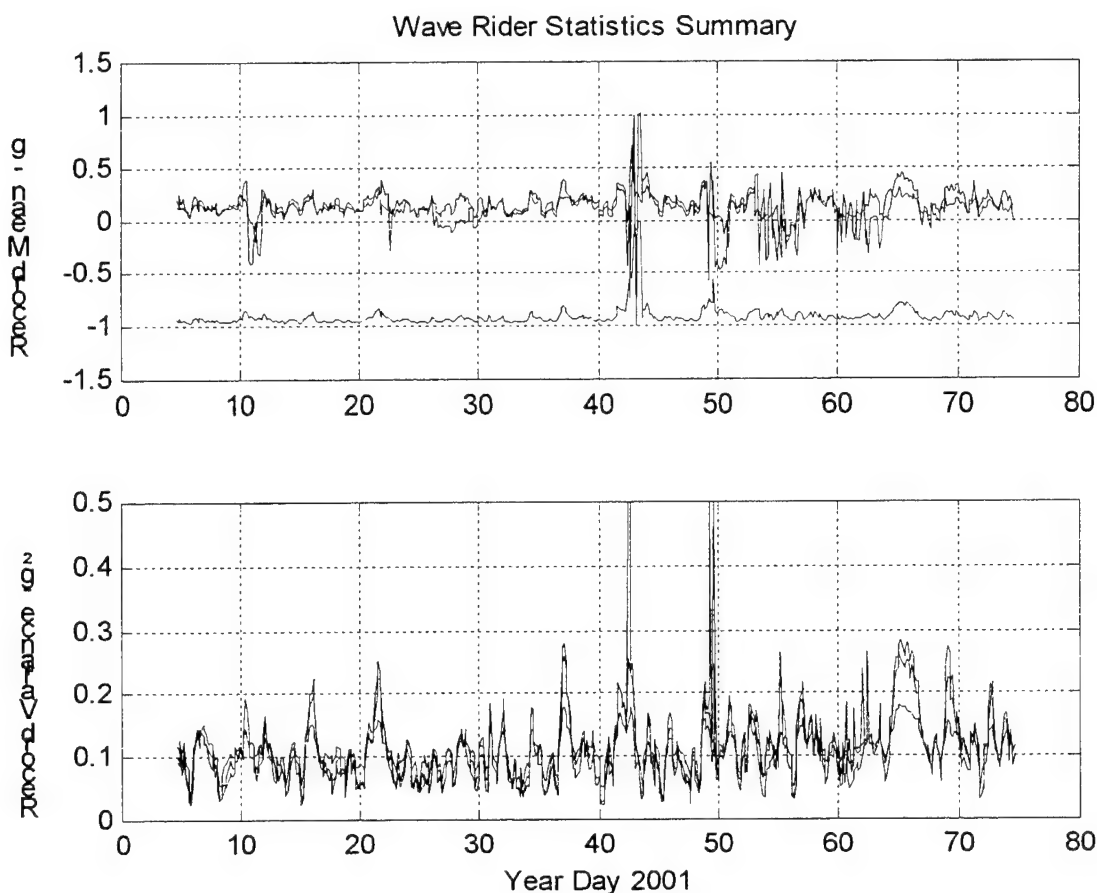


Figure 5.10. Summary statistics. The top plot shows a time series of the mean of the individual records as shown in Figure 5.9. The effects of the storm events can be seen in the change in the mean. The largest signal is seen at about year day 43 when the vertical acceleration goes to zero and one of the horizontal axis goes to 1 for a few records. The variance of each burst is plotted in the lower panel and indicates the storm periods of high waves. The largest (highest for the longest) is the 6-7 March storm around year day 66.

The tilt of the buoy with storms (probably wind on the radio mast) can be seen when the mean values of the vertical axis decrease from -1 during these storms, and the two horizontal axes increase. This indicates that the buoy is tilted over with the waves, currents and wind forcing. Taking the broadest peak during the 6-7 March Northeaster storm, the mean values indicate that the buoy is tilted about 30° from vertical. This shouldn't be a problem and is expected by the mooring and buoy configuration. However, the real surprise on year day 43 is that the vertical axis goes to zero and one horizontal axis goes to +1 g. This indicates that the buoy is tipped over on its side, and it stays there for several records. This is not normal, and is not understood. Something must have tangled around the tower, or somehow tilted the buoy, as during the largest NE storm, it didn't behave in this manner.

The storms identified by the peaks in the accelerometer variance records are tabulated in Table 5.2. This is a bit misleading as it is not the variance of the displacement or does it take into account the period of the waves, but is an indication of energetic times, and yield some information on the relative size of each event.

Table 5.2. High Acceleration Events

Event	Time and Date	Year Day	Acc Variance
1	0900 - 10 Jan 2001	10.375	0.20
2	0000 - 12 Jan 2001	12.00	0.16
3	0000 - 16 Jan 2001	16.00	0.22
4	1200 - 21 Jan 2001	21.5	0.25
5	2100 - 30 Jan 2001	30.875	0.18
6	0000 - 1 Feb 2001	32.00	0.19
7	0900 - 3 Feb 2001	34.375	0.18
8	0300 - 6 Feb 2001	37.125	0.28
9	1500 - 11 Feb 2001	42.625	~0.3
10	all day 18 Feb 2001	49-50	~0.22
11	0300 - 20 Feb 2001	51.125	0.19
12	0000 - 22 Feb 2001	53.000	0.18
13	0600 - 24 Feb 2001	55.250	0.26
14	0000 - 26 Feb 2001	57.000	0.22
15	0300 - 6 Mar 2001	65.125	0.28
16	0300 - 10 Mar 2001	69.125	0.26
17	1800 - 13 Mar 2001	72.750	0.22

The time series observations from the large 6-7 March storm are shown in Figure 5.11. The acceleration time series record is shown on top, and the vertical displacement record, obtained by a double trapezoidal integration of the acceleration in time space, is on the bottom. The peak negative displacement is cut off as probably not entirely real, but there are several waves that show greater than 12 meters peak to trough wave height, and make you glad you were not out there in the buoy's place. This wave height is typical of the 50 year Northeast storm in the Gulf of Maine.

To show the resultant signal and noise levels, a section of data when the recorder was sitting stationary in the laboratory was analyzed and the spectra of the vertical acceleration calculated and plotted as the bottom curve in Figure 5.12. This is the sensor noise level and the limit to any observation. Then, the spectra of the acceleration (top curve in Figure 5.11) from the 6 March storm was taken, and plotted as the middle curve labeled "sensor signal level." It is disconcerting to note that the low (100 second) frequency noise has risen about two orders of

magnitude above the sensor noise level as observed in the laboratory. This implies that there is some other low frequency noise in the system. It is representative of what NDBC describes as the error induced when using a strapped down accelerometer (such as used here), when the buoy is tilting in the wave field. This low frequency noise is a problem, and a limit to analyzing the data. This behavior did not appear in the motion package, and is probably due to the higher quality of the sensor, and the different movement of the fish cage in its mooring. A “stiffer” mooring constructed of two or three elastics would provide a greater downward force (three would provide over 200 lbs.) and prevent tipping of the buoy in the wave field, and reduce this spectral spillover. To do this would require the larger foam block which would provide over 1200 lbs. of buoyancy, so even if four tethers were used, there would be plenty of reserve buoyancy. This would reduce the watch circle of the buoy also, although that is of little importance here.

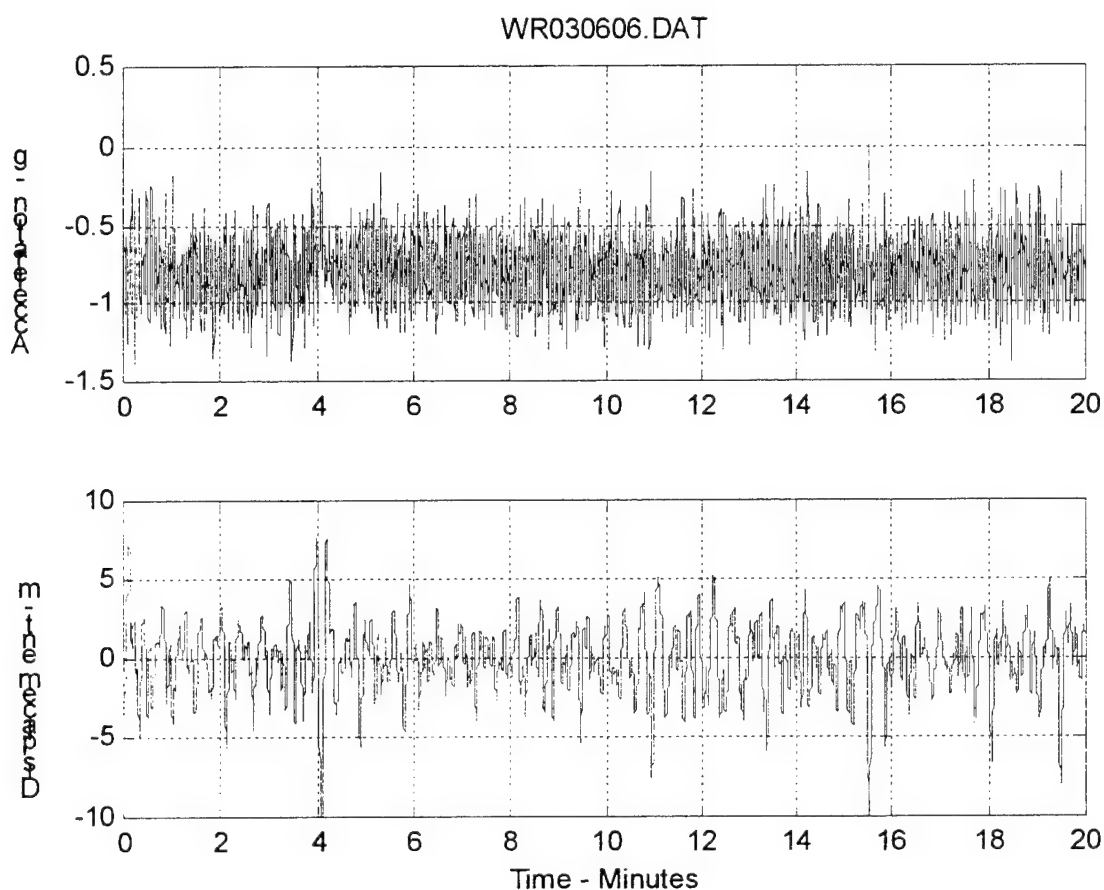


Figure 5.11. Results from the wave rider buoy for the storm event on March 6, 2001 at 0600 UTC. The top plot is the acceleration measured in g's from the vertical component (see Figure 5.10), and the bottom plot is the time space integrated displacement in meters.

Finally, the displacement spectrum from the bottom plot of Figure 5.11 was plotted as the top curve in Figure 5.12. The units are different in these last two curves so can not be directly compared. However, it is clear that the sensor and system noise is about 40 db below the signal level at the height of the largest storm observed. The cutoff observed at about 0.04 Hz is due to the 30-second cutoff of the filter used in the integration to remove the ungeophysical low-

frequency noise as discussed above. More detailed discussions of the data and analysis are being prepared in the analysis report (Irish et al., 2001b).

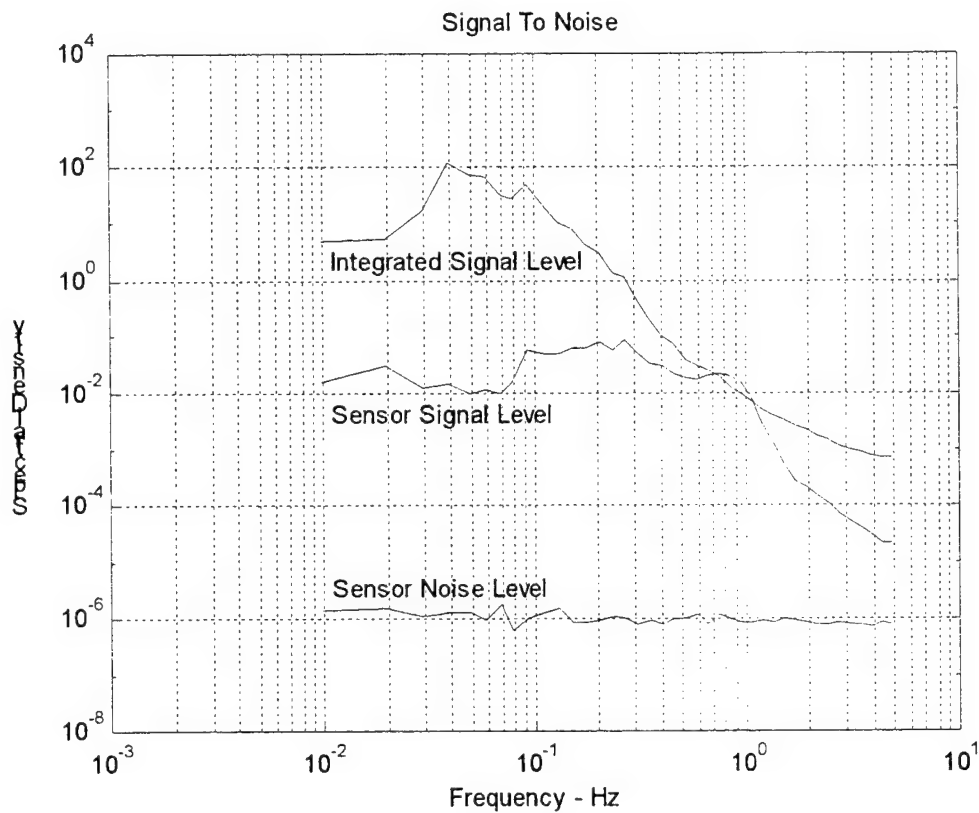


Figure 5.12. The spectral density of the signals in Figure 5.9 and 5.11 are shown in the top two curves, and the spectra of the noise with the accelerometer sitting in the laboratory with no input except gravity is the bottom curve. The noise is white and 40 db below the signal during a significant storm event. Note that the units of the bottom two curves are acceleration in g's and the top is displacement in meters.

6.0 Part 3: Fish Cage Response Monitoring

James D. Irish⁺, Arthur Newhall⁺, Craig Johnson⁺ and Glen Rice^{*}

⁺Woods Hole Oceanographic Institution, ^{*}University of New Hampshire

6.1 Motion sensor and recording system

6.1.1 Systron Donner 6-axis Motion Sensor

To measure the response (motion) of the fish cage to the wave and current forcing, a 6-axis motion package was constructed and deployed. The main motion sensor in the fish cage motion package system is a Systron Donner Motion-Pak (Figure 6.1.) It measures 6 axes of motion – three of acceleration and three of rotation. To obtain maximum sensitivity, the vertical axis is ± 2 g, and the two horizontal axes are ± 1 g. The specifications (including calibration information for the sensor used) are listed in Table 1. Data from the three accelerometers were used to calculate heave, surge and sway in response to the wave and current forcing. The three rate sensors will measure the pitch, roll and yaw of the fish cage in the current and wave field. The accelerometers in this unit are about as sensitive, but with lower noise than the accelerometers used in the wave rider buoy (see Part 2 above).

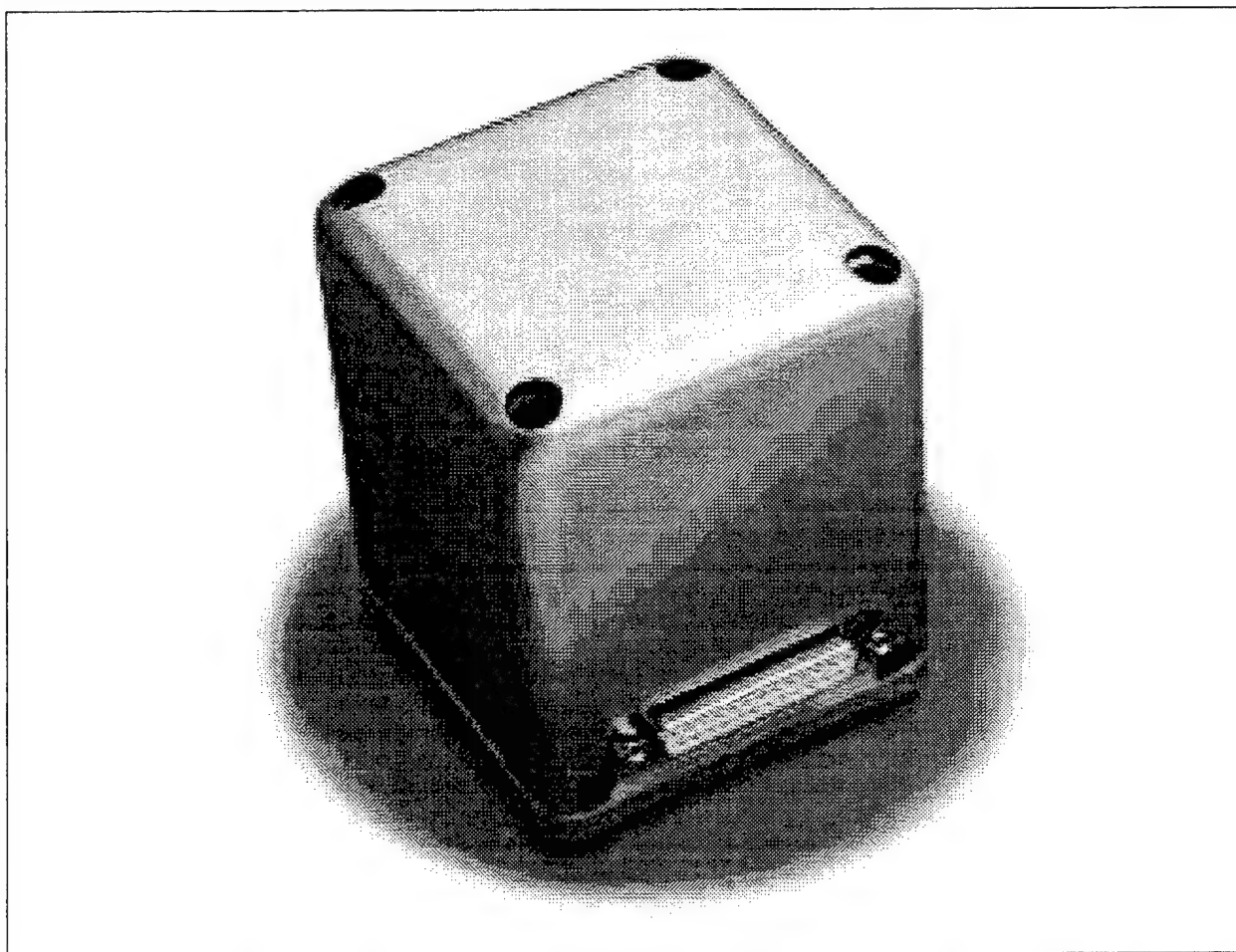


Figure 6.1. Systron Donner Six-Axes Motion-Pak is used as the principle sensor in the fish cage motion package.

Table 6.1: Motion-Pak Specifications - S/N 0548

	Angular X-Axis	Rotation Y-Axis	Angular Z-Axis	Linear X-Axis	Linear Y-Axis	Linear Z-Axis
Range	$\pm 50^\circ/\text{s}$	$\pm 50^\circ/\text{s}$	$\pm 50^\circ/\text{s}$	$\pm 1 \text{ g}$	$\pm 1 \text{ g}$	$\pm 2 \text{ g}$
Scale Factor	50.101 mV/ $^\circ/\text{s}$	49.933 mV/ $^\circ/\text{s}$	50.304 mV/ $^\circ/\text{s}$	7.504 V/g	7.458 V/g	3.742 V/g
Temp Effect	$< \pm 0.03\% / ^\circ\text{C}$	$< \pm 0.03\% / ^\circ\text{C}$	$< \pm 0.03\% / ^\circ\text{C}$	$< \pm 0.03\% / ^\circ\text{C}$	$< \pm 0.03\% / ^\circ\text{C}$	$< \pm 0.03\% / ^\circ\text{C}$
Bias (@22°C)	+0.06 $^\circ/\text{s}$	+0.14 $^\circ/\text{s}$	+0.06 $^\circ/\text{s}$	+0.33 mg	-1.76 mg	+0.83 mg
Bias Temp Effects	$< 3^\circ/\text{s}$ fr 22°C	$< 3^\circ/\text{s}$ fr 22°C	$< 3^\circ/\text{s}$ fr 22°C	100 $\mu\text{g}/^\circ\text{C}$	100 $\mu\text{g}/^\circ\text{C}$	100 $\mu\text{g}/^\circ\text{C}$
Alignment	0.21 $^\circ$	0.13 $^\circ$	0.28 $^\circ$	0.14 $^\circ$	0.18 $^\circ$	0.06 $^\circ$
Bandwidth (~90°)	>60 Hz	>60 Hz	>60 Hz	>300 Hz	>300 Hz	>300 Hz
Noise (10-100 Hz)	$< 0.01^\circ/\text{s}/\sqrt{\text{Hz}}$	$< 0.01^\circ/\text{s}/\sqrt{\text{Hz}}$	$< 0.01^\circ/\text{s}/\sqrt{\text{Hz}}$	$< 7.0 \text{ mv rms}$	$< 7.0 \text{ mv rms}$	$< 7.0 \text{ mv rms}$

The sensor is firmly mounted to the end cap of the underwater pressure case. For convenience in mounting, it was turned upside down, so that the z-axis is downward, and the acceleration of gravity appears as a positive 1 g (Figure 6.3). The x and y axis are still in the horizontal plane. As no compass was used (because the fish cage is moored with a four point mooring and couldn't turn significantly, the orientation of the pressure case and sensors relative to the mooring and earth is important, and determined by divers with a compass and visually adjusted with the fish cage. The positive x-direction was aligned with magnetic north.

6.1.2 Power requirements

The Motion-Pak sensor requires a large amount of power (Table 6.2). The power is supplied by a switched, regulated power supply off the main system's 12-15 v alkaline battery pack. This $\pm 15 \text{ v}$ supply also powers the low-pass filter board (see below) for the Motion-Pak. The sensor and filter board together draw about 0.5 amps (6 watts) from the main battery when operating, so are approximately the same power consumption as the data system. To conserve power between measurements, this power supply (and the Motion-Pak sensor) is switched off using the system's power control board (PWR CTL in Figure 6.2).

Table 6.2: Motion-Pak Power Requirements

Voltage Supply	+ 15 Vdc	-15 Vdc
Current Requirements	233 ma	188 ma

6.1.3 PC-104 recording system

The data system utilizes a PC104 computer system (Figure 6.2 and 6.3) to control sampling, sensors and storage of data. An AMPRO 386 based processor board running MS-DOS is the main controller. It uses a Real-Time Devices 16 channel 12-bit A/D converter to digitize the analog voltages from the various sensors. The digitized data is saved to system RAM via DMA under control of the A/D's clock. The A/D is easily capable of sampling 12 sensors at 10 Hz for 18 minutes 12 seconds (enough data to fill 4 pages of memory), which is then written out to hard disk. A 6 GB IDE hard drive holds the software, development system and more than a year's worth of data at these sampling rates.

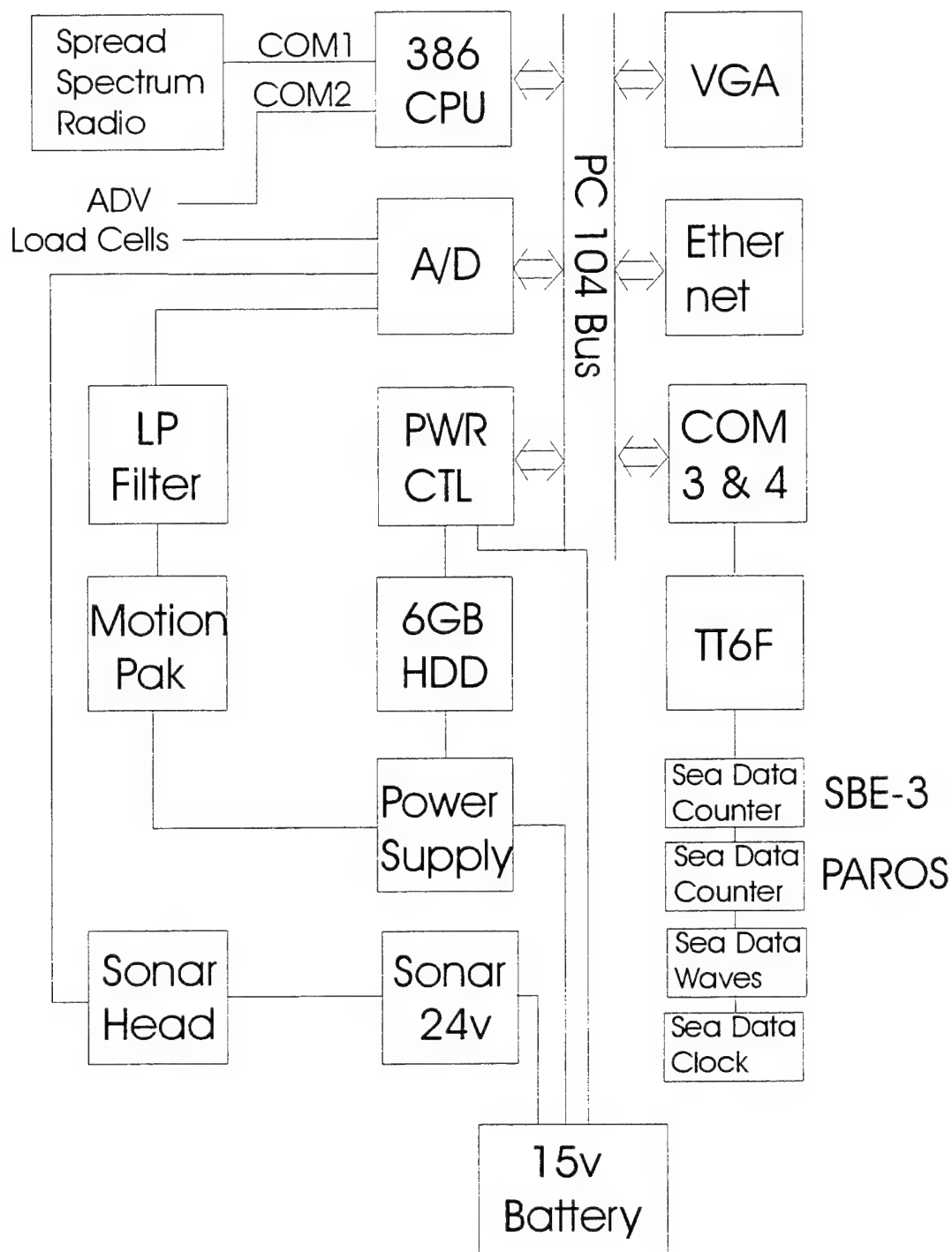


Figure 6.2. Block Diagram of the PC104 fish cage motion package data system.

The AMPRO VGA and Ethernet cards (Figure 6.2) are only plugged into the system bus when it is being run in the laboratory to dump data, check operation, develop new software, etc. These two cards draw nearly 0.5 amps together, and as they are not needed when the instrument is deployed they are removed to conserve power. To operate on batteries for long durations, additional power-saving measures are necessary and provided by a power control board (PWR CTL in Figure 6.2). This is a WHOI designed circuit for low-power applications. It has FET

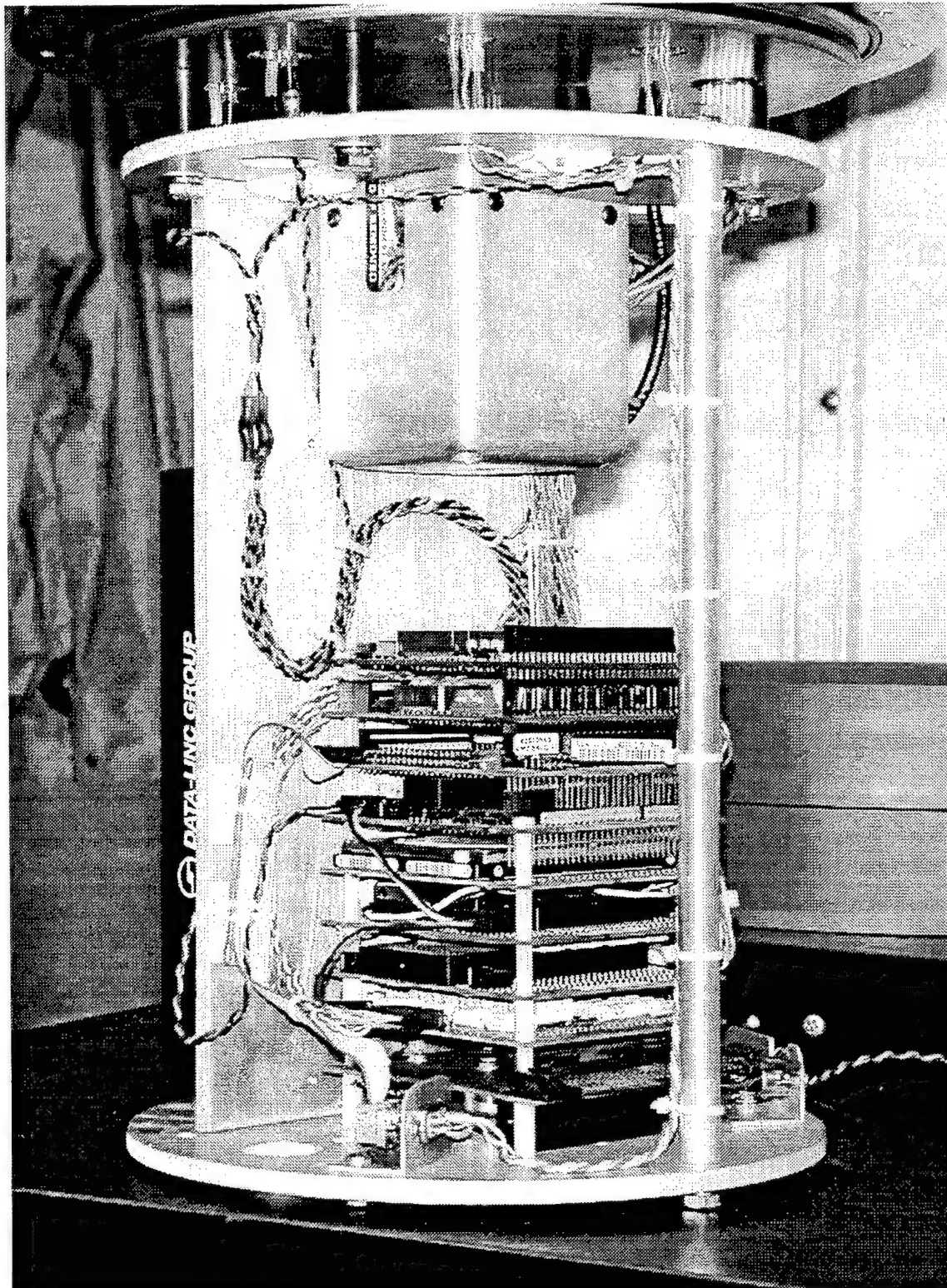


Figure 6.3. The fish cage motion package. The Motion-Pak 6 axis sensor is the cube in the top of the instrument frame. The PC104 data system is mounted below, and the Data-Linc spread spectrum telemetry radio can be seen behind the vertical plate. Connections with batteries, other sensors are through underwater connectors in the end cap at the top of the figure.

power switches and Dallas real time clock. This clock can be programmed in software to power down the entire data system, then awaken it at the proper time. This is accomplished by switching the main system power. Thus, when the system is not sampling, it is drawing less than 600 μ a. When powered up, the system draws about 0.6 amps (7 Watts) and the Motion-Pak sensor another 6 Watts when enabled. In addition, other sensors are powered from the battery under software control through the FETs on the power control board.

The data storage is on standard notebook IDE hard disk drive. A regulator off the main switched battery 12 volts supplies the 5 volts to the hard drive, and it plugs directly into the CPU board. The standard boot sectors and the autoexec.bat file are used to bring up the system from a cold start, initialize all system parameters and execute the sampling program. The basic sampling program is the last line of the autoexec.bat file, and has a number of sampling and telemetry control characters in the command line that allows the sampling program to be easily modified without recompiling. Thus, a modification to the autoexec file could be made remotely over the radio link, and the new sampling program thus implemented. The remote modification of sampling program in a PC-104 system when it is plugged into the LEO-15 and Martha Vineyard Coastal Observatories with power and two-way telemetry was worked well, so we expect it will also do so in this application. The two-way control and transfer of software and data was used with these same radios between a buoy system in a nearby building and the laboratory with computer and software documentation.

The hard disk also holds the sampling software and development system, so (with the video and Ethernet boards) the system can be used to write, compile and test software as well as run it. The hard drive is partitioned into 2 GB sections as required by DOS, and the second drive is used to store the data. The data files are stored under subdirectory by month to get around the DOS 511 file limit to a disk directory, as subdirectories are dynamically allocated. There is no real limit to the number of files that can be stored on them and they could all be stored in one subdirectory if desired. For convenience, the file name is created from the data and time to make a unique tag on the data. The two digit numbers for the year, month, day, and hour make up the main name with the minute as the extension. Thus 6 March 2001 at 15:00 UTC would be "01030615.00." Thus it is easy to find a particular date and time in the resulting series of files recorded. A similar method is used in the load cell and wave rider recorders, where instead of the year, alphabetical characters represent the instrument, e.g. WR for wave rider.

There are several power supplies in the system that are controlled by software through the power control card. These power supplies are set up to power the disk drive, the motion package filter board and sensor, load cells on the fish cage, and the scanning sonar system. This last capability was added so that we could attach one of our fan or pencil beam sonar systems, and log the data on the data system and power it through the main batteries. The design of this was borrowed from our sediment transport work (Irish et al., 1999, and Irish et al., 2001).

Unlike the accelerometer in the wave rider buoy, the Motion-Pak does not come with internal low pass filters to prevent aliasing, so a separate filter board was constructed and added to the PC-104 stack (Figures 6.2 and 6.3). This board was designed at WHOI for Mark Grosenbaugh for use with the Systron Donner Motion-Pak, and we were fortunate enough to find a spare PC board and were able to populate it with appropriate components for this application. The board holds eight 4-pole low-pass Butterworth filters and power supply. The system is set with a 3 Hz cutoff to prevent aliasing at the system 10 Hz sampling frequency. This system is powered from the regulated supply for the Motion-Pak and is switched with the sensor power.

6.1.4 Software and Sampling Program

The system was designed to be capable of sampling to resolve the full spectrum of the expected wave forcing and system resonance. A 3-hour burst interval was selected so as to be compatible with the standard wave spectral time scale, and to minimize the system power and data storage requirements. A 20-minute burst is recorded by the wave rider and the load cell systems, but for this fish cage motion system an 18 minute 20 second interval was selected. This was the result of borrowing much of the software from Ken Prada and Mark Grosenbaugh at WHOI, that writes data in blocks of one page of DOS memory or 65,536 Bytes. 10 Hz was selected to resolve waves and any system resonance. This resulted in a 18 minute 12 second record being obtained from the 6 axes motion package, optical backscattering sensor (see environmental sensors below), and the two load cells on the fish cage (see Part 1 above). It was decided to leave the sampling program as it was and accept the shorter record as it nearly gives the same record length as the wave rider and load cell recorders, and reduce system power by 10% (a critical factor in this system). The number of records taken is set by a parameter in the control line in the autoexec.bat file. Thus, the sample length can easily be set to be multiples of 4 minutes 33 seconds. If the number of sensors sampled is changed (requiring software modifications), the record length will change.

The power control board is set to wake the system on the hour every three hours. The system boots in about 20 seconds, then samples the battery voltage after the system boots, but before it starts running the main sampling routine. If the battery voltage has decreased to 10.0 volts (see Figure 6.4), then the system does not sample, but goes back to sleep and tries again at the next scheduled sampling interval. This prevents the system from discharging the batteries to the extent that it might effect system operation and damage the data already stored on the hard disk. If the battery voltage is acceptable, the system powers up the sensors (load cells, OBS, Motion-Pak and filter) then starts digitizing the results for 18 minutes 12 seconds. The data is then dumped from RAM to hard disk (with file name convention as mentioned above). The system then checks to see if the telemetry flag is set in the autoexec.bat file. If so, it powers up the Data-Linc spread spectrum radio, opens the file and sends the data out the radio. If not, then the system goes back to sleep until the next sample interval.

6.1.5 Spread spectrum telemetry link

It was thought desirable to telemeter the fish cage motion data to shore for analysis and input into the fish cage management program. A Data-Linc Group SRM600 frequency hopping, spread spectrum radio modem was used (see Parts 1 and 2 above). This system would also allow two-way telemetry between the fish cage and shore to allow the sampling plan to be changed in response to storms to optimize sampling and battery life. To coordinate the normal telemetry of data at the UNH-OOA site, the motion package was assigned the telemetry time starting at 18 minutes after the hour. The 18 minutes time was most compatible with the PC-104 data system, as with the boot process, and its sampling scheme, it was ready to telemeter data at about 18 minutes 25 seconds after the hour. The telemetry of the 18-minute burst takes about 4 minutes, so the system would be completed sending data by the time that the environmental buoy had collected its data and was ready to telemeter it. If the weather was poor and the telemetry link slow, then the transfer of data could extend out of the allocated time slot. Finally, after telemetering the data, the system would program the real-time clock for its next wakeup time, and put the system to sleep.

6.2 Mounting, battery and electronic pressure cases, antenna

6.2.1 Battery supply and life

The entire system when operating is quite power hungry, drawing about 1.1 amps at 12 volts for the duration of the burst, and 0.76 amps during telemetry. Thus, an average power over a 3 hour sample interval is about 0.128 ah, or just over 1 ah per day (1.03ah). The most efficient power (cost, weight and size) has proven to be the standard alkaline "D" size flashlight battery. They can be combined in packs of 10 cells each to provide the basic 15-volt supply, and packs paralleled together to provide the power required. One problem with drawing this level of power out of alkaline batteries, is that their capacity decreases, but with multiple packs, the decrease is minimized as all packs share the load. WHOI has designed and successfully used a basic 120 ah pack of batteries for several projects. These have powered the PC104 systems, sensors and telemetry without difficulty in similar applications. Therefore, the power would be built around systems of these packs. If a single pack were to be used the life would be significantly reduced by the high drain. If the full 4 packs were used, the life would be near full battery capacity.

For the two field deployments, only one battery pack was used. Because we were unsure of its life (estimated at 6 weeks), we decided to deploy for about 1 month. After 21 days the system was recovered, and the battery was in good condition. The discharge is shown in the voltage as a function of time plot (Figure 6.4). During the summer this battery was again connected to the system and fully discharged to the point that the software cutoff stopped sampling. The battery pack voltage was down to nearly 10 volts, and had lasted another 29 days. Thus, we were able to obtain nearly 50 days energy from that battery pack.

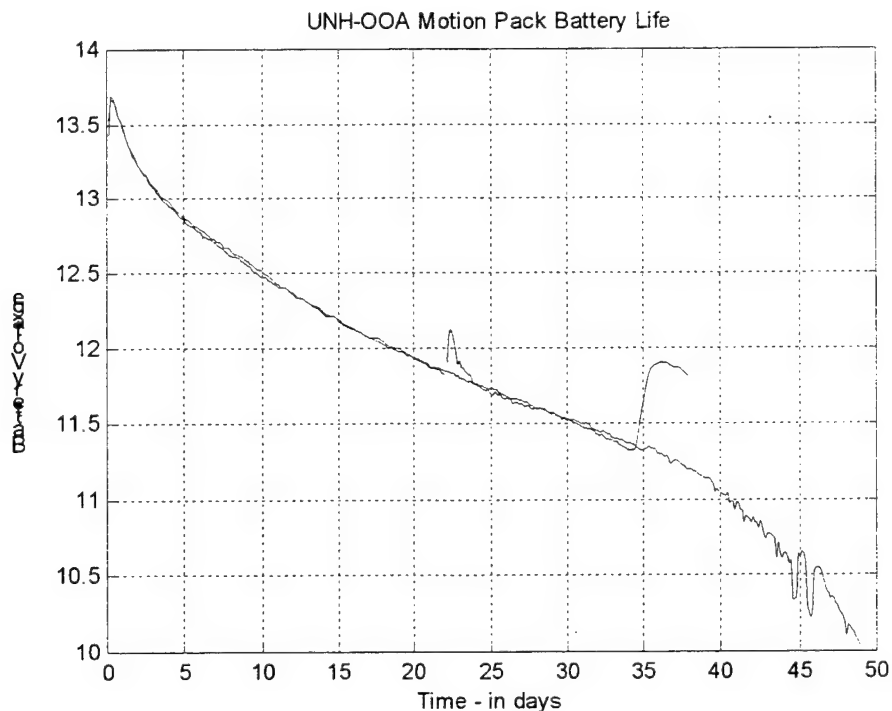


Figure 6.4. The battery discharge curve for the motion package for its two deployments, and subsequent laboratory life test for the battery used in deployment 1.

6.2.2 Pressure cases

The pressure cases (Figure 6.5) for the electronics and batteries are the same size, with the battery case holding two of the basic battery packs, and the electronics, only the motion package sensor and recording electronics. To provide power for a four-month deployment, it was determined that four battery packs would adequately supply the power with safety and derating for power usage. Thus two pressure cases would be used for batteries and one for electronics. Underwater connectors would connect the batteries to the electronics, and the batteries could be unplugged, removed from the fish cage and new batteries (already in spare pressure cases) installed and plugged into the electronics. These pressure cases with batteries were 24 inches tall (connectors extra) and weight about 120 lbs each. The electronics pressure case weights less than 30 lbs.



Figure 6.5. The battery pressure case (front left), the electronics pressure case (front right) and the mounting silos (rear) for the motion package on the top of the fish cage central spar.

6.2.3 Mounting silos

The servicing plan for the fish cage motion package was to construct it to last for 4 months so that it would not have to be serviced during the winter months. The package would be mounted on top of the fish cage, which would be at the surface, so that we could telemeter the data to shore, but would be capable of being fully submerged without flooding. The servicing would have to be done by divers as the normal servicing vessel could not approach the fish cage

when it was at the surface without the potential for damaging the net. Therefore, the diver would swim to the fish cage with a line, pull a battery over with the line, and lift it up into a silo that was bolted to the top of the fish cage. The silo would allow the battery to be placed in it, then finally secured later without danger of losing the battery over the side or danger to the diver. The two batteries and electronics would thus require three silos. In addition, there are wires coming up from the environmental sensors, and load cells that need to be routed to the electronics, and the telemetry package from the Northeast grid corner load cell package (see Part 1 above) that need to be accommodated. Therefore, a four-silo arrangement as shown in Figure 6.4 was selected [see Appendix 9.5.2]. There is a connecting pipe between the silos to run wires, and tops that close to prevent wave damage to the wires and connectors in the top of the pressure cases. The silos would be freely flooding and be the structural part of the system, while the pressure cases would contain the batteries and electronics would keep things dry and operational.

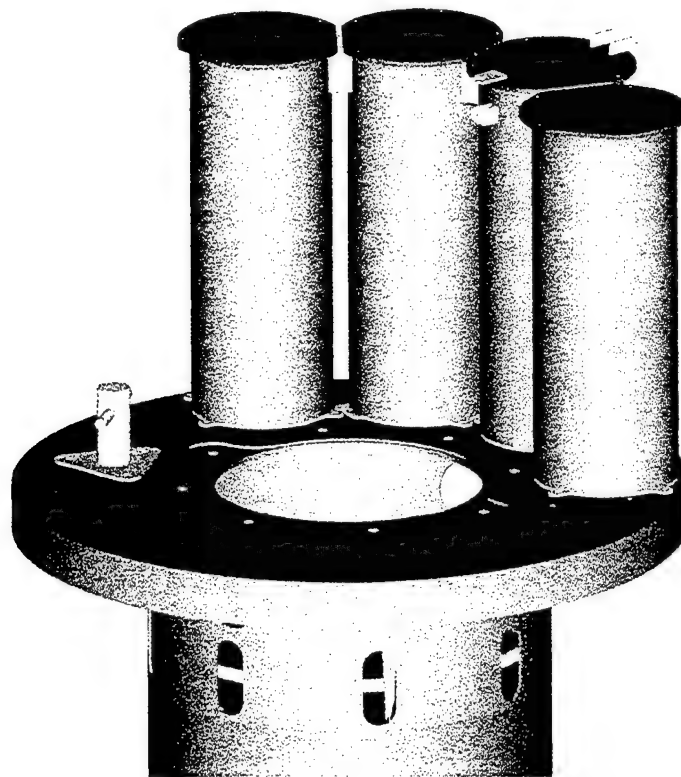


Figure 6.6. A drawing of the four silos (Figure 6.5) mounted on the fish cage top plate. The tubes between the silos can be seen at the top, and one lid fastening and hinge is shown. For scale the top plate of the fish cage is 5 feet across and the silos are 35" tall.

6.2.4 Spar in-water mounting system

However, the best planning often misses some important fact. We had been using the PC-104 systems in buoys and submerged without problems. While we were preparing this system for deployment, another group at WHOI was testing a PC-104 system on the WHOI dock in December. The temperature dropped below freezing and the hard disk could not spin-up as the lubrication became too viscous. With this warning, it was decided that we should try for an in-water mounting solution, as the fish cage was to be at the surface during the winter. The

coldest the water gets at the UNH-OOA site is 4° C, so we would expect no problems. The implications of this were (1) that we could not use telemetry, as we would have to plug and unplug the coax connector underwater, (2) that the deployments would have to be shorter as the battery pack would have to be in the electronics pressure case, (3) the environmental sensor interface would have to go as the space would be needed for the battery pack, (we could still record the load cells on the fish cage), (4) we would not put the silos on the fish cage, so we could not use the load cell telemetry system (see Part 1 above). There was some concern that the silos mounting plan had gotten a little "out of hand" and that the added weight of the silos, batteries, electronics and antennas would begin to effect the fish cage itself. The smaller mounting system underwater would solve these problems, but required diver servicing more often. As UNH was willing to undertake this, we could get the data recorded with the existing hardware without rebuilding or reworking.

Attaching the motion package to the spar saved space on top of the spar, and kept the hard drive in warmer temperature, helping to insure its operation. A frame was custom made from concrete reinforcing bar - rebar (Figure 6.7 and 6.8) to contain the motion package and to fit onto the side of the spar. The rebar was covered with fire hose as electrical insulation to isolate it from the aluminum pressure casing of the motion package to reduce dissimilar metal corrosion. The frame was attached to the spar with two-inch nylon ratchet straps approximately ten feet from the top of the spar. The motion package was placed inside the frame, and attached using one-inch nylon ratchet straps. A pigtail with an underwater plug was attached before deployment for connection to the load cells.

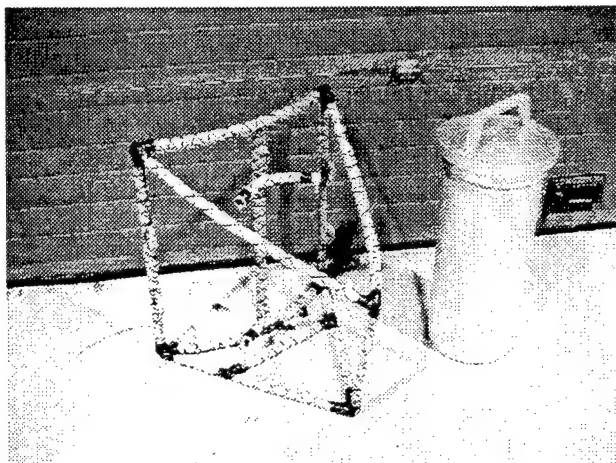


Figure 6.7. The mounting frame on the fish cage central spar (left) that holds the motion package (right). The frame is strapped to the central spar of the fish cage.

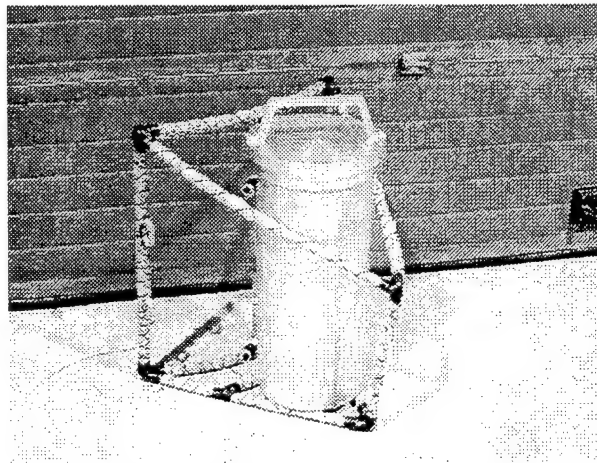


Figure 6.8. The motion package in the fish cage mounting frame. The pressure case is held firmly to the frame by straps.

6.3 Environmental Sensing Package

6.3.1 Sensors (pressure, temperature, OBS and currents)

To supplement the environmental buoy and gain additional information on the environment in the fish cage, additional sensors were mounted in the fish cage itself (Figure 6.9). The sensor suite consisted of a Paroscientific pressure sensor, a Sea Bird temperature sensor, a Sea Point optical backscattering sensor and a Nortek Aquadopp acoustic Doppler current meter.

The Paroscientific pressure sensor was housed in a PVC pressure case, and in addition to the pressure sensing quartz crystal, also has a temperature sensor to correct for pressure sensor temperature effects. The output is a frequency proportional to pressure and a frequency proportional to temperature. These two signals were sent up the cable and digitized in a separate electronics package (see Figure 6.10) in the motion package electronics pressure case. The pressure sensor was sampled in two ways. First, half hourly averages of pressure were made and saved in a Tattletale 6F microcomputer. Thus, the system was powered up continually, but only drew about 20 ma with all sensors powered. In addition, when the motion package was burst sampling the Motion Pak, it raised a logic line to the environmental sensor system so that it would burst sample the pressure sensor for waves at 10 Hz. This data was again stored in the Tattletale 6F data logger until the end of the burst, when the full data set was transferred to the PC-104 data system for storage and telemetry.

The water temperature was measured with a Sea Bird SBE-3 sensor that output a frequency-modulated signal. It was digitized by the environmental electronics system to provide half hourly averages. This would provide the temperature at about the middle depth in the fish cage to assess the environment that the fish were seeing. Also, the Sea Point OBS sensor would sample the particulates in the water column in the fish cage (as well as any fish that swam in front of it). Interpretation of this would be difficult as the sensor is sensitive to biofouling, and fish swimming in front of the sensing window. However, it would be a measure of the water clarity that could be compared with the observations made on the environmental mooring (Bub et al., 2001).

The last sensor was an acoustic Doppler current meter. Of concern was the flow through the cage, and particularly the velocity at the central spar, which is a large drag. If the fish net were fouled, this velocity would decrease. Good knowledge of this velocity would improve the modeling effort, and allow better estimates of the blockage of the flow by the extent of biofouling on the net. The sensor would be set to sample two horizontal components of velocity and a third at 45 degrees upward which would allow calculation of the three components of velocity. The sampling volumes would be a meter or two removed from the central spar to get out of the immediate flow effects. This instrument would store the data internally as well as send it to the motion package data system for telemetry to shore.

6.3.2 Mounting on fish cage

To attach the sensors, a system had to be devised that would allow this to be done when the fish cage was fully assembled in the water. The mounting plate that holds the sensors bolted to the through-spar bolt holding the feeding tube in place on the opposite side of the spar. Welded to this plate was a tube that ran up the spar. The other end of the tube was bolted to the top plate of the spar. The wires to the sensors were run through the pipe for protection. The sensors were attached to the mounting plate with PVC blocks (see Figure 6.9). The sensors were installed in the fish cage during the June 2000 assembly and mooring at the UNH-OOA site. The cables were installed at the same time and were coiled up in the space between the top of the buoyancy and the top plate for storage.

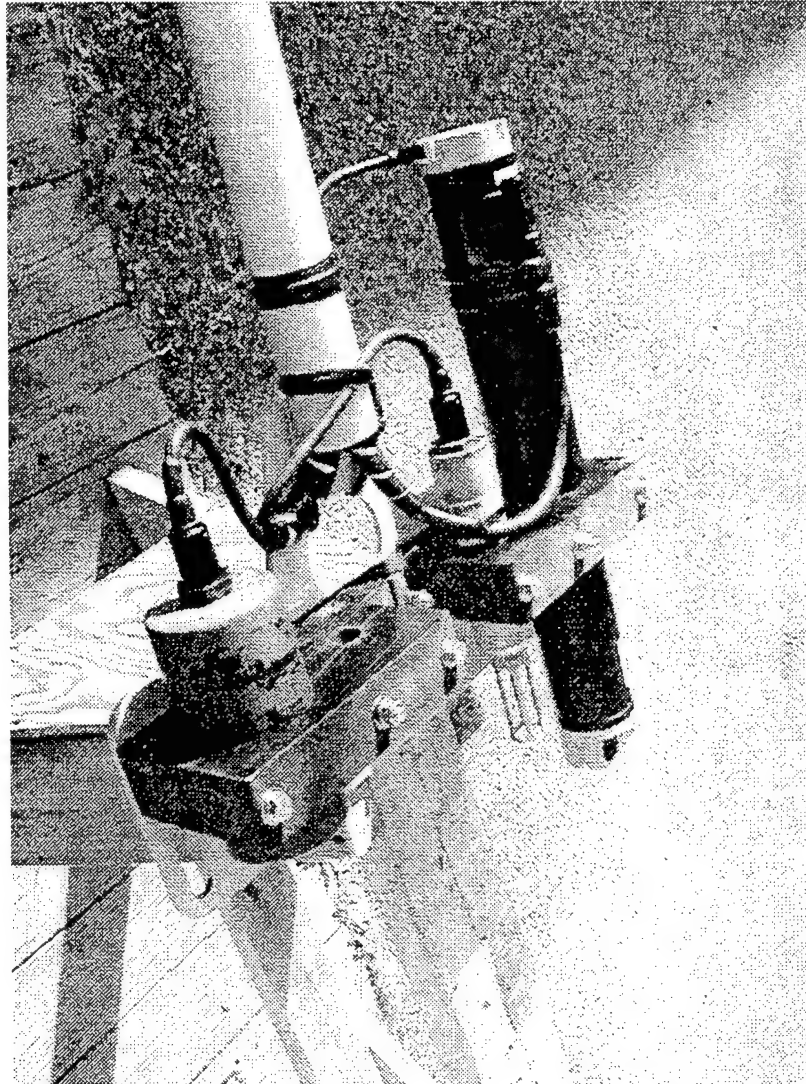


Figure 6.9. The environmental sensor package on its mounting bar before assembly on the fish cage spar. The Paroscientific pressure sensor is on the left, the Nortek Aquadopp acoustic current meter on the right with the Sea Bird temperature sensor just to the left. A Sea Point Optical Backscattering sensor is shown taped to the Nortek (high on the right).

6.3.3 Environmental Sensor Data system

The environmental sensor electronics package consisted of a series of Sea Data boards with clock, frequency counter, a special "waves" board with frequency multiplier phase lock loop and timing (Figure 6.10). The system was hard wired together and when started would run on its own. It was set to count the input frequencies of the pressure sensor, the pressure sensor temperature and the water temperature over half hour intervals to get cage depth and conditions. Upon command from the PC-104 system, the hardware would burst sample the pressure sensor.

The Sea Data clock board controls the counter boards and basic timing, and latches the counts into serial shift registers for output. For this application, a Tattletale 6F microcontroller was used to shift the data out and save it for three hours, then send the data to the PC-104 data system through a COM port (Figure 6.2). A latch on the Tattletale interface board woke the

system up when data was available to shift out, and format for telemetry. During the 18-minute motion package burst sample, another latch system shifted the environmental sensor system into burst mode where the pressure sensor was sampled at 2 Hz and the data stored for telemetry with the half hourly averages. This pressure observations would complement the sensor on the UNH environmental mooring (Bub et al, 2001) and give an indication of the relative motion of the fish cage as well as the mean depth changes with time.

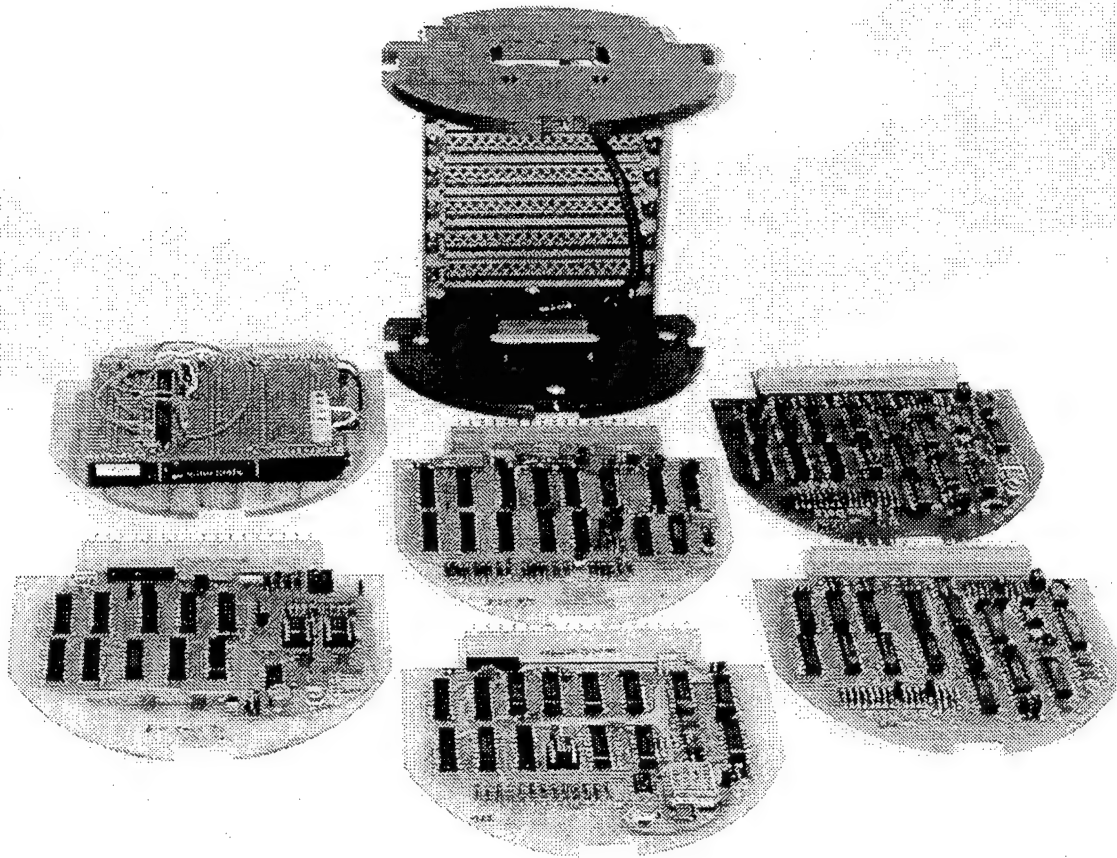


Figure 6.10. The Sea Bird/Tattletale environmental sensor data system. The rack holding the cards is shown in the rear. The Tattletale 6F recorder and interface logic is shown in the left rear. The clock is in the center front and the two AC counter boards on the right. the special waves control board is center rear, and another counter card front left.

However, because of the temperature problem with the hard disk drive that was not realized until the system was constructed and ready to deploy, the change that put the battery in the electronics pressure case necessitated the removal of the environmental sensing package. It is ready to reconnect and interface with the PC-104 data logger any time. The method of distributed processing (using dedicated low-power microprocessors) to reduce power needs for the PC-104 system often works well in this type of sampling application, but we were not able to take advantage of it in this deployment.

6.4 Deployments, Operation and Preliminary Results

The revised motion package system with battery and electronics in one pressure housing was delivered to UNH after Christmas 2000. The startup procedure was reviewed so that UNH personnel could start and deploy the motion package without WHOI involvement when a good weather window became available. The initial setup set the Dallas real-time clock relative to WWV, set the command line in the autoexec.bat file for the sampling program and tested to see that the system cycled properly. Therefore, all that needed doing to start the system was to plug in the battery and close the pressure case. The motion package system was started on 18 January 2001 and deployed for a first good sample on bottom of 1800 UTC, 18 Jan 2001 (see Table 6.3).

Table 6.3. Motion Package Start and End times

Deployment	First Sample	First "On Bottom"	Last "On Bottom"	Last Sample
1	1500, 18 Jan 2001	1800, 18 Jan 2001	1200, 09 Feb 2001	1200, 09 Feb 2001
2	1800, 09 Feb 2001	1800, 09 Feb 2001	1800, 15 Mar 2001	1500, 19 Mar 2001

All times are in Coordinated Universal Time (UTC)

We were concerned on the life of the motion package with the single battery pack (12 parallel packs of "D" cells) in the electronics pressure case. Therefore, a first deployment duration of about 1 month was selected to assure that the battery did not go flat, and to measure the battery discharge curve to estimate optimum deployment lengths. At the first weather window (9 February) when the UNH boat was available, an extra battery, support equipment (video and Ethernet cards), notebook computer, and monitor and keyboard were loaded on the R/V Gulf Challenger to service the motion package. Divers recovered it from the fish cage, the system was checked, and had recorded good data for the first deployment. The data was dumped to the notebook computer over the Ethernet link, and the data checked. As the disk drive had plenty of storage space, the data was left on the disk as a backup to the data dumped to the notebook computer. The new battery was installed, the system checked and redeployed (see Table 1). Only one sample was lost during this servicing.

After the large 6-7 March 2001 storm, it was decided to recover the motion package and recover the data to see what the motion of the fish cage was. Also, during this storm, the counter weight broke off the fish cage, and it was riding at the surface for about a month until a new counter weight was obtained and attached (see mooring tension in Figure 4.30). The system was recovered on 15 March, and on 19 March WHOI brought support equipment to UNH and dumped the data from the motion package, backed it up on CD-ROM, notebook and desktop PC.

The data system was checked for calibration of the A/D, and then the data was normalized using the factory calibrations. A basic burst record as recorded by the 6-axes motion package is shown in Figure 6.11. The acceleration observations are shown in units of g 's (9.8 m/s^2) and the angular rate (rotation) observations in degrees/second. The basic statistics of these records for 6 February at 0300 are shown in Table 6.4. This event was selected as being the largest storm (see Figure 5.11 from the wave rider buoy) from which we have motion package data with the counter weight in place.

The vertical axis shows nominally +1 g acceleration due of gravity (the + sign because the Motion-Pak was mounted upside down). This sensor measures the heave or vertical motion of the fish cage on this axis, and is seen as fluctuations about 1 g mean. To the first order, these will be a scaled version (due to system response) of the wave forcing amplitudes.

The x and y accelerations are centered near zero and measure the surge and sway of the fish cage in the wave and current field. That the y-axis is not centered around zero, is an indication of a tilt in the fish cage in this axis, but not in the x axis. When the cage was placed in its mount on the fish cage, the divers oriented the pressure case with the x direction aligned approximately with magnetic North (16° magnetic variation at this location). Therefore, there must be some error in alignment, as the fish cage would tilt due to tension variations in the mooring lines due to uneven tensioning of the fish cage, and currents on the system. This tilt would be aligned at 45° true with the mooring lines, and not along one of the motion package axes if the x-axis were aligned with magnetic north.

The three rate sensors (the bottom three panels in Figure 6.11) measure the rotational speed around each axis. Thus, the z rate motion is back-and-forth motion in the horizontal plane around the z-axis, and the x and y axes are the pitch and roll motions around these two axes. As might be expected the x and y rates are higher than the z rate, as the mooring is restricted to rotational motions around the vertical axis by the mooring system (see Figures 4.1 and 4.2).

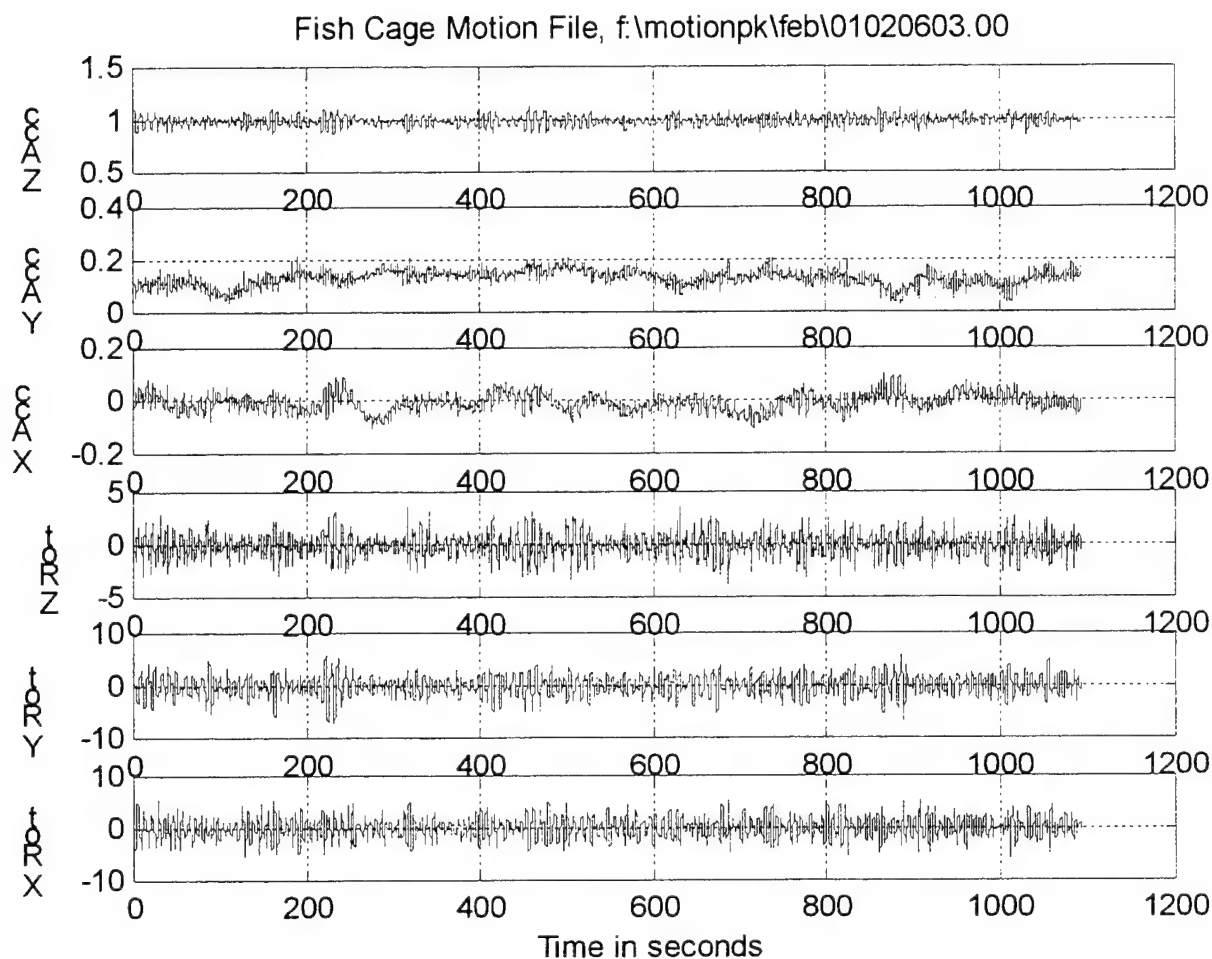


Figure 6.11. Time series plots from the 6 February 2001 storm. The top three panels are the accelerations and the bottom three the rotation rates. The statistics of these records is given in Table 6.4. Note that the scales of the panels are different.

Table 6.4: Statistics for 6 February 2001 storm record shown in Figures 6.14, 15, 16 and 17

	Zacc	Yacc	Xacc	Zrate	Yrate	Xrate
Maximum	1.1285	0.2137	0.0972	3.6681	6.0617	5.5520
Minimum	0.8481	0.2137	-0.1115	-3.8017	-7.1320	-5.7468
Mean	0.9900	0.1305	-0.0104	-0.0809	0.0499	-0.0074
Std Deviation	0.0438	0.0288	0.0327	0.9144	1.8241	1.9046
Units	g's	g's	g's	%/s	%/s	%/s

The power density spectra of the three acceleration records (Figure 6.11) is shown in Figure 6.12. The three acceleration record spectra have different shapes. The most energetic record, as might be expected is the vertical, which shows a peak at about 8 second period (0.125

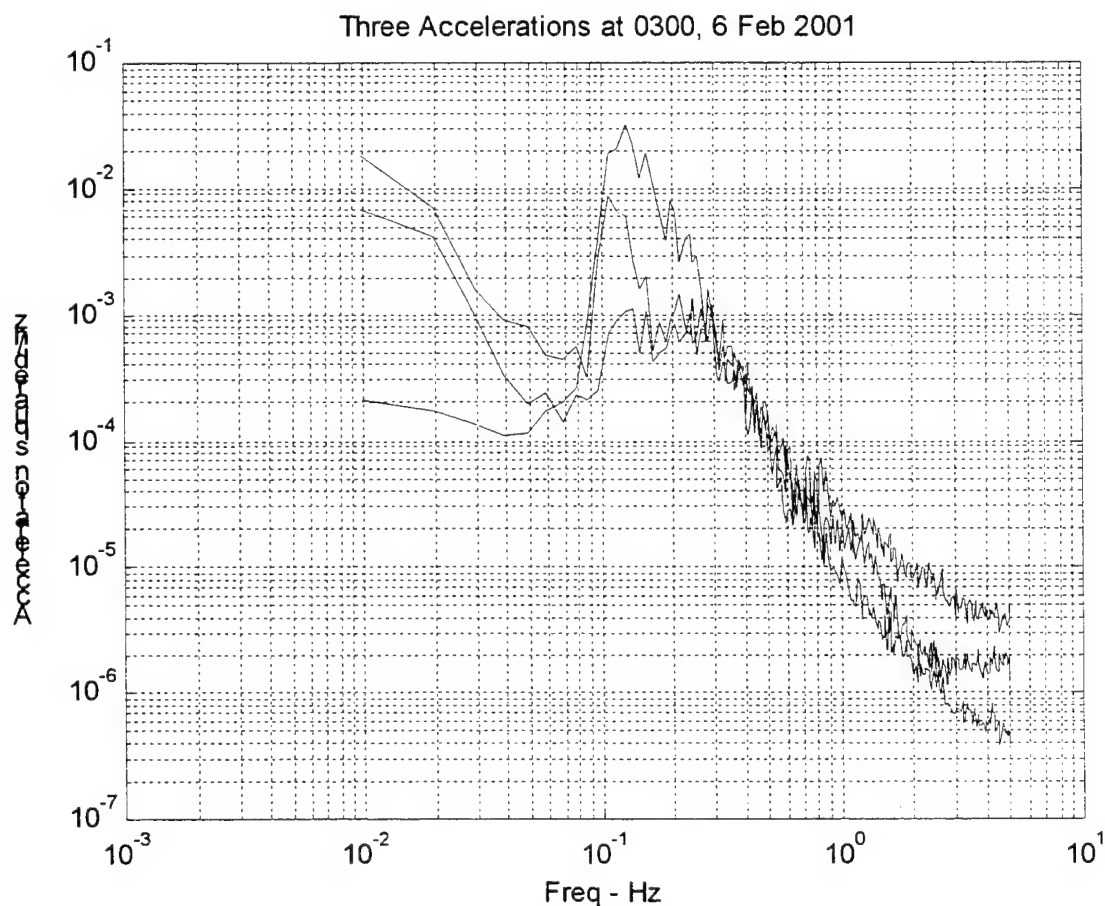


Figure 6.12. Spectra of the three acceleration records shown in Figure 6.11. The low frequency signal is mostly sensor noise, and the high frequency falloff where the three axes are equal is probably also noise. The signals show a broad peak in the vertical record which has the most energy, a shaper peak around 8 seconds in one horizontal axis, and a broad flat area out to about 3 seconds period in the other horizontal axis. At about 3 seconds period, the three observations become equal.

Hz) and a f^{-4} fall off out to 1 Hz. The horizontal axes are quite different. One shows a slight rise to a plateau at 0.1 Hz, and flat across until it intersects the f^{-4} fall off in the other tow records. The last sensor shows a sharp peak at 0.125 seconds, then falls off more rapidly, and levels out with the second sensor before intersecting and falling off with the other two records.

Another interesting feature is at low frequencies where the vertical acceleration shows a plateau some 25 db below the peak. This is the sensor noise floor for the measurement and is quite reasonable. The two horizontal acceleration spectra show increasing low frequency energy that may be due to the horizontal current and mooring motion response.

The spectra of the rate sensor records (Figure 6.13) shows a different picture. The spectra again have a peak at the 0.12 Hz, but the vertical axis shows the lowest energy. However, this appears to level out in the 0.4 to 1 Hz region, then fall off rapidly. The two horizontal axes rotation spectra appear to be very nearly the same in energy and spectral behavior. Again the low frequency energy is more than 20 db below the signal levels and well behaved with no indications of spectral spillage as observed in the wave rider data.

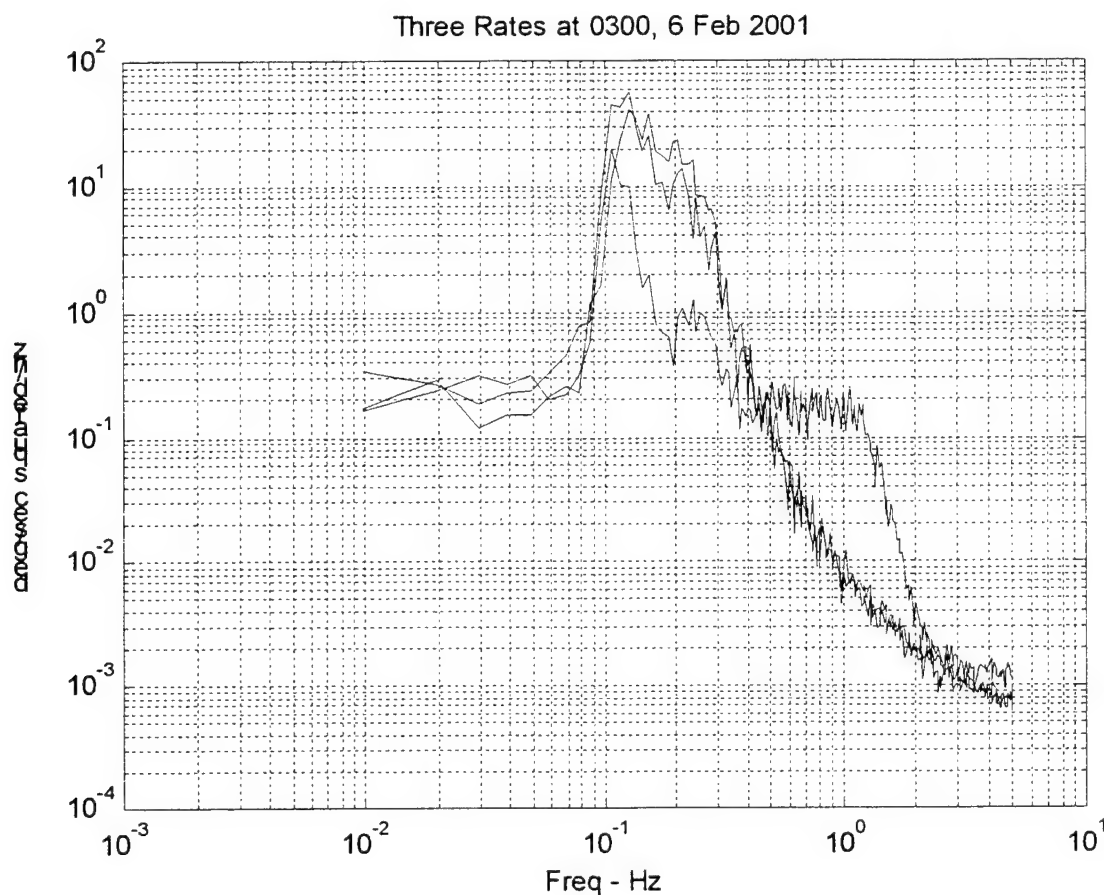


Figure 6.13. Spectra of the three rate sensor records shown in Figure 6.11. The vertical axis shows the least energy at the 8-second wave forcing, but an interesting flattening out of the spectra in a broad back around 1 Hz. The two horizontal rate records are very similar with a smooth fall of without the flat plateau in the vertical rate sensor.

To get a general idea of the entire record from the motion package and show the temporal change in statistics, the means and standard deviations of the six outputs of the Motion-Pak during each 18 minute burst were calculated and plotted in Figures 6.14, 6.15, 6.16 and 6.17. The mean of each burst record (e.g. as shown in Figure 6.13) show little effects of the storms seen in the standard deviation record (Figure 6.15), but do show a sudden change in values and behavior on 6 March when the fish cage counter weight was lost and the fish cage rose to the surface and was more strongly influenced by the waves. The fish cage also shows a tilt at this time that appears in changes in the mean values (change in orientation relative to gravity). The records indicate a change from nearly 0° tilt to about 18° tilt. This tilt is probably due to the unequal tension in the mooring lines due to either unequal initial tensioning or tilt of the mooring system with the mean currents. This record is further indication that the mooring was not deployed so that all four legs had the same tension as was suggested by the load cell records (see Part 1 above). The sinusoidal record after the fish cage counterweight was released was tidal, and shows the changes in tilt with the tidal currents. Although these variations were present earlier, they were much damped (due to the counter weight and position of the fish cage).

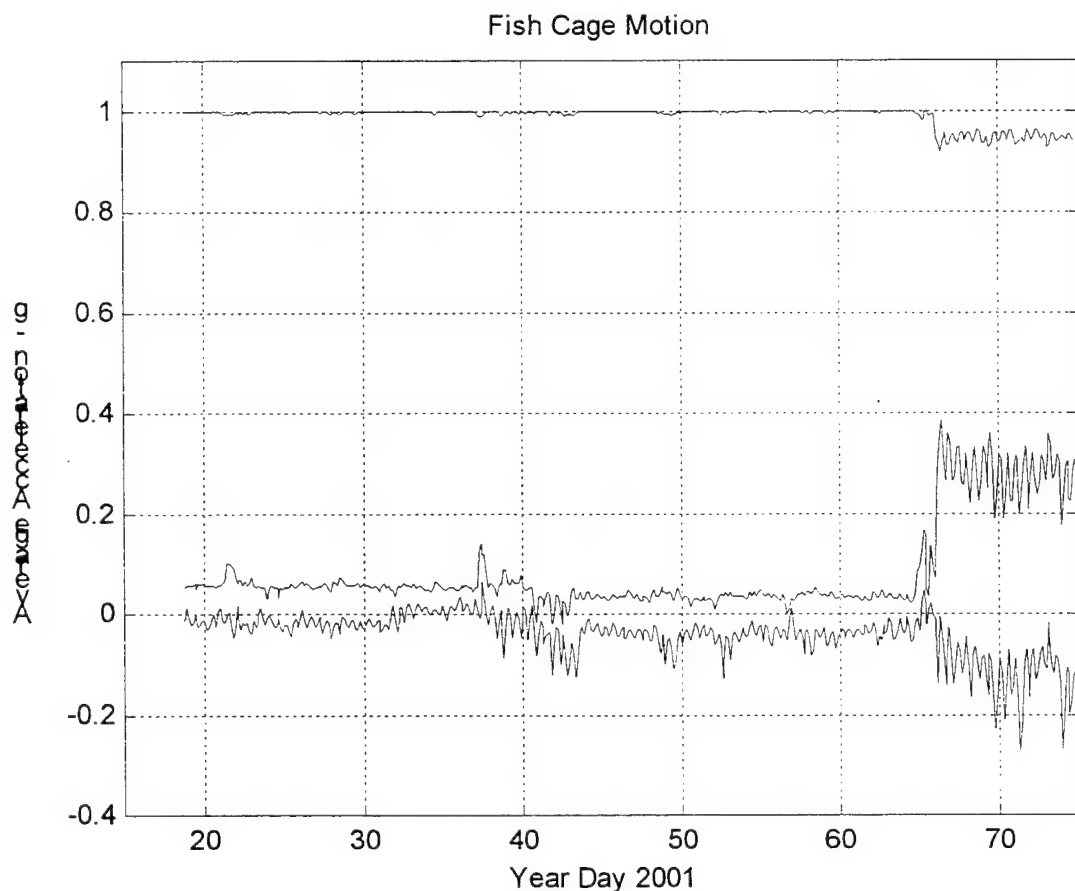


Figure 6.14. Fish cage motion package shown by the means of the three acceleration sensors for each 18-minute burst. The sudden change about year day 67 is when the fish cage counter weight came off and the cage tilted.

The motion caused by the storms is more obvious in the time series plot of the standard deviation of the accelerations in each burst as shown in Figure 6.15. The 6 February storm, which appears around year day 37 and whose record is shown in Figure 6.11, produces the strongest response until the 6-7 March storm and, which is also the strongest storm in the wave rider acceleration records (Figure 5.11). There is a visual correlation between the peaks in the waves as indicated by the wave rider acceleration in Figure 5.11 and the response to these waves as seen in the motion package accelerations as shown in Figure 6.15. There are a number of storms that excite the cage from different directions, with different frequencies. These will give us a representation of various forcing and response to understand the mooring and fish cage dynamics and aid in the validation/improvement in the models. The nature of the record changes after year day 64 with the loss of the counter weight where the fish cage is observed to move more, even in the relatively calm periods between the storms. The frequency space transfer function, is the fish cage response function to the wave forcing, and is a critical measurement for the modeling effort. Further discussion of this is put off until the data report (Irish, et al., 2001).

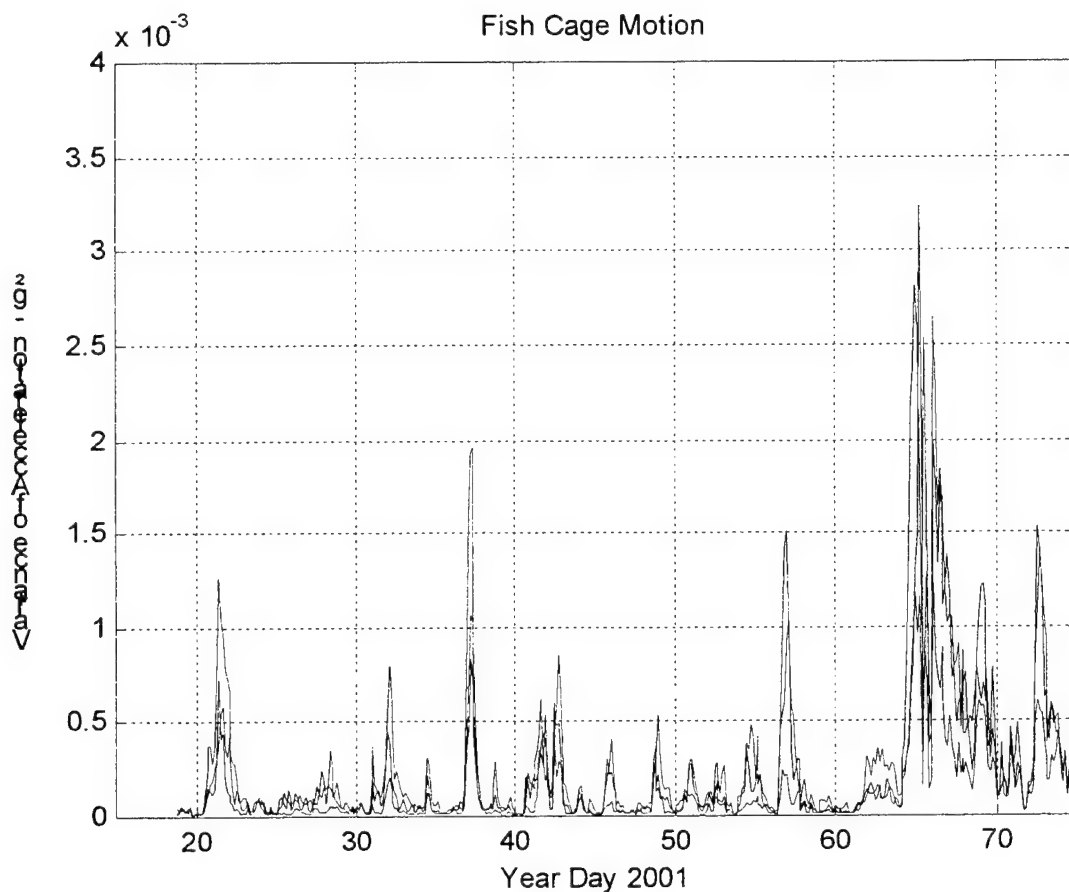


Figure 6.15. Fish cage motion package variance of the acceleration during each 18-minute burst sample. The increased variance in the records during storm activity is clear, as is the change at about year day 64 with the loss of the fish cage counter weight.

The average of each burst from the rate sensors (Figure 6.16), again does not indicate much as the fish cage is held against rotation in the vertical (z) axis by the mooring, and against

pitch and roll by the mooring and the counter weight. The nature of the signal can again be seen to change with the loss of the counter weight. The energy in the rotation is seen in the variance records (Figure 6.16) where the storm activity, and the change in nature after the loss of the counter weight is again evident. The means of the bursts records shown in Figure 6.16 probably indicates the accuracy and noise level of the rate sensors, and is probably not significant. It is obvious that the average is zero, as the cage is upright and in the same orientation a year after the deployment.

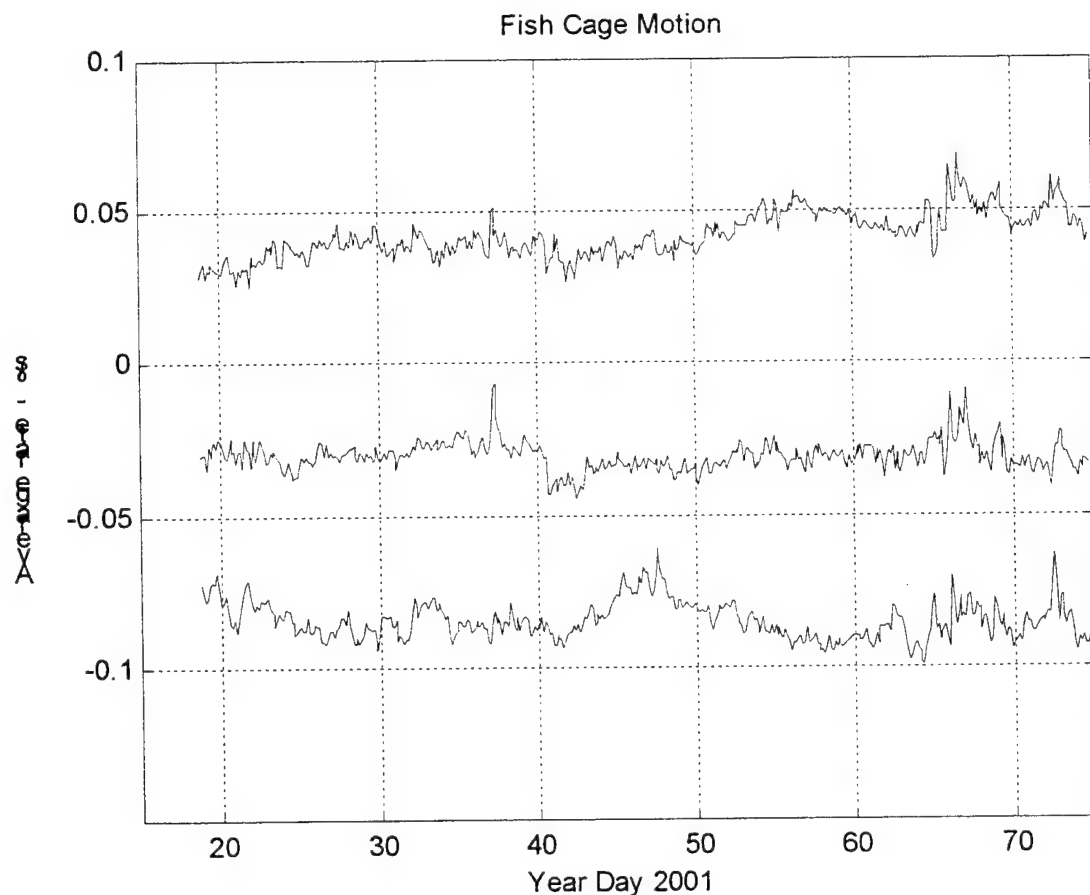


Figure 6.16. The fish cage motion package mean of the rate sensors. As the mooring constrains the fish cage so that it is basically in the same position, this record gives an indication of how constant the sensor is in this application. The lower curve is vertical and the upper two are the horizontal rotational means.

The standard deviation of the rate sensors (Figure 6.17) show the response to the wave forcing, and appears visually correlated with the wave rider accelerations (Figure 5.11) and the motion package accelerations (Figure 6.11). Again, as expected, the rotations around the vertical axis are the smallest, and the pitch and roll around the two horizontal axes are larger. The sudden change in behavior after the fish cage counter weight was lost is also clearly evident. Again, the records are yielding information on the fish cage response to wave and current forcing that is important to understanding the fish cage and mooring response. This better understanding will allow better offshore aquaculture moorings to be constructed as the dynamics of these complicated system will be better understood.

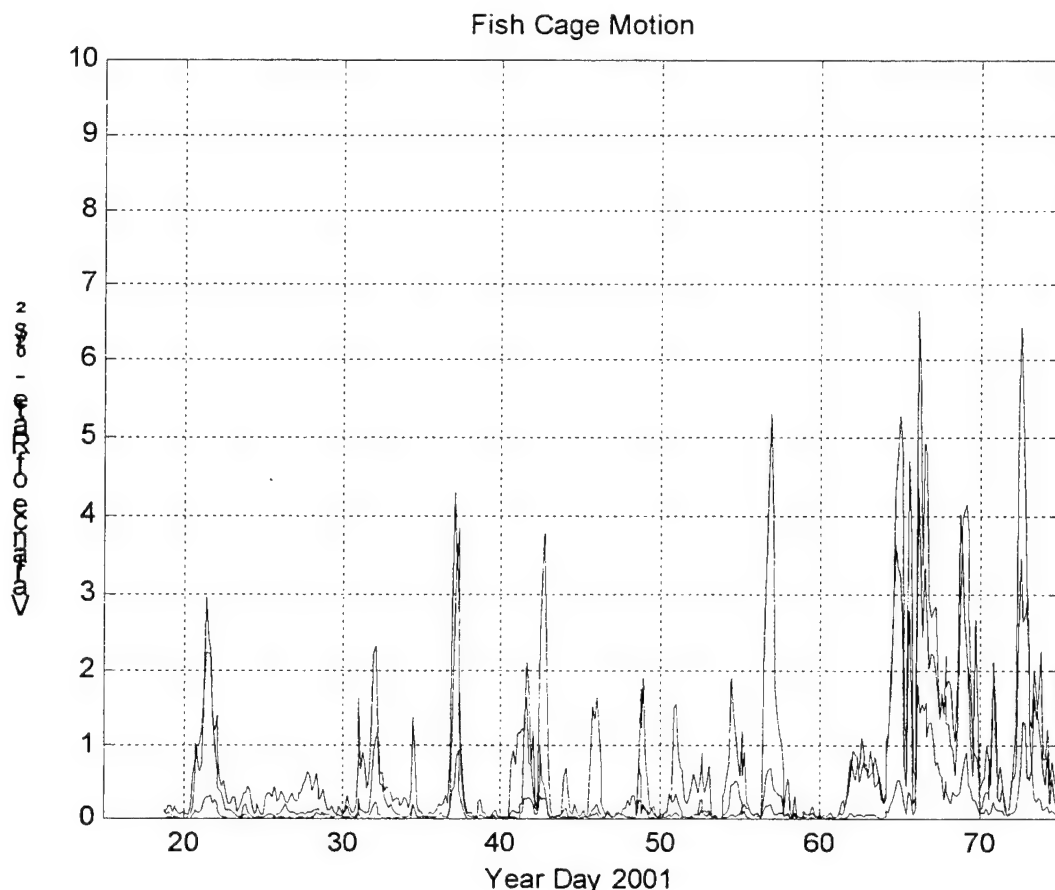


Figure 6.17. The fish cage variance of the rate sensors. Again, these records show the increased activity related to the storms as seen in the variance of the accelerations in Figure 6.11. The largest signals are the horizontal pitch and heave, and the lowest is rotations about the vertical.

The data from (1) the load cells in the mooring lines as discussed in Part 1, (2) the wave rider buoy which measures the higher frequency forcing of the fish cage, (3) the fish cage motion package, and (4) the Acoustic Doppler Current Profiler on the UNH environmental mooring that gives the low frequency forcing due to the weather forced currents and the tides are further discussed in a preliminary data analysis report for the 2001 data sets (Irish et al., 2001b) now being prepared.

7.0 Acknowledgements

Funding for this effort was provided by the National Oceanic and Atmospheric Administration for the Open Ocean Aquaculture Project under Contract No NA86RG0016 to the University of New Hampshire and under Subcontracts 00-394 and 01-442 to the Woods Hole Oceanographic Institution. Diving support for this project was supplied by UNH, and the divers, particularly Michael Chambers, Glenn Rice and Dave Fredriksson are to be thanked as their effort made the monitoring program possible. Ship time on the R/V *Gulf Challenger* was also supplied by UNH, and Captian Paul Pelletier is to be thanked for his support. Ship time for the mooring and load cell deployment was on the F/V *Nobska* with help from Captain Matt Stommel

and crew, as well as the UNH divers and small boat R/V *Galen J.* John Godley and Tom Sullivan and all the Persistor staff provided a superb product and support on their microcomputer system. The UNH engineering team of Barbaros Celikkol, Rob Swift, Igor Tsurkov, Ken Baldwin, Dave Fredriksson, Rob Steen and Glen Rice contributed to discussions and integration of the WHOI effort into the OOA program. Michael Chambers is to be commended on his management of the field effort that really made a difference in interfacing WHOI's effort with the UNH program.

8.0 References

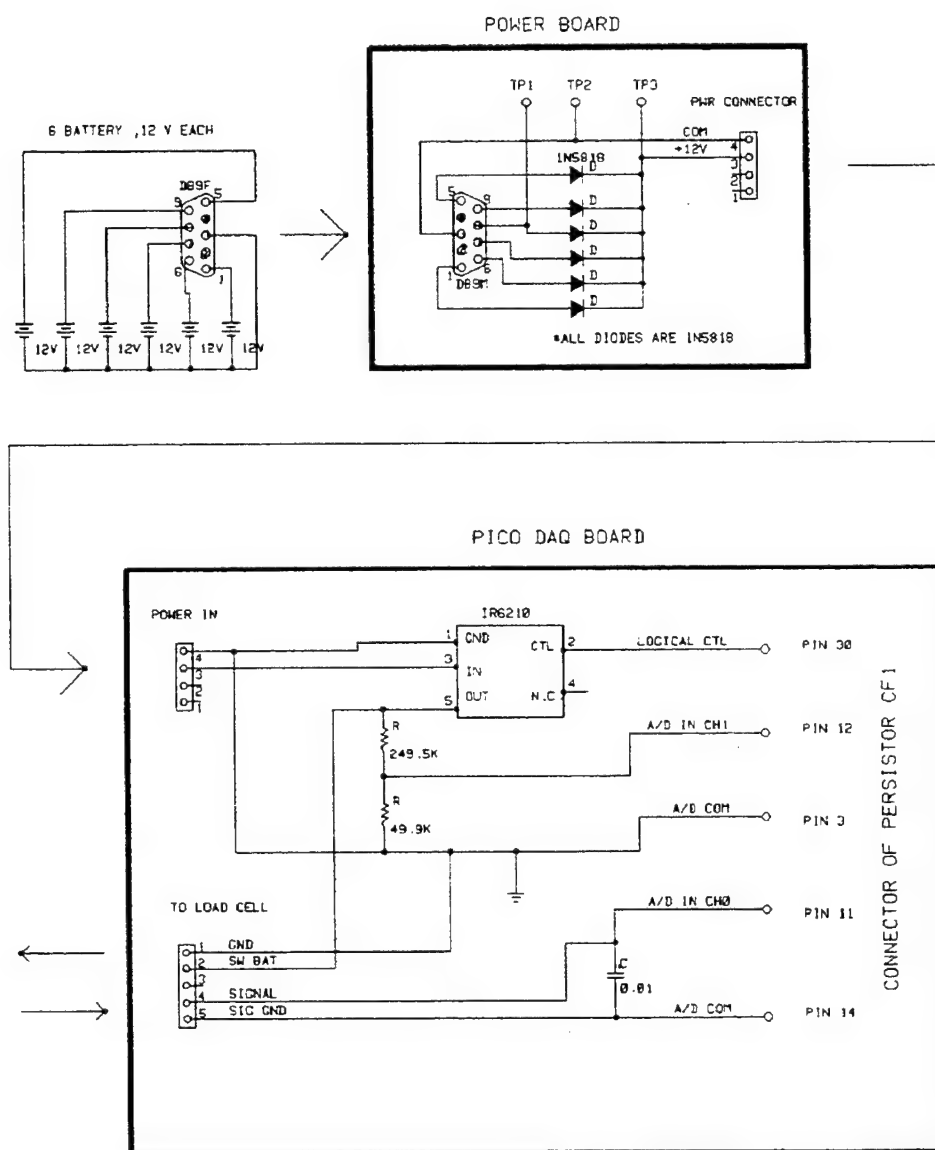
- Baldwin, K., B. Celikkol, R. Steen, D. Michelin, E. Muller and P. Lavoie, "Open Ocean Aquaculture engineering: Mooring & Net Pen Deployment," *Mar. Tech. Soc. Jour.*, 34(1), 53-58, 2000.
- Bub, F., J. Lund and M. Brodeur, "Measurements of the Physical Environment: What Have We Learned and What Do We Need," *Open Ocean Aquaculture IV*, June 17-20, St. Andrews, NB, Canada, Mississippi-Alabama Sea Grant Consortium, Ocean Springs, MS. MASGP-01-006, 2001 (submitted).
- Fredriksson, D.W., M.R. Swift, E. Muller, K. Baldwin and B. Celikkol, "Open Ocean Aquaculture Engineering: System Design and Physical Modeling," *Mar. Tech. Soc. Jour.*, 34(1), 41-52, 2000.
- Fredriksson, D.W., "Open Ocean Fish Cage and Mooring System Dynamics," Ph.D. Thesis submitted to the University of New Hampshire in partial fulfillment of the Engineering Systems Design Program. Durham, NH, September 2001.
- Irish, J.D., and S. Kery, "Elastic Tether Technology for Shallow Water Moorings in Harsh Environments: Results from Georges Bank," *Proc. Oceans '96*, 635-639, 1996.
- Irish, J.D. "Elastic Tether Mooring Technology: Experiences in the Gulf of Maine and on Georges Bank," *Sea Technology*, 38(10), 61- 69, 1997.
- Irish, J.D., J.F. Lynch, P.A. Traykovski, A.E. Newhall, K. Prada, and A.E. Hay, "A Self Contained Sector Scanning Sonar for Bottom Roughness Observations as Part of Suspended Sediment Studies," *Jour. Atm. and Oceanic Tech.*, 16, 1830-1841, 1999.
- Irish, J.D., W. Paul W. Ostom, Michael Chambers, Dave Fredriksson, and Matt Stommel, "Deployment of the Northern Fish Cage and Mooring, University of New Hampshire – Open Ocean Aquaculture Program, Summer 2000," Woods Hole Oceanog. Inst Tech. Rept., WHOI-01-01, 57pp, 2001a.
- Irish, J.D. D.W. Fredriksson, F. Bub and K. Morey, "Open Ocean Aquaculture Monitoring: Preliminary 2001 data Analysis," Woods Hole Oceanog. Inst Tech. Rept., in preparation, 2001b.
- Irish, J.D., A.E. Hay, P. Traykovski, A. Newhall, R. Craig, and W. M. Paul, "On Attaching Acoustic Imaging Instrumentation to the LEO-15 Observatory for Sediment Transport and Bottom Boundary Layer Studies," Submitted to IEEE Ocean Engineering, Sept. 2001c.
- McDonald, G. and D. Peters, "Mechanical Systems for the Portable Coastal Observatory," *Proc. ONR/MTS Buoy Workshop 2000*, Woods Hole MA, April 2000.

- Muller, E., "Development of an Offshore Aquaculture Site". Master's Thesis submitted to the University of New Hampshire in partial fulfillment of the Ocean Engineering Program. Durham, NH, December, 1999.
- Panchang, V., B. Pearce and Y. Puri, "Hindcast Estimates of Extreme Wave Conditions in the Gulf of Maine". *Applied Ocean Research*, Vol 12, No. 1, p.43-40, 1990.
- Paul, W., "Design Considerations for Stretch Conductors in Oceanographic Moorings," Woods Hole Oceanog. Inst. Tech. Rept. WHOI 95-15, 1995.
- Paul, W., J. Irish, J. Gobat and M. Grosenbaugh, "Taut Elastomeric and Chain Catenary Surface Buoy Moorings," *Proc. Oceans'99*, 418-426, 1999.
- Paul, W. and D. Bentley, "Conductor Survival in Lightweight Upper Ocean Working Cables," *Proc. 11th (2001) International Offshore and Polar Engineering Conference*, Vol. II, pp 708-714 Stavanger, Norway, June 2001
- Tsukrov, I.I., M. Oxbay, D.W. Fredriksson, M.R. Swift, K. Baldwin and B. Celikkol, "Open Ocean Aquaculture engineering: Numerical Modeling," *Mar. Tech. Soc. Jour.*, 34(1), 29-40, 2000.
- Wood, J.D. and J.D. Irish, "A Compliant Surface Mooring System for Real Time Data Acquisition," *Proc. of OCEANS '87*, 652-657, September 1987.
- Wyman, D.M., "Elastic Tethering Techniques for Surface and Near-Surface Buoy Systems," *Proc. Oceans 82*, 61--613, 1982.

9.0 Appendices

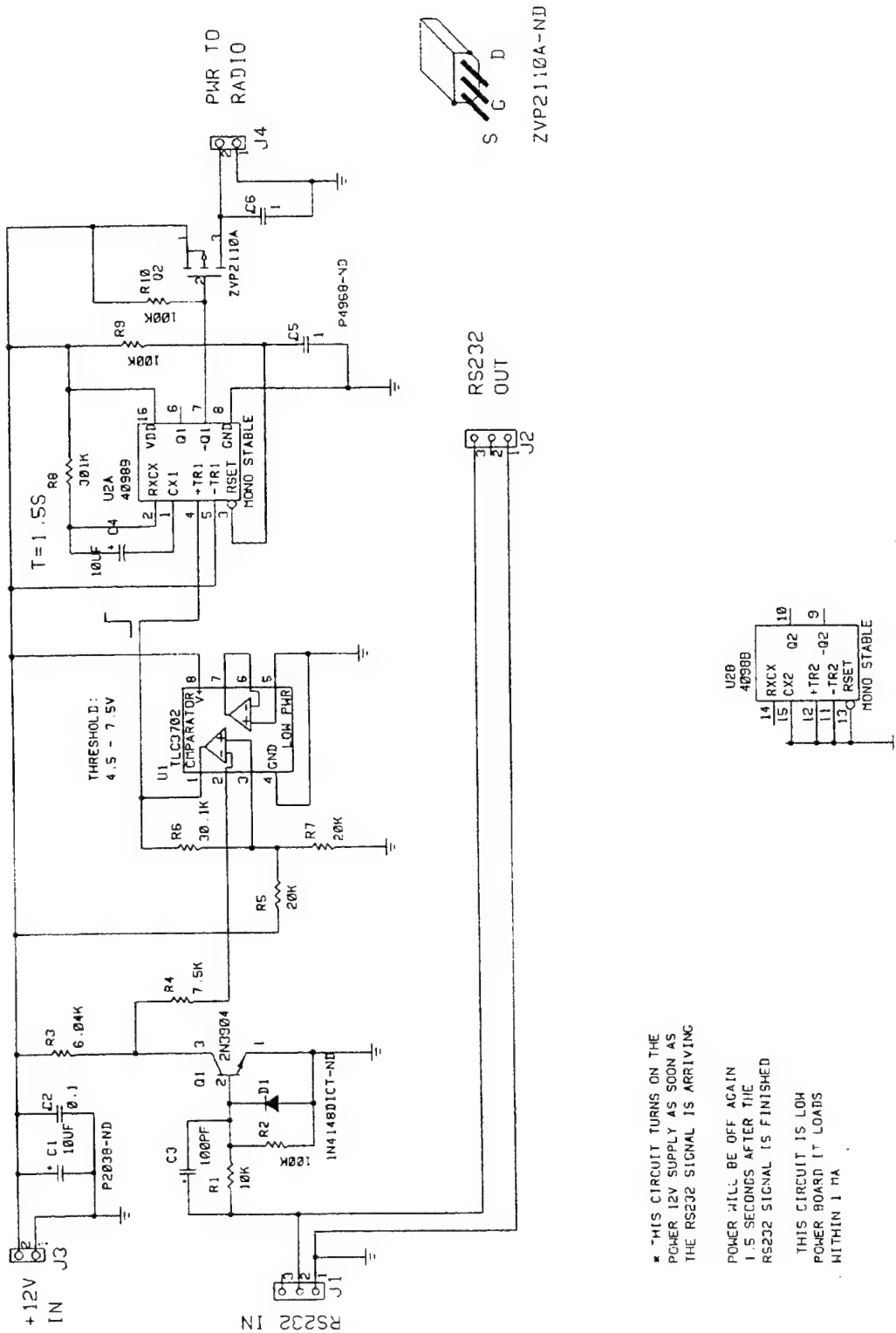
9.1 Load Cell Electronics

9.1.1 Power switch on load cell recorder



[illegible]

9.1.3 Telemetry link on fish cage



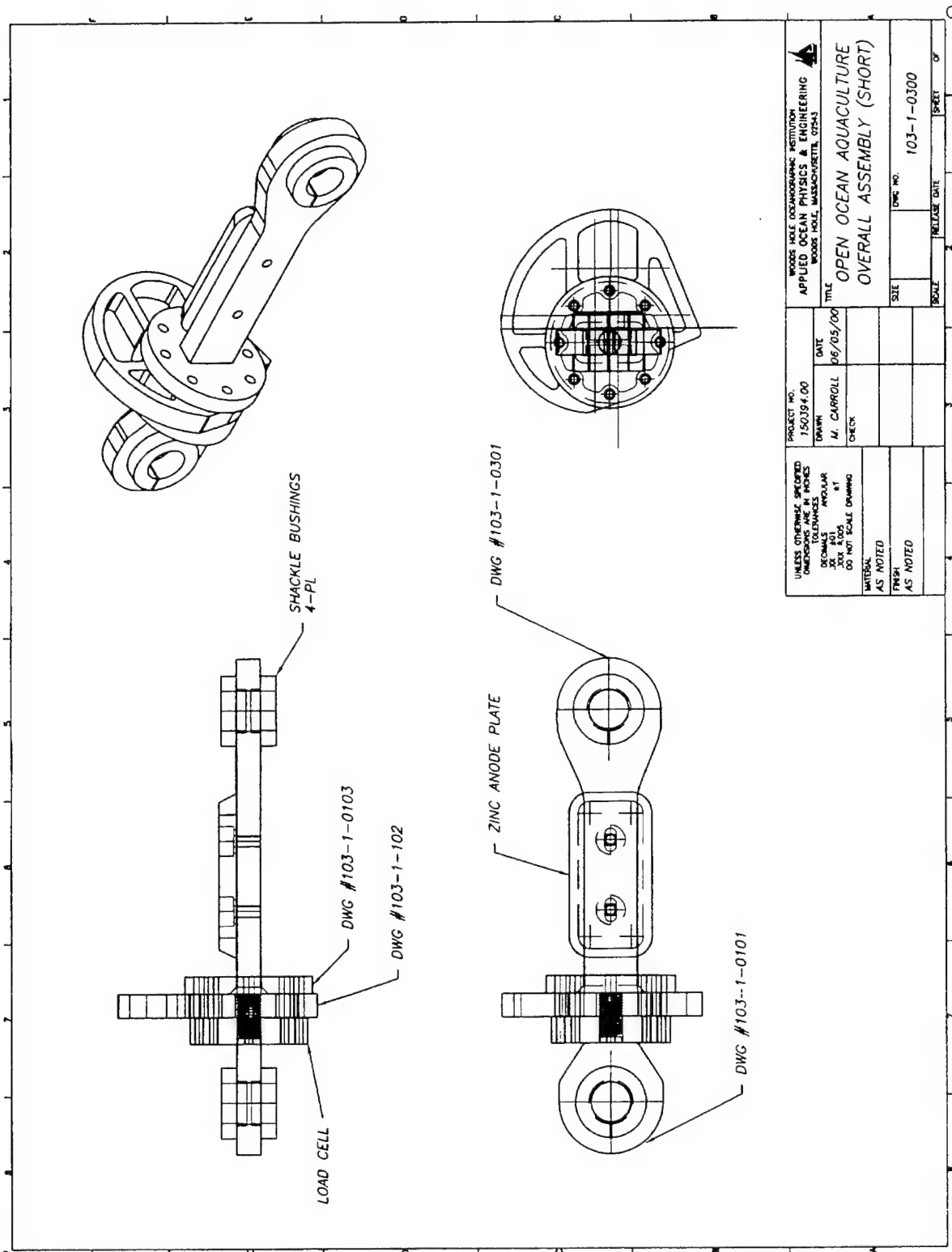
* THIS CIRCUIT TURNS ON THE POWER 12V SUPPLY AS SOON AS THE RS232 SIGNAL IS ARRIVING

POWER WILL BE OFF AGAIN 1.5 SECONDS AFTER THE RS232 SIGNAL IS FINISHED

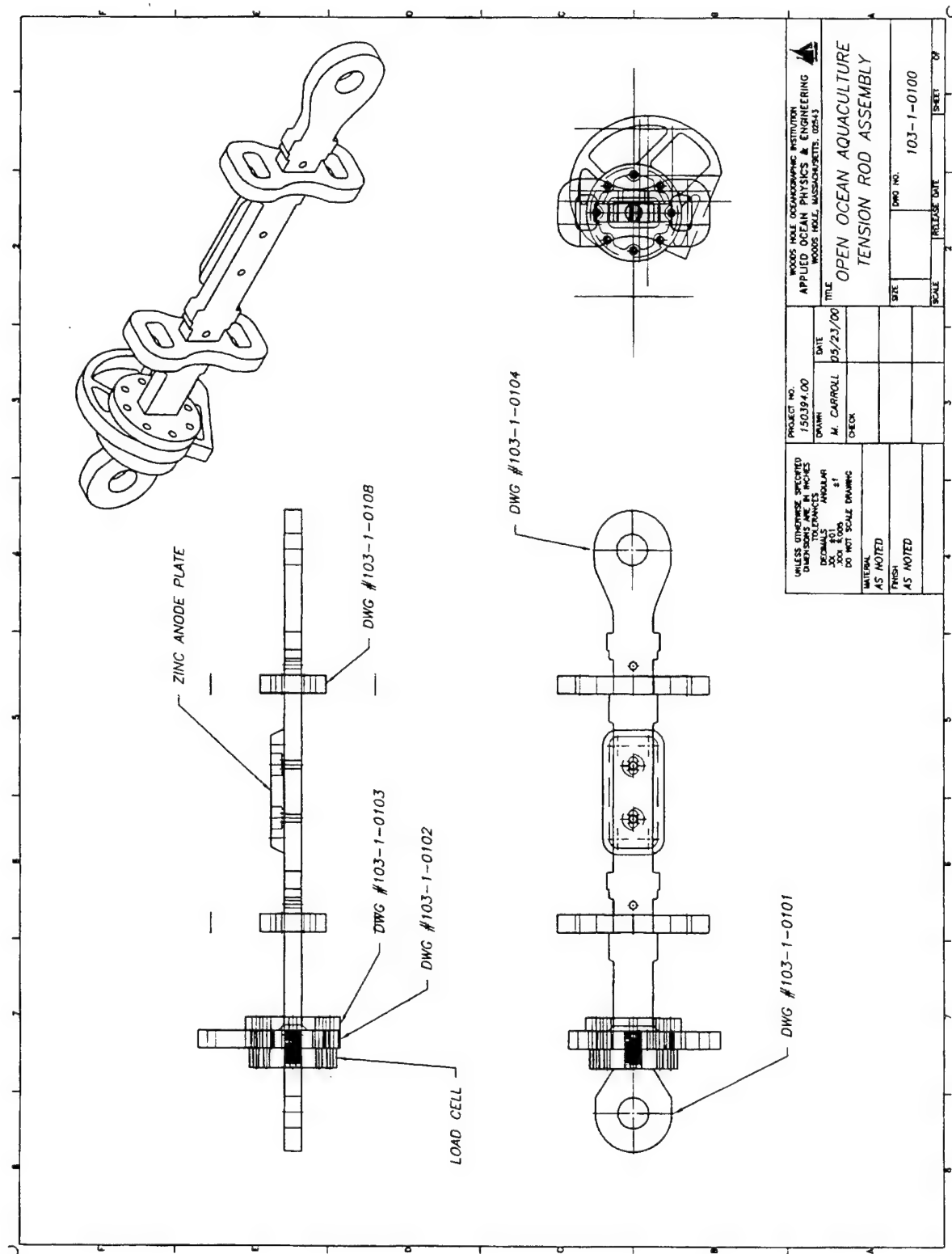
THIS CIRCUIT IS LOW POWER BOARD IT LOADS WITHIN 1 mA

9.2 Load Cell Mechanical

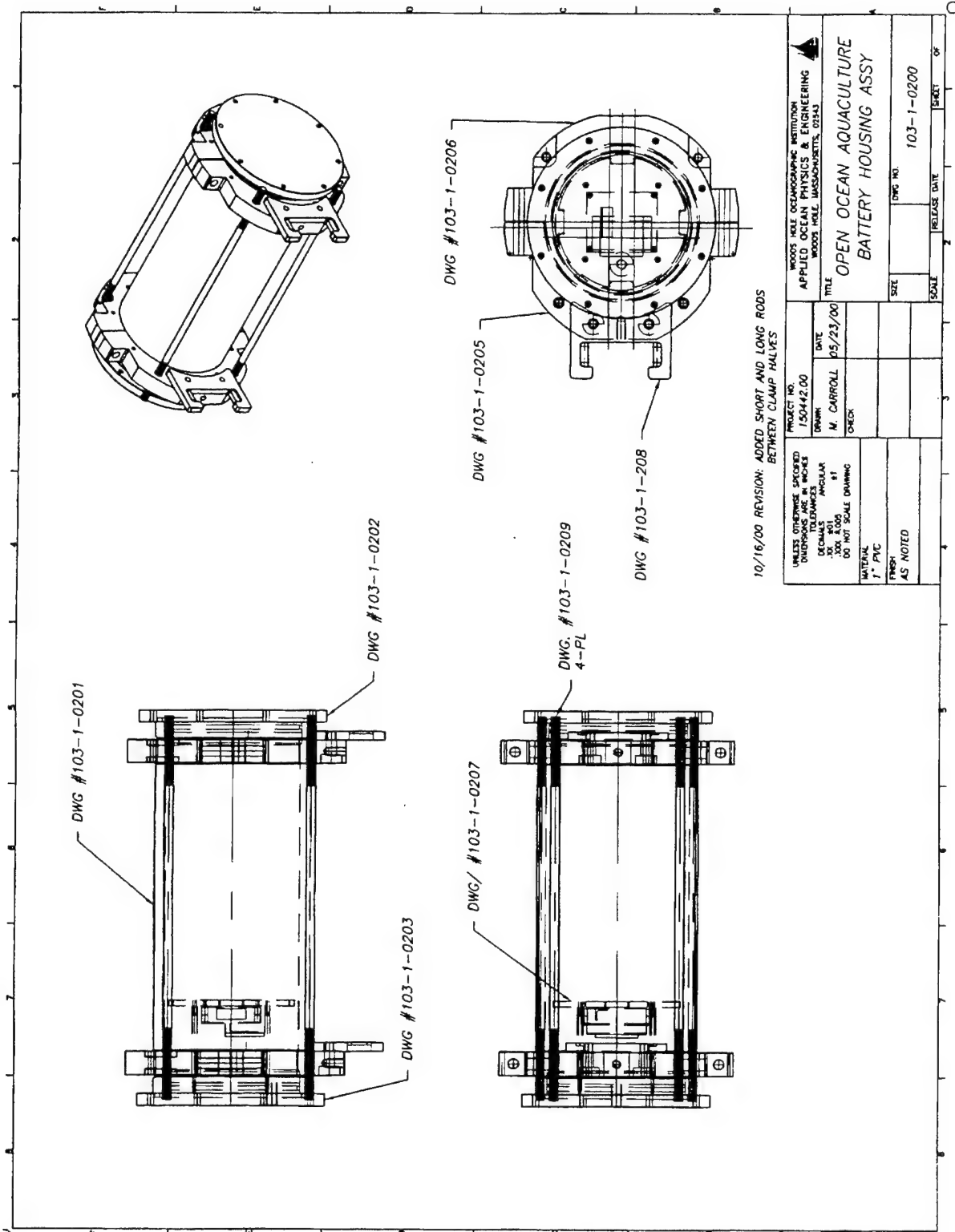
9.2.1 Strongback/load cell mounting



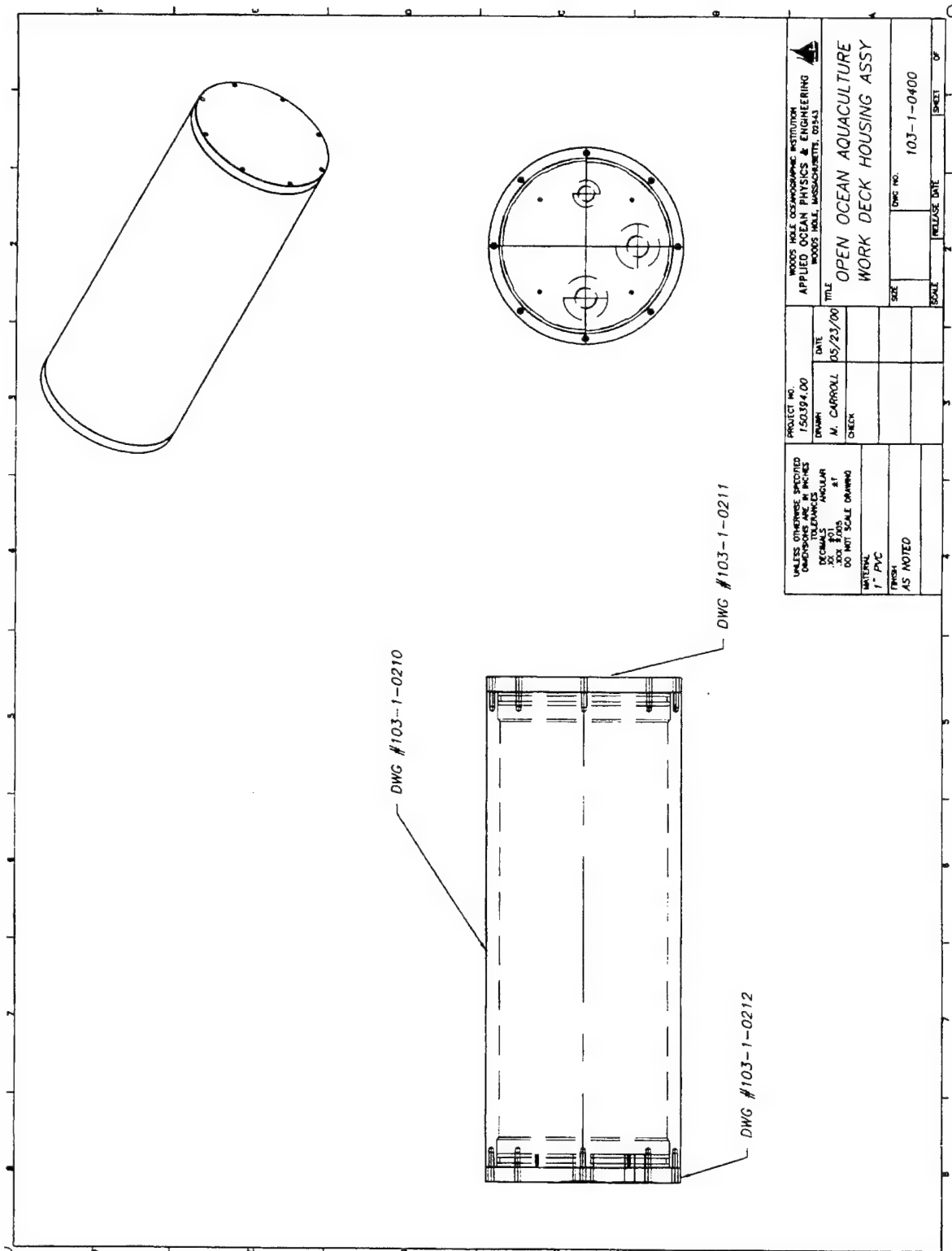
9.2.2 Strongback/load cell for recorder pressure case mounting



9.2.3 Recorder pressure case

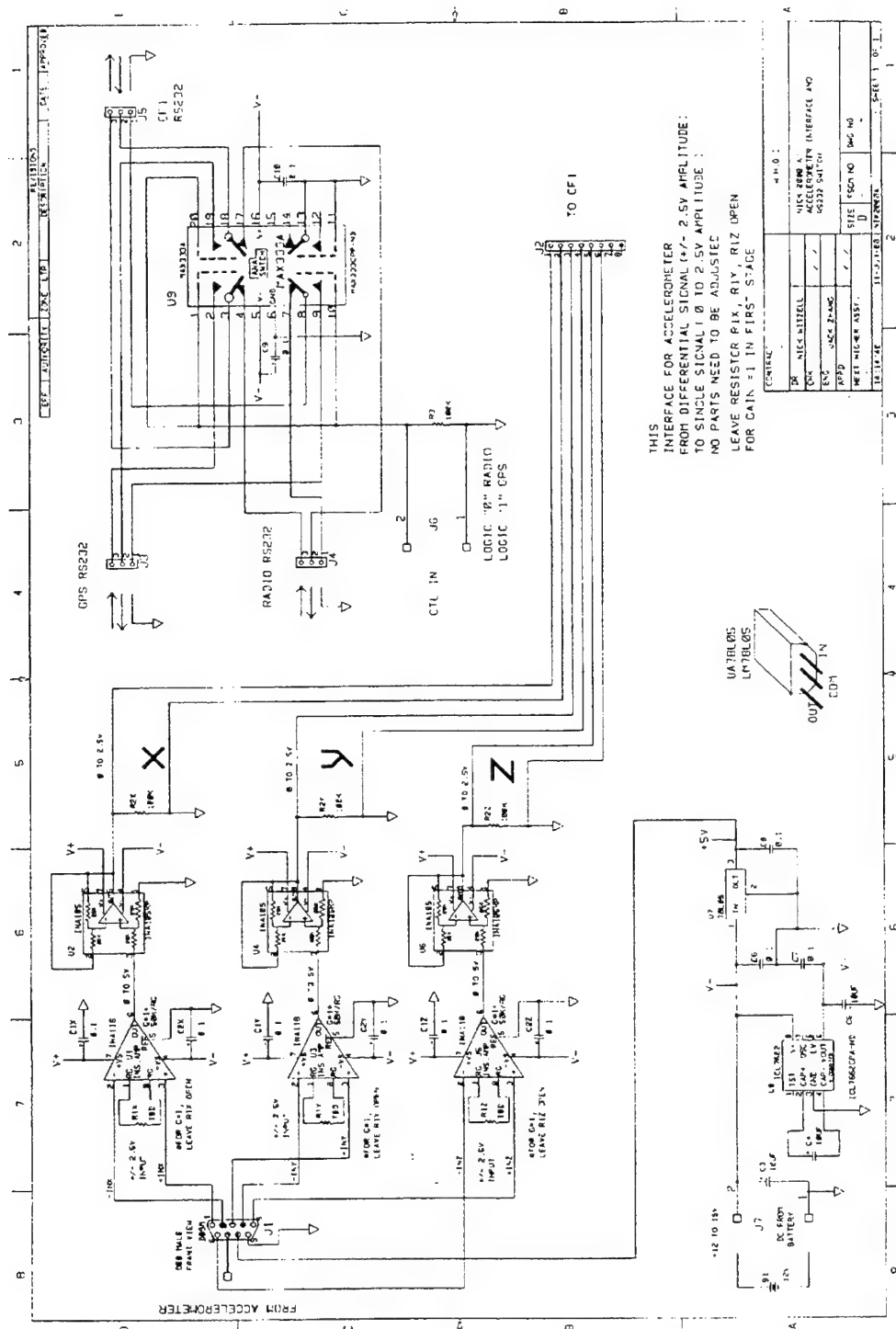


9.2.4 Fish cage telemetry pressure case



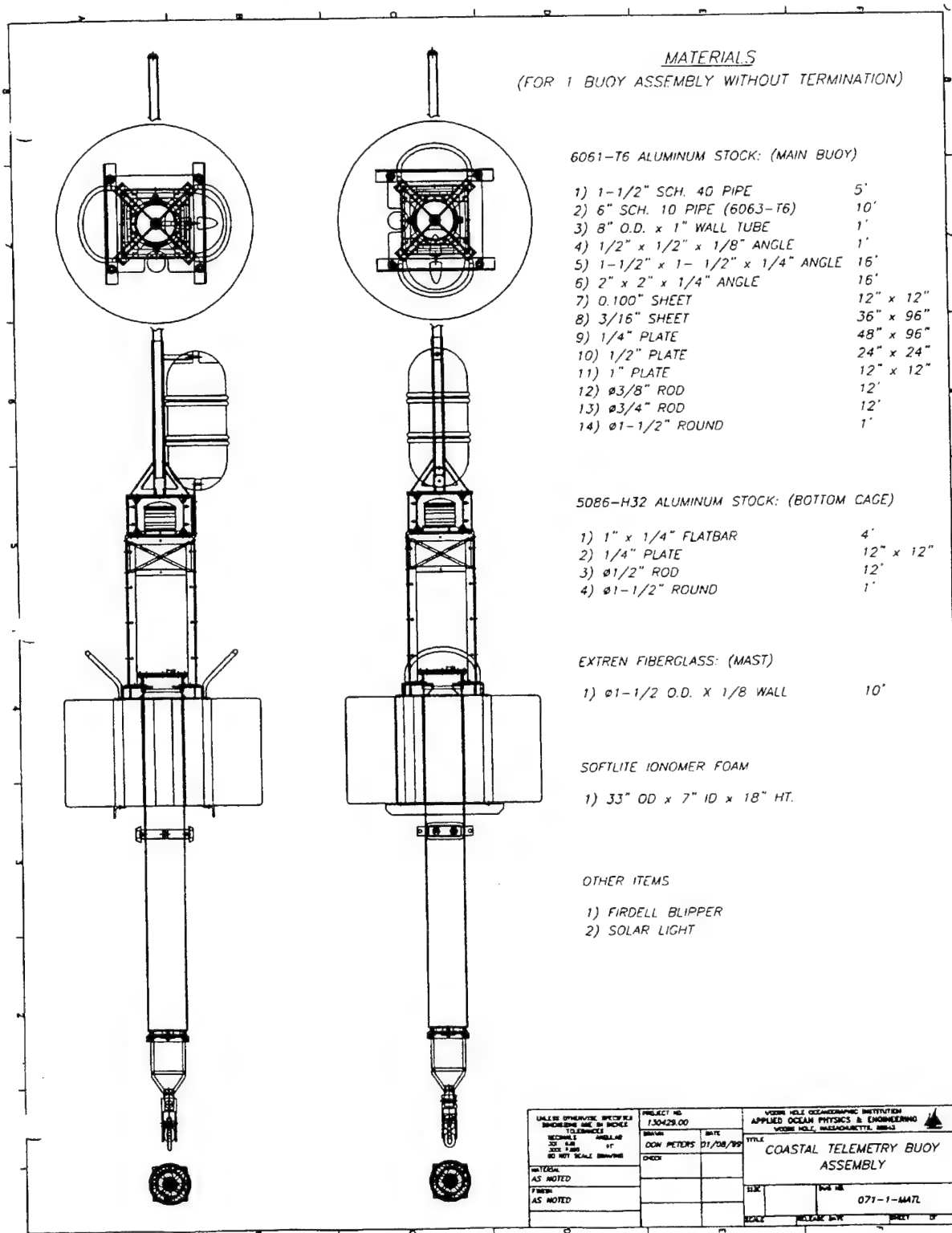
9.3 Wave Rider

9.3.1 Electronics schematic



9.4 Wave Rider Buoy and Mooring

9.4.1 Buoy assembly drawing



9.4.2 Wave rider mooring hardware list

See Figure 5.8 mooring diagram.

From Top of Mooring Down:

1. 5/8" chain shackle into wave rider buoy
2. 5/8" chain shackle into 1/2" chain
3. 1 meter of 1/2" chain
4. 5/8" chain shackle into 1/2" chain
5. 5/8" pear link
6. 3/4" shackle into tether
7. 10 m of 1" compliant elastic tether
8. 3/4" shackle into tether
9. 5/8" pear link
10. 3/4" shackle into tether
11. 10 m of 1" compliant elastic tether
12. 3/4" shackle into tether
13. 5/8" pear link
14. 5/8" anchor shackle
15. 3 ton swivel
16. 5/8" anchor shackle
17. 5/8" pear link
18. 13 mm shackle to wire rope
19. 23 m of 5/16 jacketed wire rope
20. 13 mm shackle to wire rope
21. 5/8" chain shackle into 1/2" chain
22. 1 meter of 1/2" chain
23. 5/8" chain shackle into 1/2" chain
24. 5/8" pear link
25. 3/4" shackle to anchor
26. 500 lb. anchor
27. 3/4" shackle
28. 5/8" peak link for deployment slip line

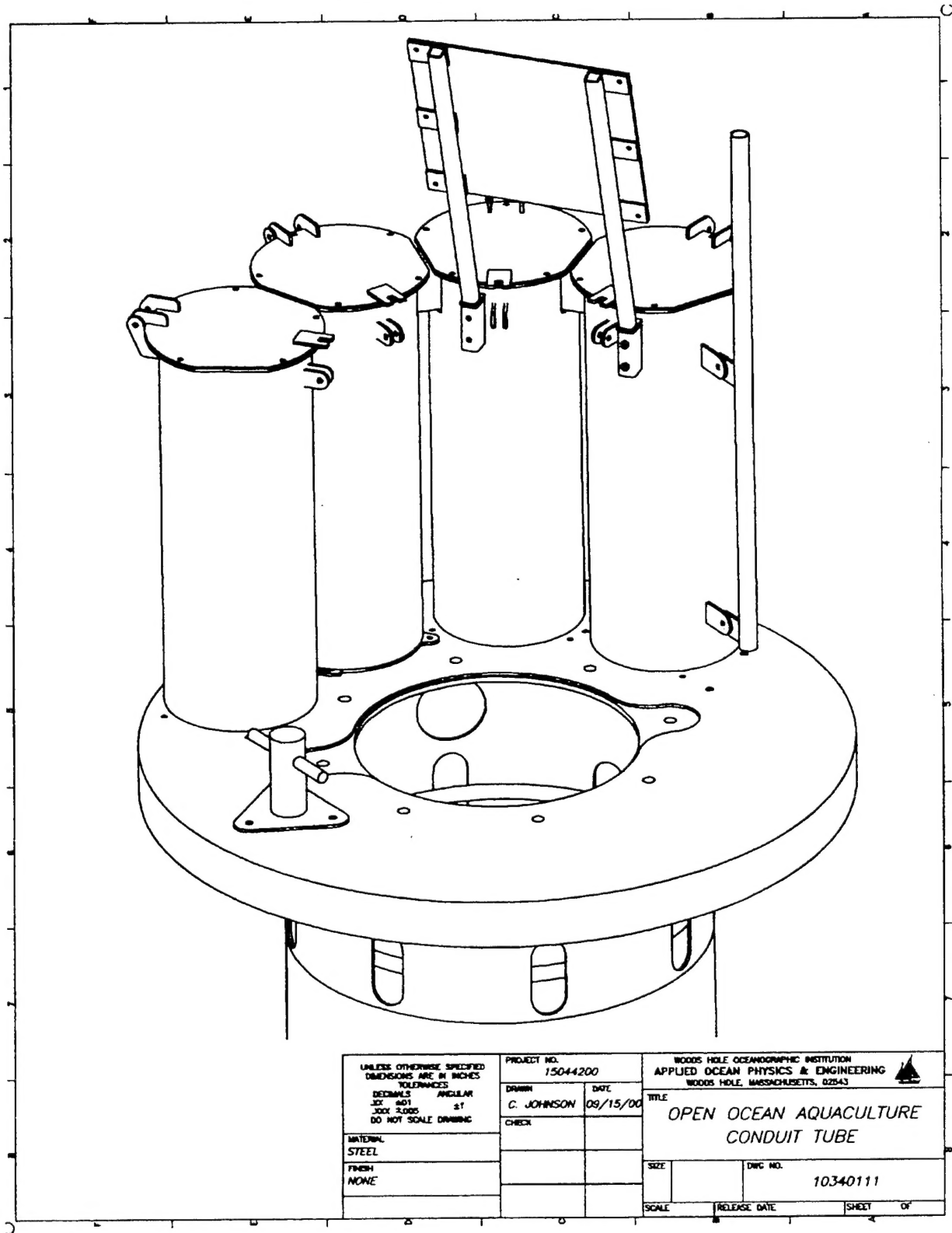
Hardware Count/List

	Hardware List	Number Required
1	5/8" chain shackles	7
2	3/4" shackles	6
3	Pear links	6
4	1 meter of 1/2" chain	2
5	10 m tether – terminated	2
6	3 ton swivel with zinc	1
7	13 mm shackles	2
8	5/15 wire rope	23 m, terminated
9	500 lb anchor	1

9.5.1 Electronics and battery case pressure case

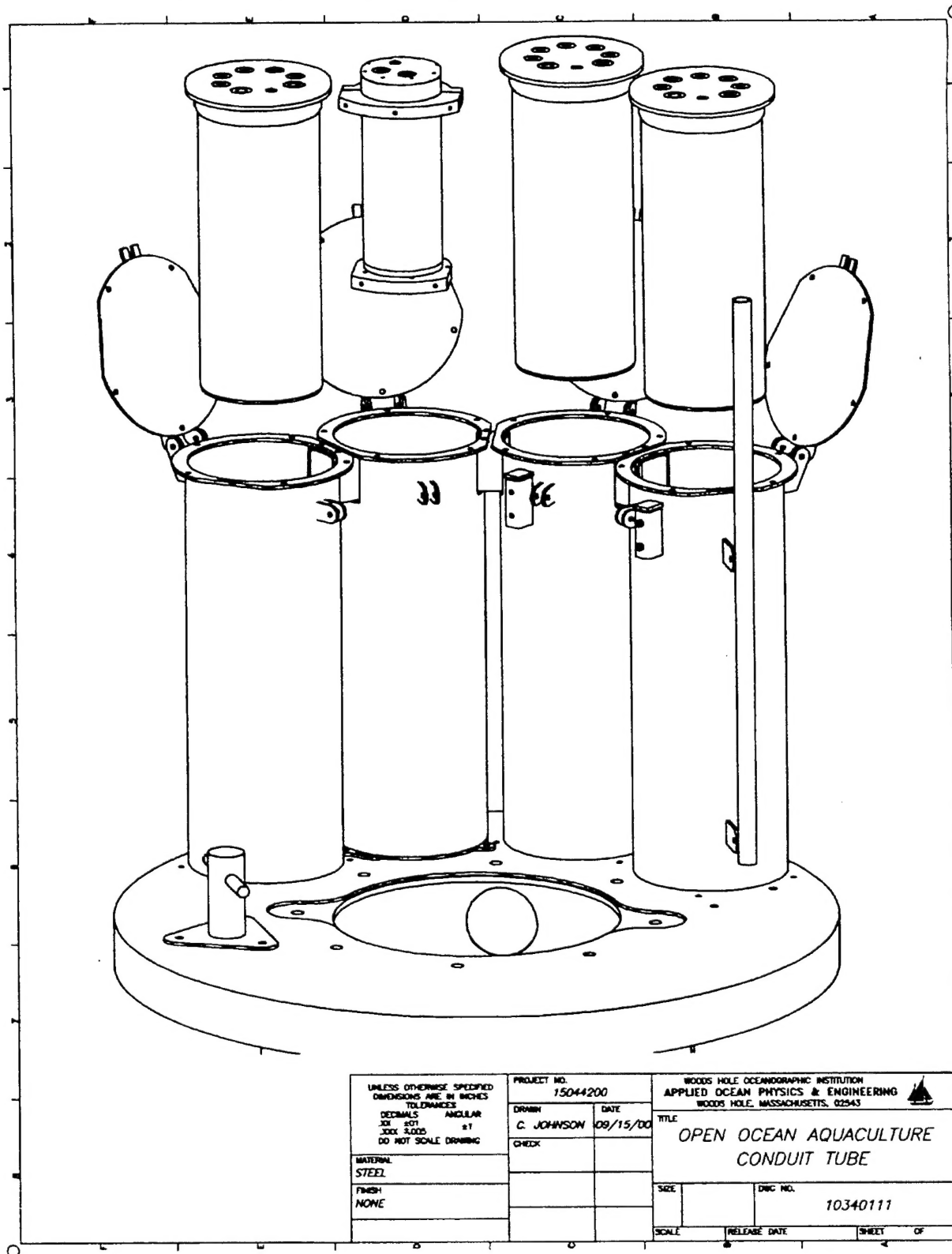


9.5.2 Silo assembly on spar



Fish cage spar with the four silos in place. The antenna is on the pole on the right, and the solar panel charges the load cell telemetry unit. The silo open to access the electronics pressure cases.

9.5.2 Silo Assembly with pressure cases



Silo assembly showing the two battery pressure cases (each end), the load cell telemetry unit (left center), and the motion package pressure case (right center) above their respective silos.

DOCUMENT LIBRARY

Distribution List for Technical Report Exchange - July 1998

University of California, San Diego
SIO Library 0175C
9500 Gilman Drive
La Jolla, CA 92093-0175

Hancock Library of Biology & Oceanography
Alan Hancock Laboratory
University of Southern California
University Park
Los Angeles, CA 90089-0371

Gifts & Exchanges
Library
Bedford Institute of Oceanography
P.O. Box 1006
Dartmouth, NS, B2Y 4A2, CANADA

NOAA/EDIS Miami Library Center
4301 Rickenbacker Causeway
Miami, FL 33149

Research Library
U.S. Army Corps of Engineers
Waterways Experiment Station
3909 Halls Ferry Road
Vicksburg, MS 39180-6199

Marine Resources Information Center
Building E38-320
MIT
Cambridge, MA 02139

Library
Lamont-Doherty Geological Observatory
Columbia University
Palisades, NY 10964

Library
Serials Department
Oregon State University
Corvallis, OR 97331

Pell Marine Science Library
University of Rhode Island
Narragansett Bay Campus
Narragansett, RI 02882

Working Collection
Texas A&M University
Dept. of Oceanography
College Station, TX 77843

Fisheries-Oceanography Library
151 Oceanography Teaching Bldg.
University of Washington
Seattle, WA 98195

Library
R.S.M.A.S.
University of Miami
4600 Rickenbacker Causeway
Miami, FL 33149

Maury Oceanographic Library
Naval Oceanographic Office
Building 1003 South
1002 Balch Blvd.
Stennis Space Center, MS, 39522-5001

Library
Institute of Ocean Sciences
P.O. Box 6000
Sidney, B.C. V8L 4B2
CANADA

National Oceanographic Library
Southampton Oceanography Centre
European Way
Southampton SO14 3ZH
UK

The Librarian
CSIRO Marine Laboratories
G.P.O. Box 1538
Hobart, Tasmania
AUSTRALIA 7001

Library
Proudman Oceanographic Laboratory
Bidston Observatory
Birkenhead
Merseyside L43 7 RA
UNITED KINGDOM

IFREMER
Centre de Brest
Service Documentation - Publications
BP 70 29280 PLOUZANE
FRANCE

REPORT DOCUMENTATION PAGE	1. REPORT NO. WHOI-2001-15	2. UNH OOA	3. Recipient's Accession No.
4. Title and Subtitle Instrumentation for Open Ocean Aquaculture Monitoring			5. Report Date October 2001
			6.
7. Author(s) James Irish, Megan Carroll, Robin Singer, Art Newhall, Walter Paul, Craig Johnson, Nick Witzell, Glen Rice, Dave Frericksson			8. Performing Organization Rept. No. WHOI-2001-15
9. Performing Organization Name and Address Woods Hole Oceanographic Institution Woods Hole, Massachusetts 02543			10. Project/Task/Work Unit No.
			11. Contract(C) or Grant(G) No. (C) NA86RG0016 (G) WHOI 00-394 WHOI 01-442
12. Sponsoring Organization Name and Address NOAA Woods Hole Oceanographic Institution			13. Type of Report & Period Covered Technical Report
			14.
15. Supplementary Notes This report should be cited as: Woods Hole Oceanog. Inst. Tech. Rept., WHOI-2001-15.			
16. Abstract (Limit: 200 words) The Woods Hole Oceanographic Institution is assisting the University of New Hampshire by instrumenting a fish cage and mooring as part of their Open Ocean Aquaculture demonstration program in the Gulf of Maine. To understand these systems, the wave and current forcing and the response of the mooring and the fish cage needed to be measured. A UNH mooring with an ADCP measured the current forcing. Tension in the mooring lines was measured by load cells deployed with the mooring during servicing in August 2000. Load cells were placed in each anchor line, and, in the NE corner, also in the two grid lines and the riser line to the fish cage. Low power recording systems were deployed on the load cell mounting bars by divers on 22 October 2000, recorded good data through January 2001, when they were turned around and redeployed. Three single load cell recorders were recovered in July 2001 and recorded through 23 June when their data storage filled. The four load cell system was recovered in March after a large winter storm, and had failed in early March. The wave forcing was measured with a wave rider buoy with a 3-axis accelerometer measuring its motion. The acceleration was integrated twice to obtain wave displacement. The system mooring contained a compliant elastic. The wave rider was deployed on 4 January 2001 and recovered on 17 March 2001 after a major Northeast storm. It recorded data throughout its deployment. The motion of the moored fish cage was measured by a motion package constructed around a 6-axis Motion-Pak and a PC-104 data system. The motion package was deployed on the fish cage from Jan into March 2001 and recorded motions throughout without difficulty. It observed the major storm in early March where the counter weight was lost from the fish cage, and its increase in motion thereafter.			
17. Document Analysis a. Descriptors open ocean aquaculture motion monitoring mooring line tension b. Identifiers/Open-Ended Terms c. COSATI Field/Group			
18. Availability Statement Approved for public release; distribution unlimited.	19. Security Class (This Report) UNCLASSIFIED	21. No. of Pages 99	
	20. Security Class (This Page)	22. Price	